QCD in the LHC Era

Precision Measurements and Searches for New Phenomena with Jets

in Proton-Proton Collisions

Katerina Lipka, DESY

https://twiki.cern.ch/twiki/bin/view/AtlasPublic

https://twiki.cern.ch/twiki/bin/view/CMSPublic/PhysicsResults

Jahrestagung der Deutschen Physikalischen Gemeinstraft DPG 2014 in Mainz

Particle production in proton-proton collisions

proton structure hard interaction

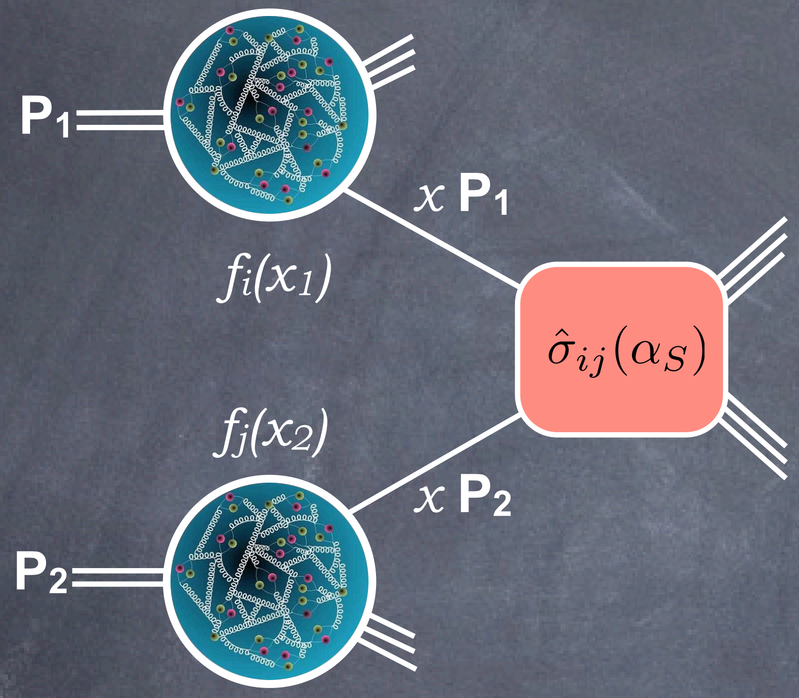

Factorization: proton structure ⊗ sub-process ME

$$\sigma(s) = \sum_{i,j} \int_{\tau_0}^{1} \boxed{\frac{d\tau}{\tau} \cdot \frac{dL_{ij}(\mu_F^2)}{d\tau}} \cdot \hat{s} \cdot \boxed{\hat{\sigma}_{ij}}$$

Particle production in proton-proton collisions

proton structure   hard interaction

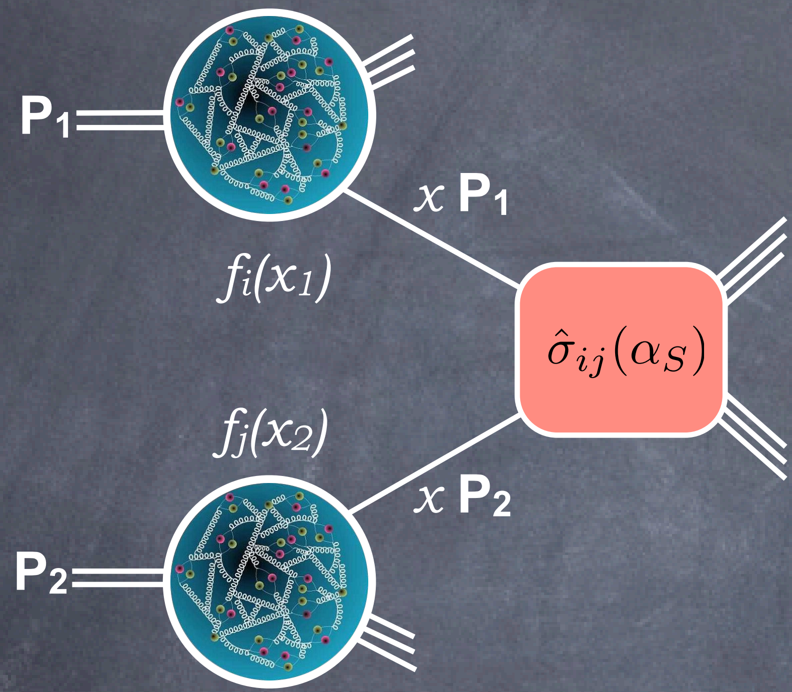

Factorization: proton structure ⊗ sub-process ME

$$\sigma(s) = \sum_{i,j} \int_{\tau_0}^{1} \boxed{\frac{d\tau}{\tau} \cdot \frac{dL_{ij}(\mu_F^2)}{d\tau}} \cdot \hat{s} \cdot \boxed{\hat{\sigma}_{ij}}$$

parton luminosity:

$$\tau \cdot \frac{dL_{ij}}{d\tau} \propto \int_0^1 dx_1 dx_2 (x_1 f_i(x_1, \mu_F^2) \cdot x_2 f_j(x_2, \mu_F^2)) + (1 \leftrightarrow 2) \delta(\tau - x_1 x_2)$$

parton distribution functions (PDFs)

Particle production in proton-proton collisions

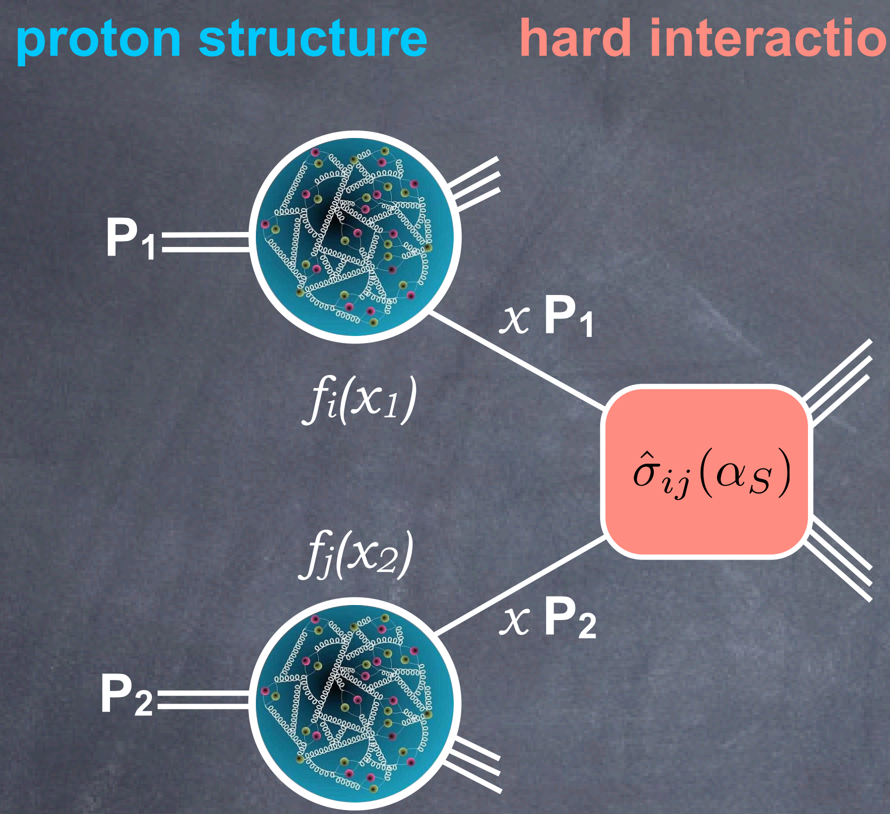

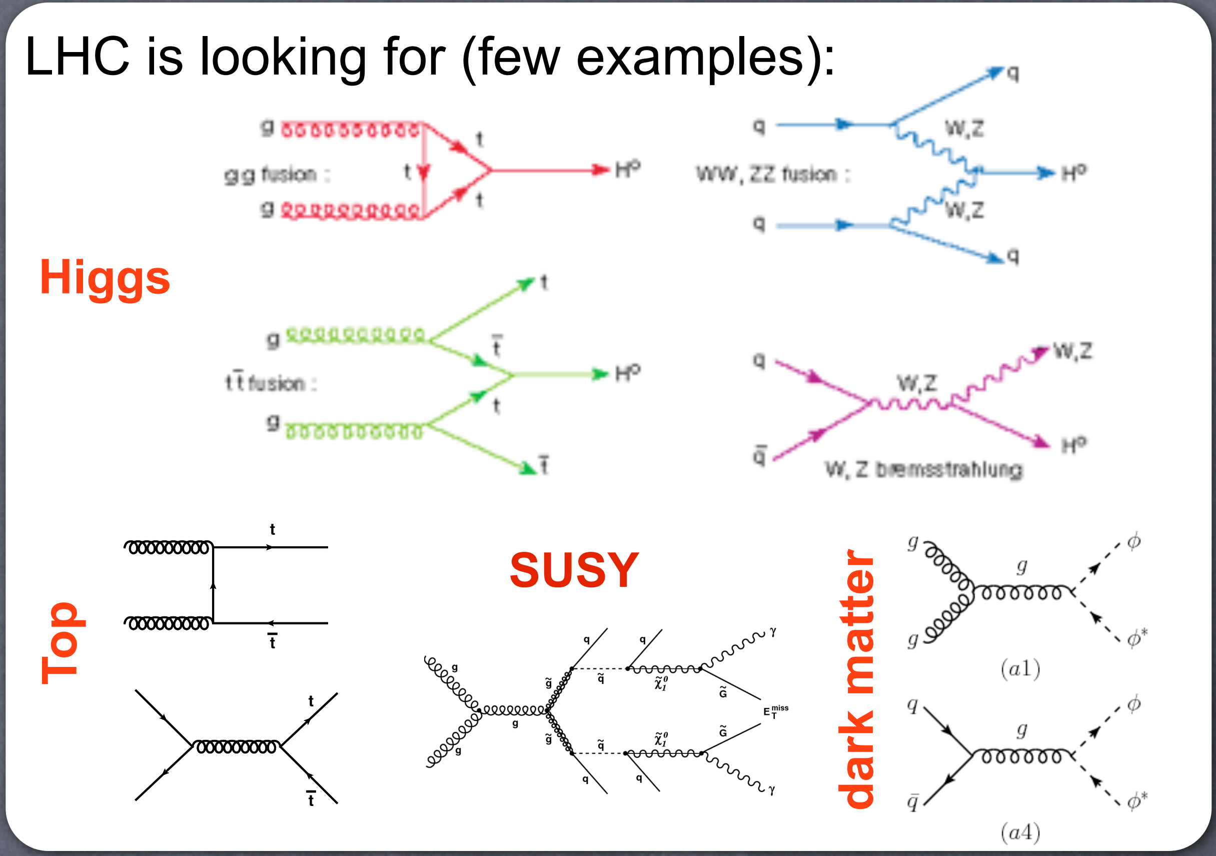

Factorization: proton structure ⊗ sub-process ME

$$\sigma(s) = \sum_{i,j} \int_{\tau_0}^{1} \boxed{\frac{d\tau}{\tau} \cdot \frac{dL_{ij}(\mu_F^2)}{d\tau}} \cdot \hat{s} \cdot \boxed{\hat{\sigma}_{ij}}$$

Imporant for interpretation of pp collisions:

- exact calculations to highest order,
- precision of strong coupling,
  quark masses,
  parton distributions (PDFs)

Particle production in proton-proton collisions

proton structure **hard interaction**

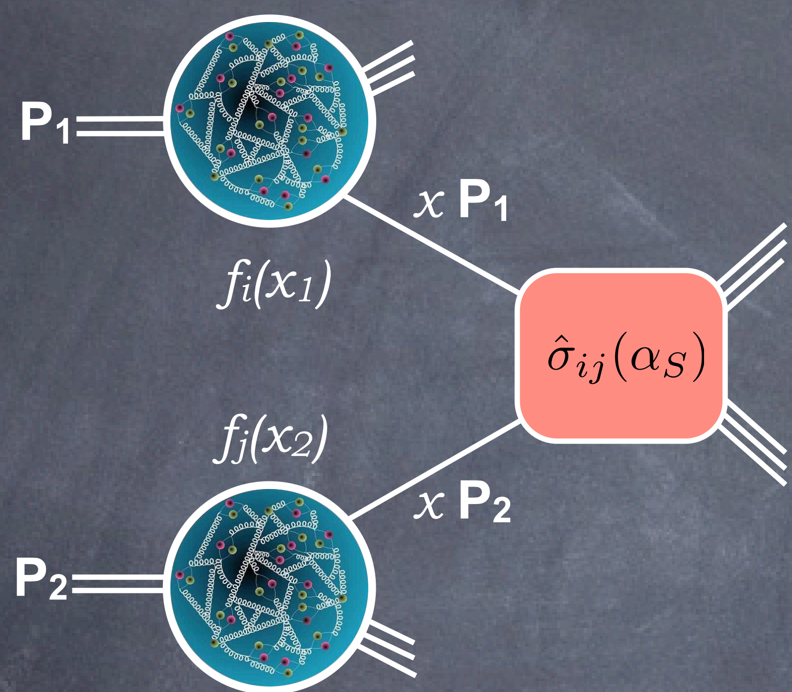

Higgs production at the LHC at NNLO

https://twiki.cern.ch/twiki/bin/view/LHCPhysics/CrossSections

		σ (8 TeV)	uncertainty
NNLL QCD +NLO EW	gg→H	19.5 pb	14.7%
	VBF	1.56 pb	2.9%
NNLO QCD +NLO EW	WH	0.70 pb	3.9%
	ZH	0.39 pb	5.1%
NLO QCD	ttH	0.13 pb	14.4%

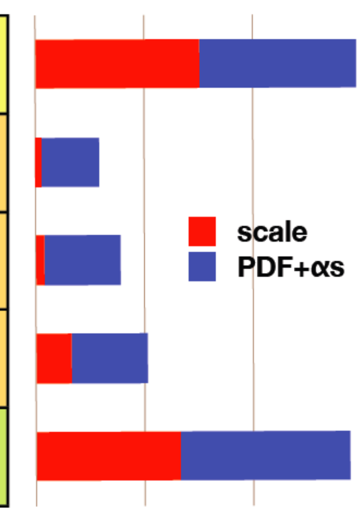

...summary J. Campbell ICHEP 2012

Particle production in proton-proton collisions

proton structure   hard interaction

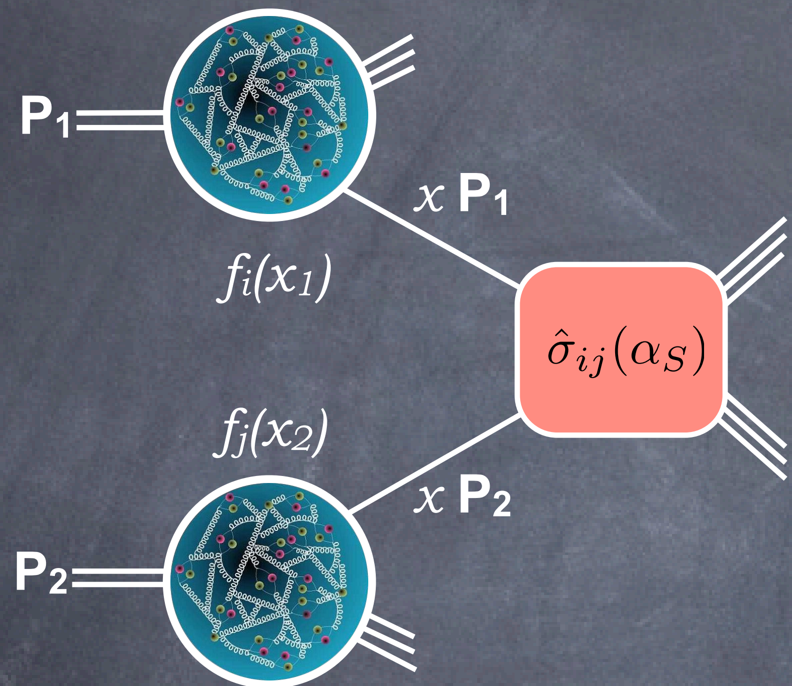

Higgs production at the LHC at NNLO

https://twiki.cern.ch/twiki/bin/view/LHCPhysics/CrossSections

		σ (8 TeV)	uncertainty
NNLL QCD +NLO EW	gg→H	19.5 pb	14.7%
NNLO QCD +NLO EW	VBF	1.56 pb	2.9%
	WH	0.70 pb	3.9%
	ZH	0.39 pb	5.1%
NLO QCD	ttH	0.13 pb	14.4%

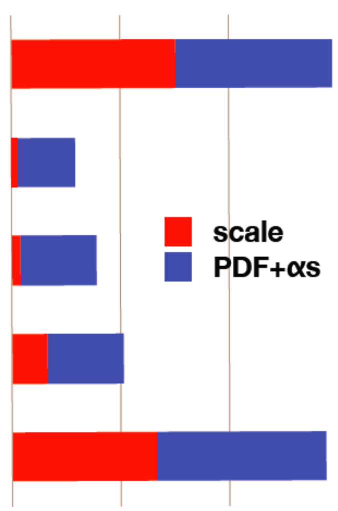

...summary J. Campbell ICHEP 2012

Searches at the LHC:

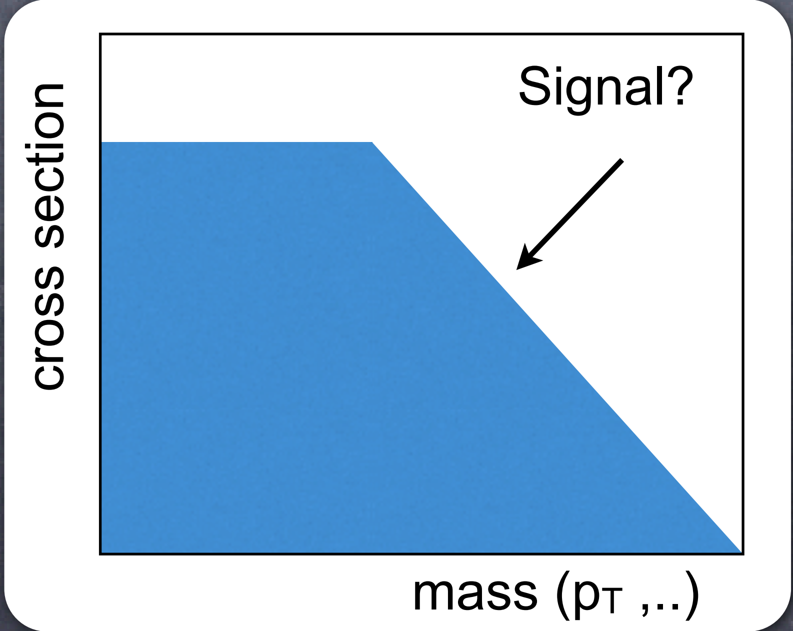

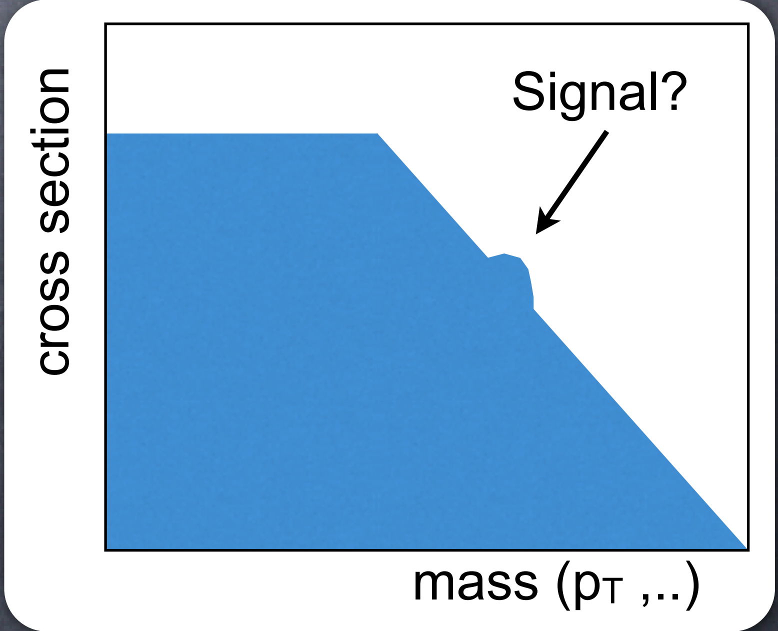

...G. Salam ICHEP 2010...

Particle production in proton-proton collisions

proton structure **hard interaction**

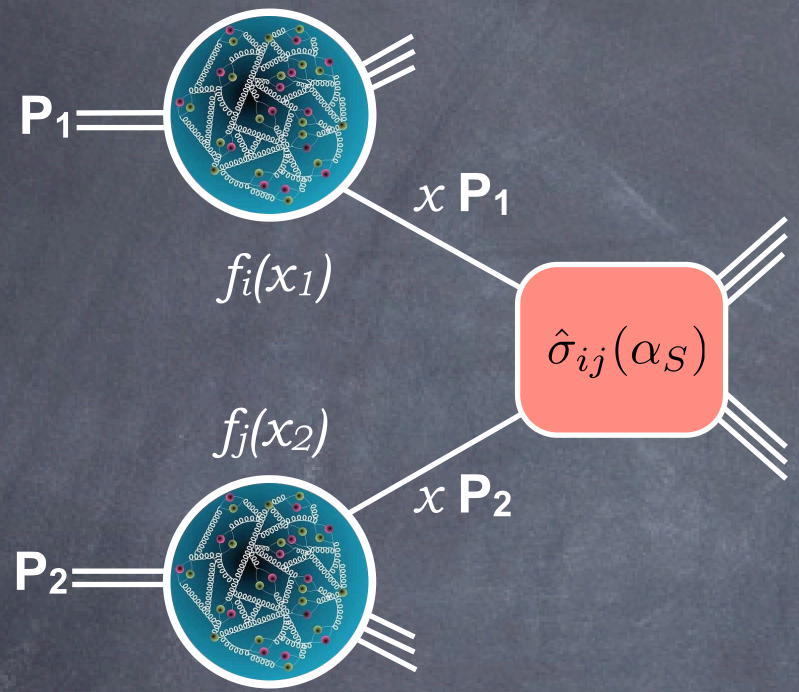

Higgs production at the LHC at NNLO

https://twiki.cern.ch/twiki/bin/view/LHCPhysics/CrossSections

		σ (8 TeV)	uncertainty
NNLL QCD +NLO EW	gg→H	19.5 pb	14.7%
NNLO QCD +NLO EW	VBF	1.56 pb	2.9%
	WH	0.70 pb	3.9%
	ZH	0.39 pb	5.1%
NLO QCD	ttH	0.13 pb	14.4%

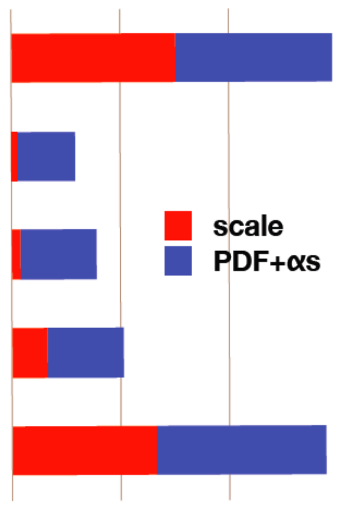

...summary J. Campbell ICHEP 2012

Searches at the LHC:

- excess in a flat signal: need precise QCD to estimate background

- sharpen a 'bump' : learn from QCD how to reduce background

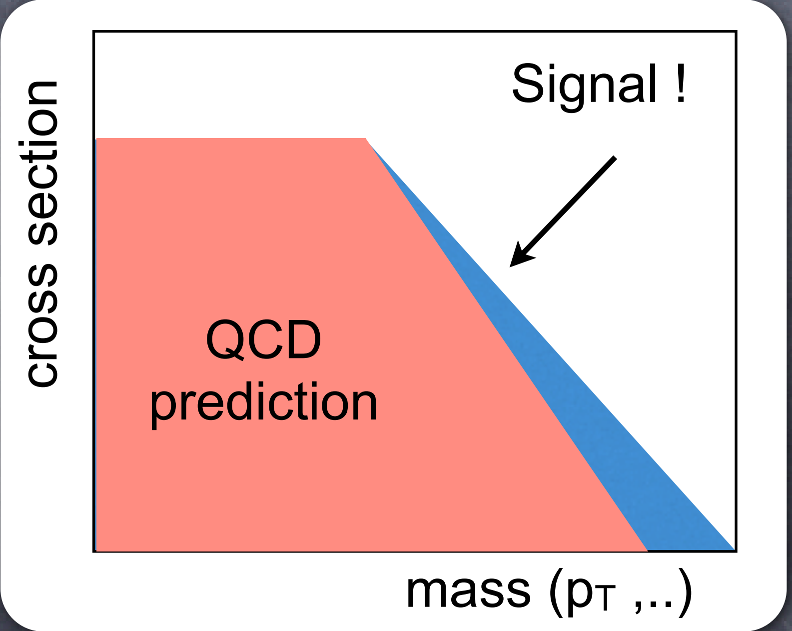

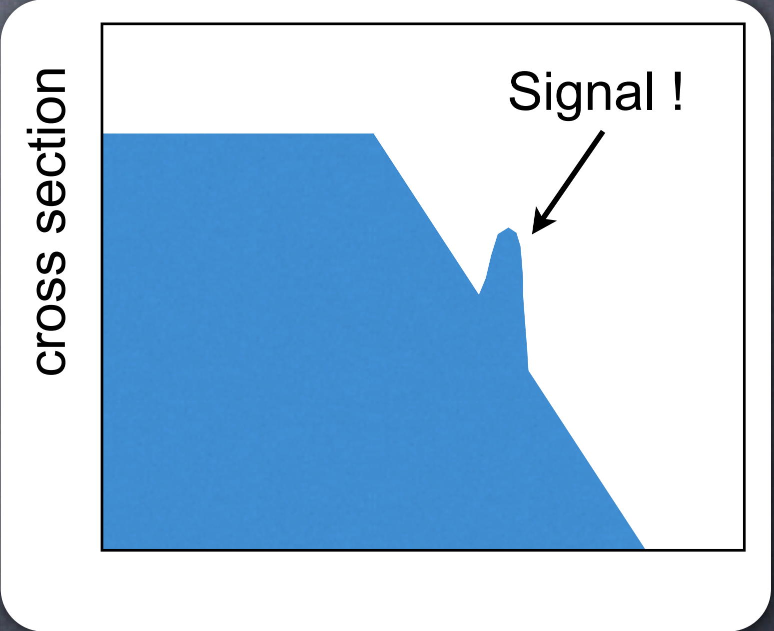

...G. Salam ICHEP 2010...

Particle production in proton-proton collisions

proton structure hard interaction

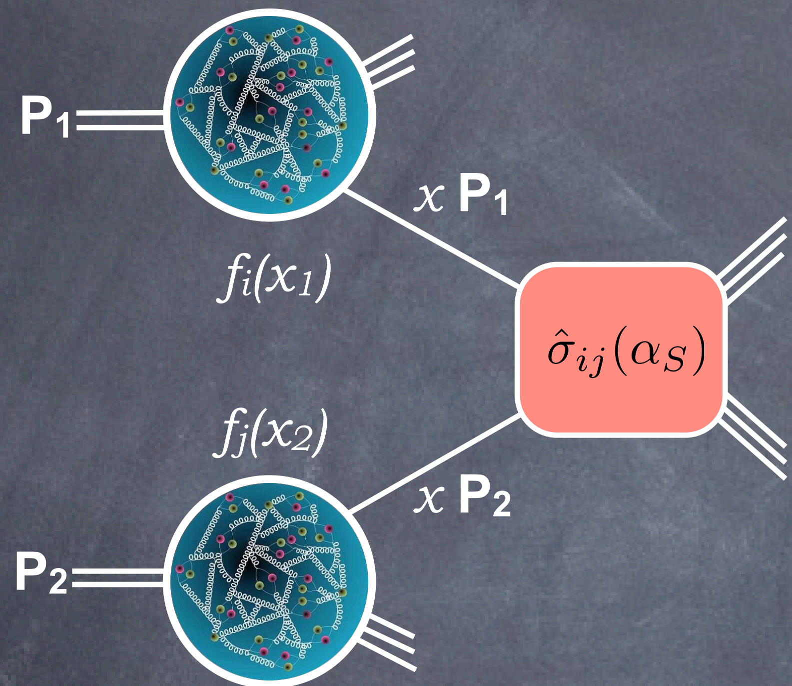

Higgs production at the LHC at NNLO

https://twiki.cern.ch/twiki/bin/view/LHCPhysics/CrossSections

		σ (8 TeV)	uncertainty
NNLL QCD +NLO EW	gg→H	19.5 pb	14.7%
	VBF	1.56 pb	2.9%
NNLO QCD +NLO EW	WH	0.70 pb	3.9%
	ZH	0.39 pb	5.1%
NLO QCD	ttH	0.13 pb	14.4%

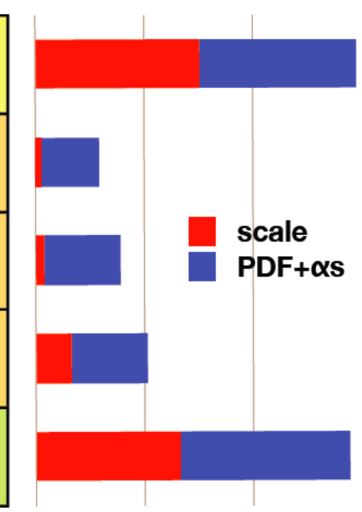

...summary J. Campbell ICHEP 2012

Searches at the LHC:

learn from QCD how to reduce background

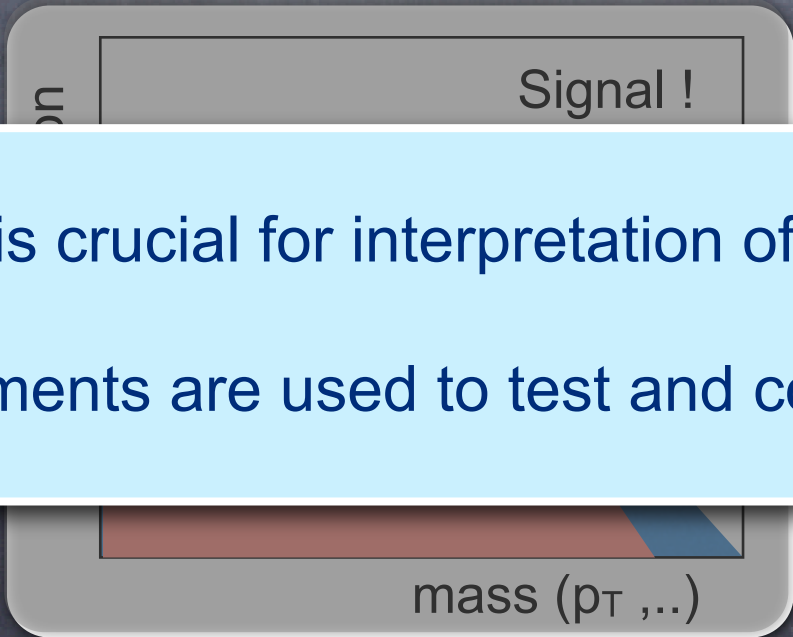

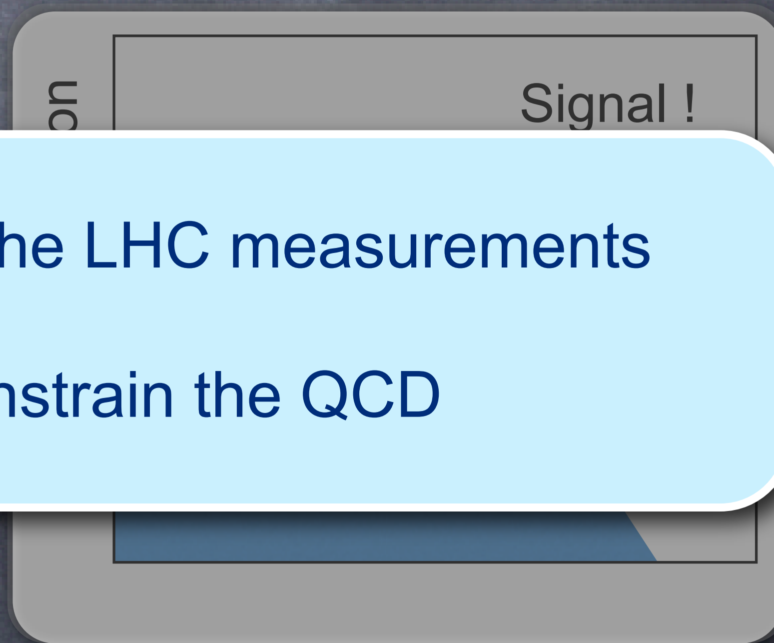

Improvement in QCD is crucial for interpretation of the LHC measurements

LHC measurements are used to test and constrain the QCD

...G. Salam ICHEP 2010...

In this talk

1) LHC data testing QCD

(Multi) jet production in pp collisions:
tests of QCD factorization,
standard candle for searches

2) LHC data improving QCD precision

Expected constraints from LHC
➡ *at high x*:
- jet production: gluon, light quarks
- top-pair production: gluon
- prompt photons: gluon

➡ *at medium x:*
W, Z, W+c production: valence, sea

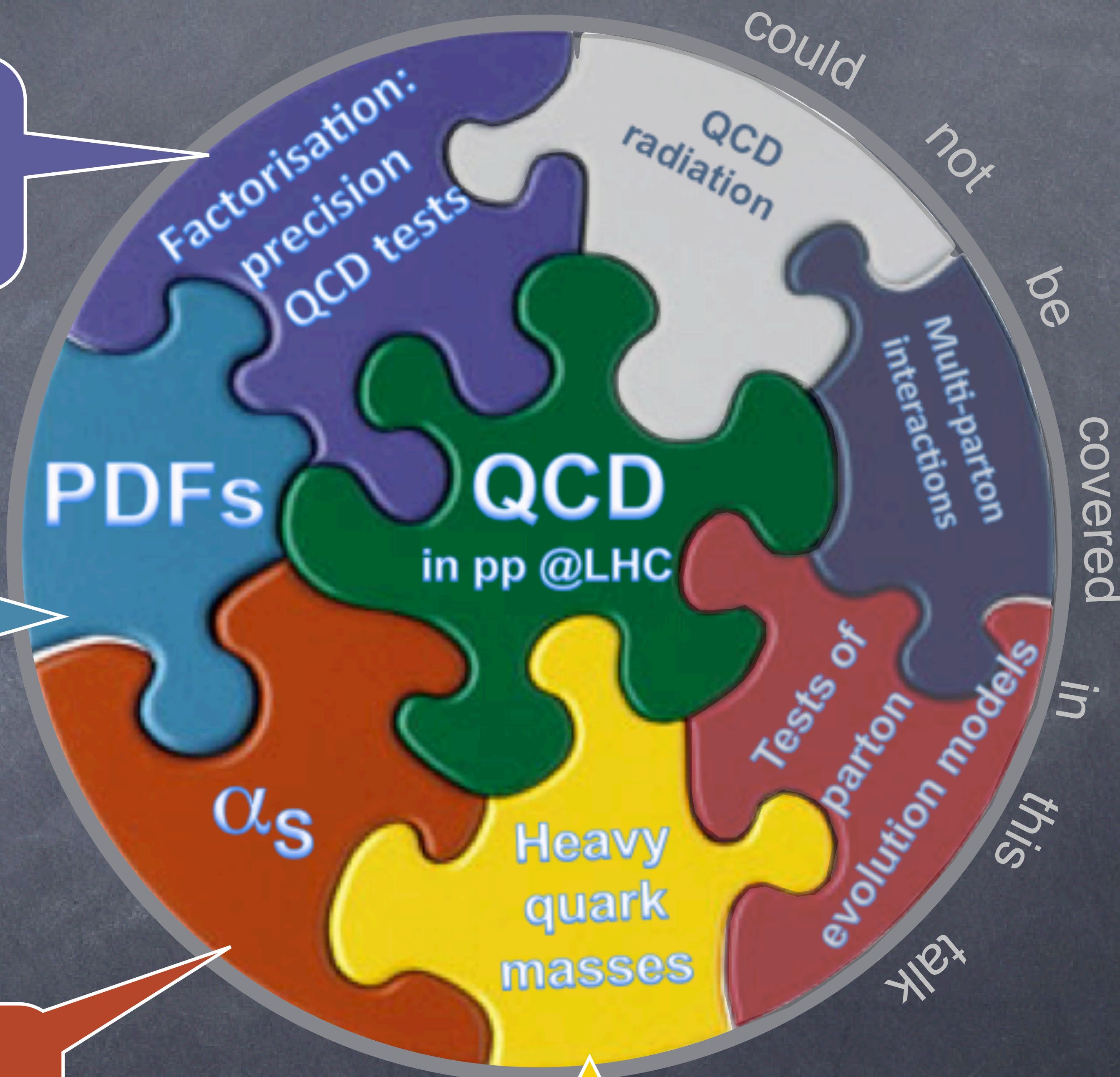

Determined using jet and top-pair production, measurement of running is one of the most important tests of SM

top-pair production:
unambiguously defined top-quark mass

1) LHC data testing QCD

(Multi) jet production in pp collisions:
- test QCD factorization through data/theory comparison

Directly sensitive to PDFs and α_S

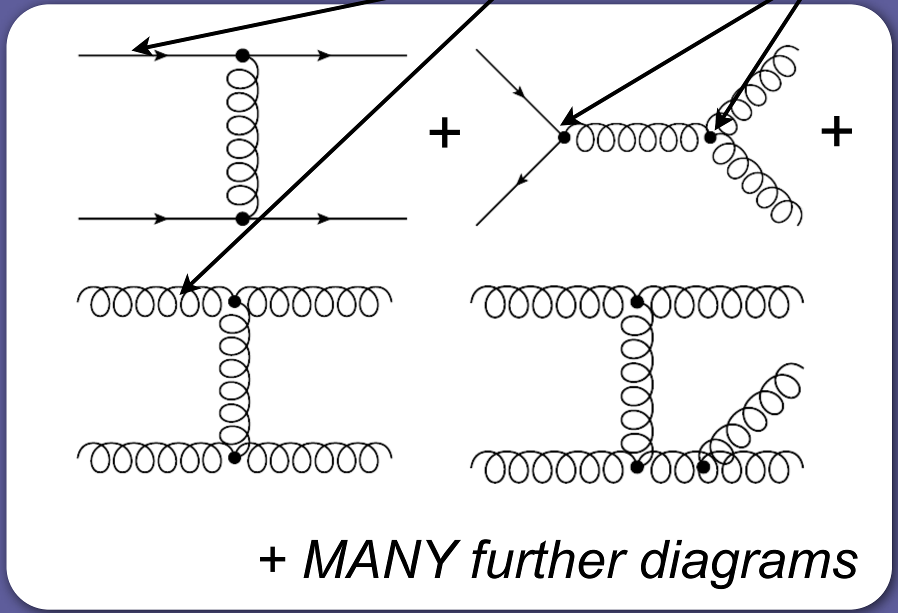

- standard candle to search for new phenomena

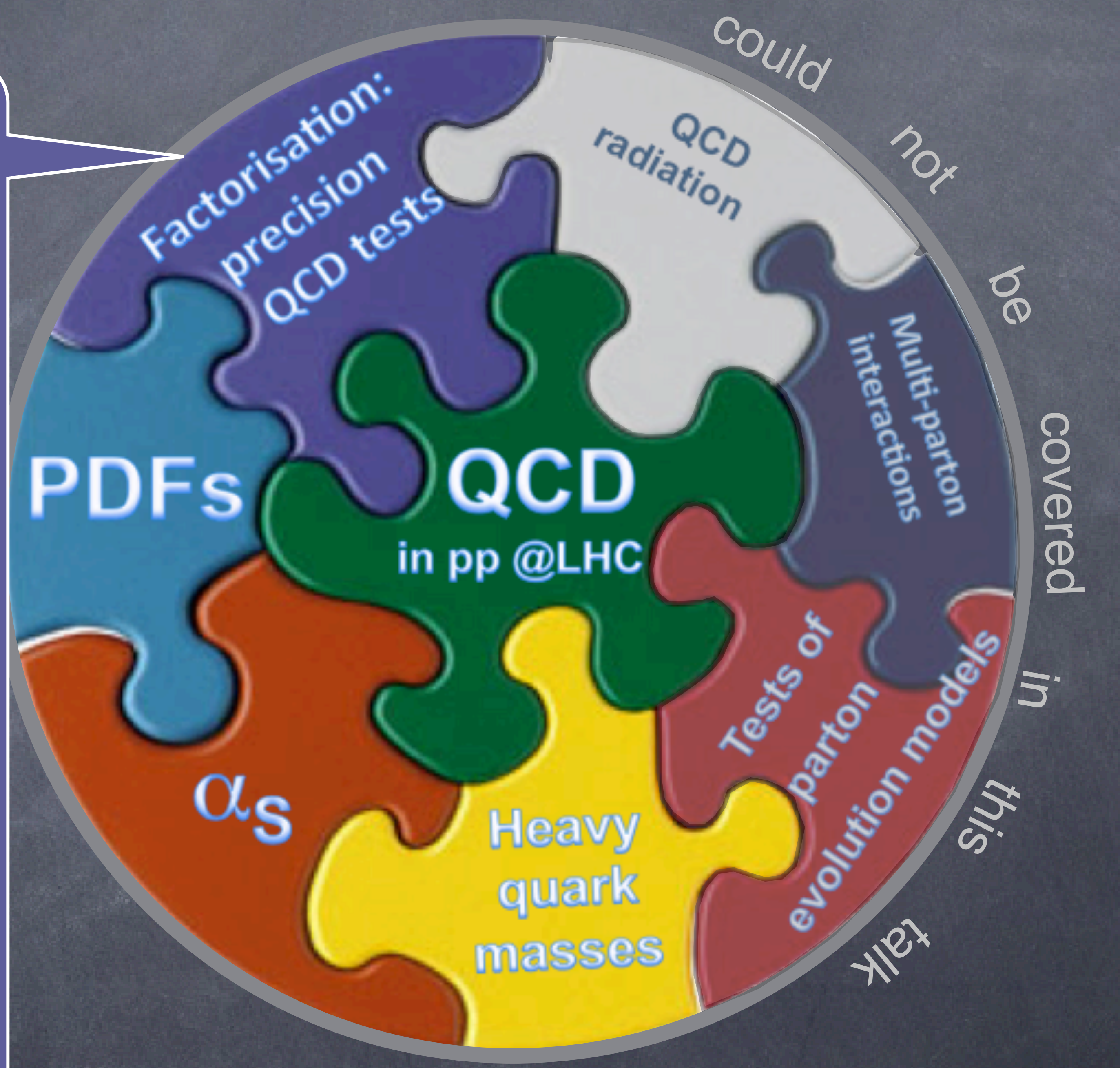

Inclusive jet production: precision test of factorization

Confront theory calculations with high precision measurements

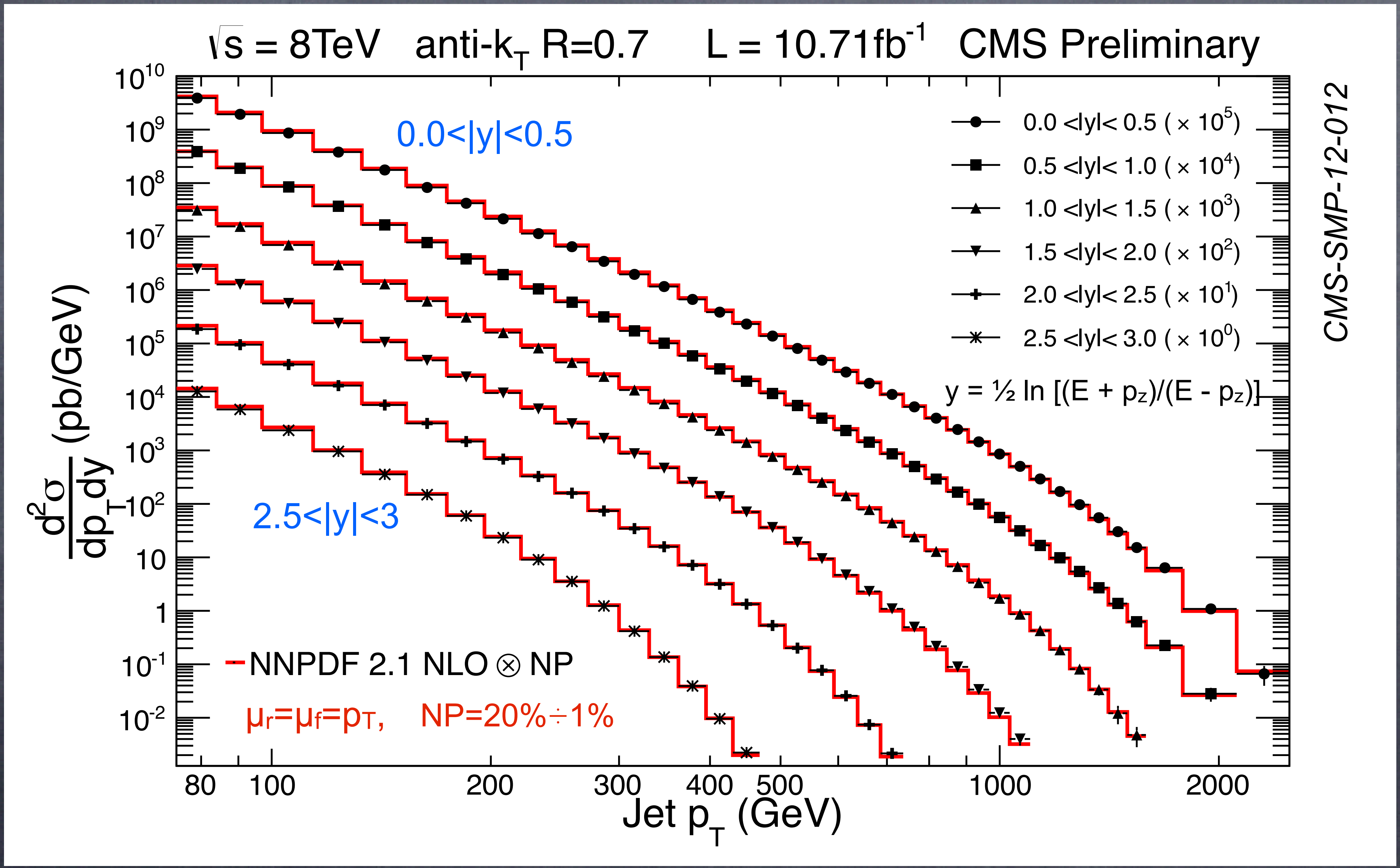

Transverse momenta range from 74 GeV to 2.5 TeV. Good description by **NLO QCD**

Inclusive jet production: precision of data vs theory

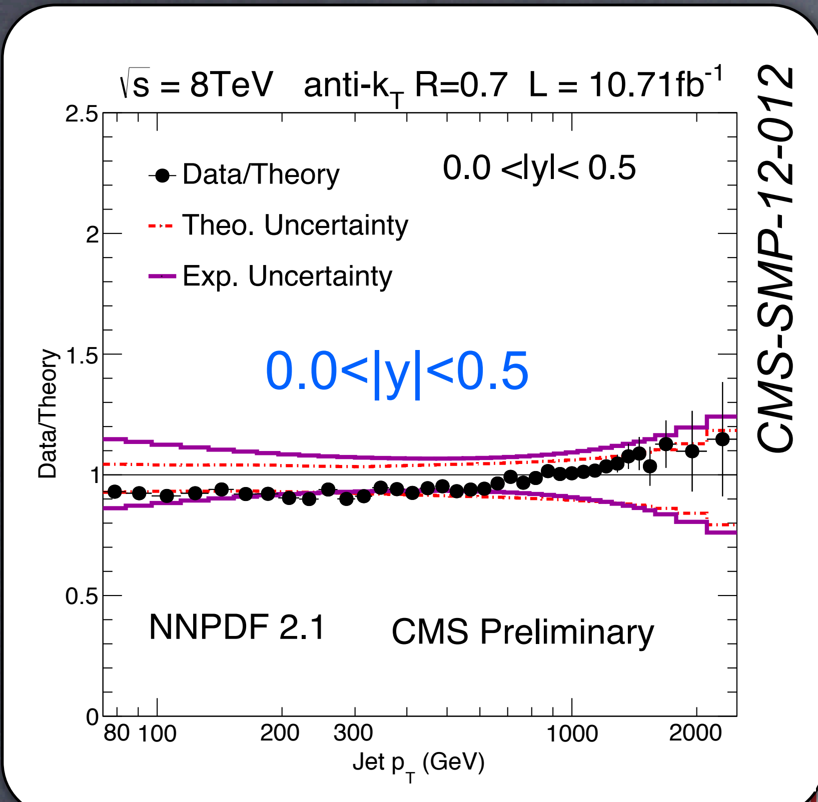

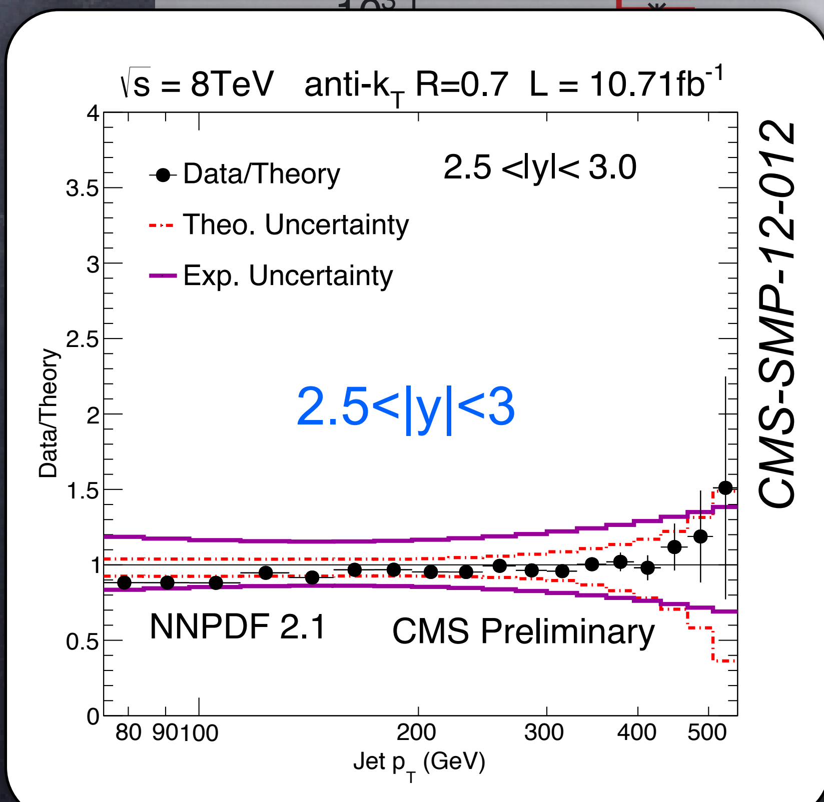

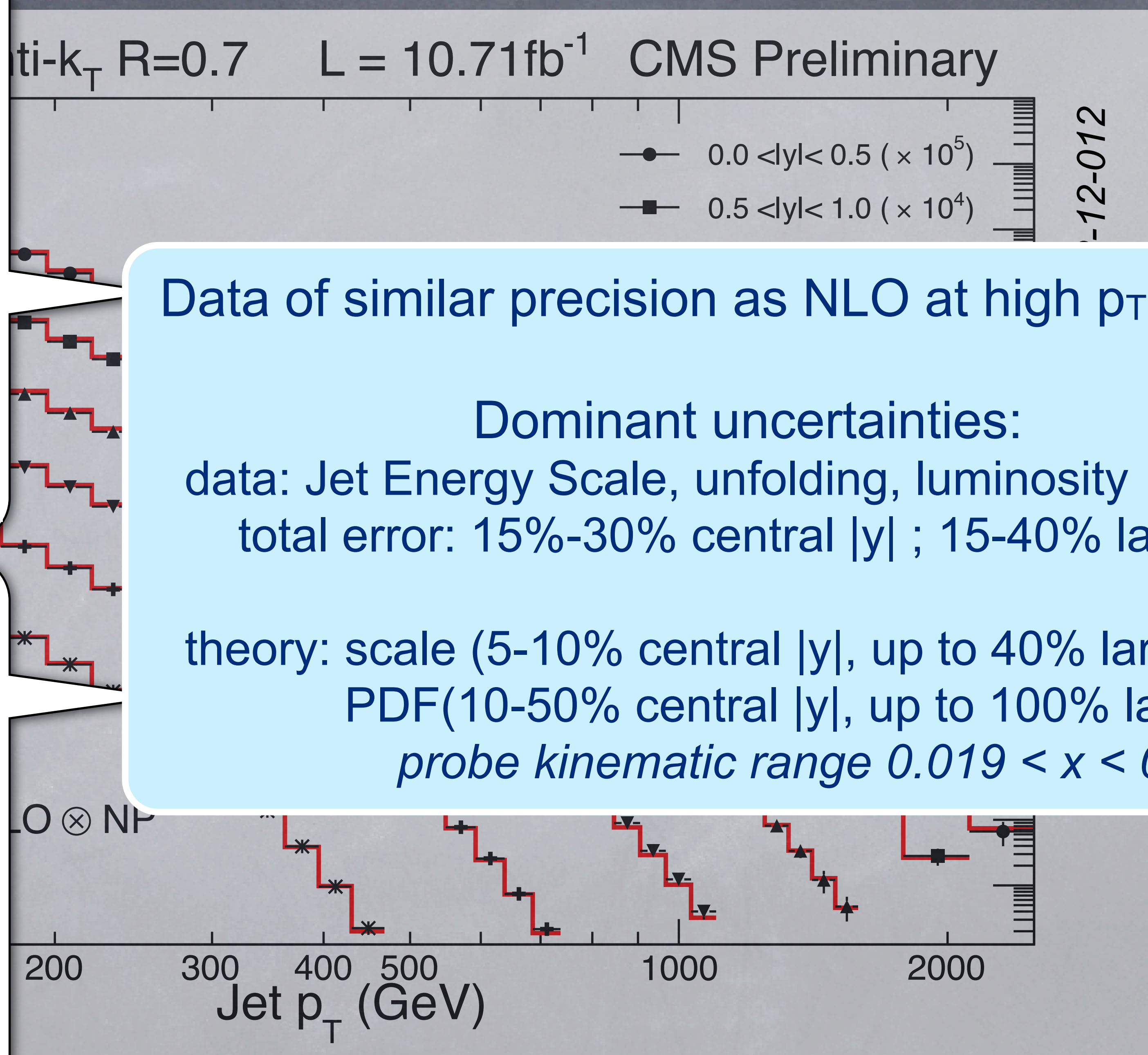

Data of similar precision as NLO at high p_T (high x)

Dominant uncertainties:

data: Jet Energy Scale, unfolding, luminosity

total error: 15%-30% central |y| ; 15-40% larger |y|

theory: scale (5-10% central |y|, up to 40% larger |y|

PDF(10-50% central |y|, up to 100% larger |y|)

probe kinematic range 0.019 < x < 0.625

Inclusive jet production: sensitivity to PDFs

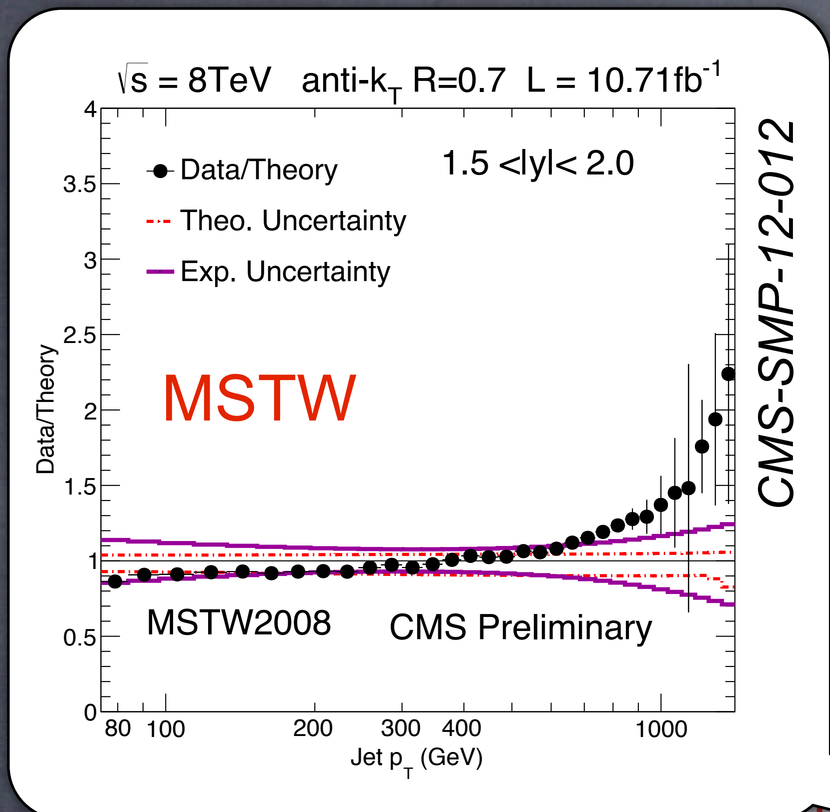

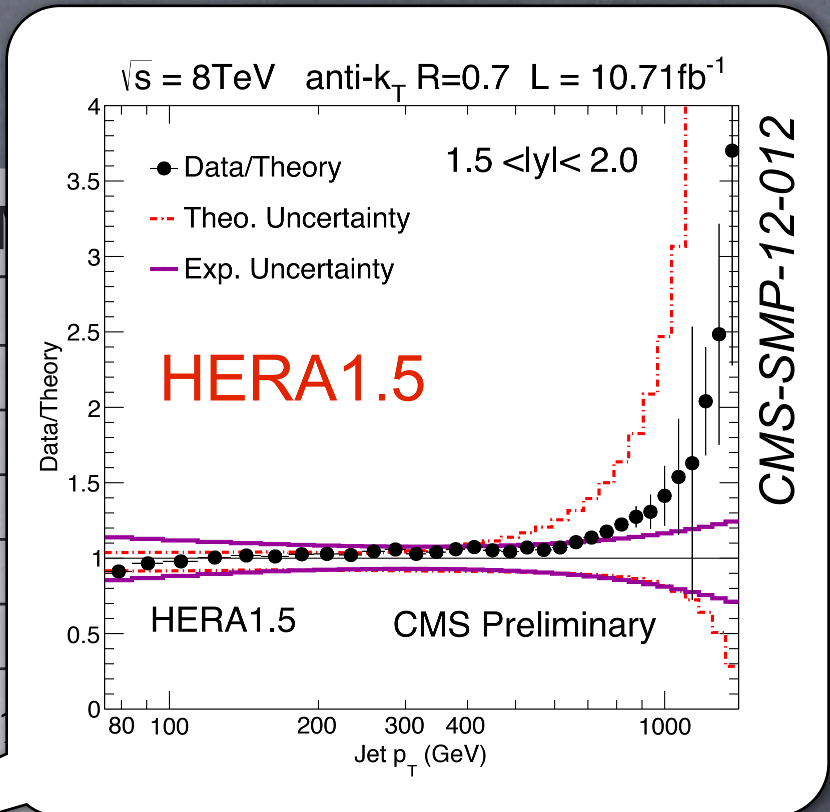

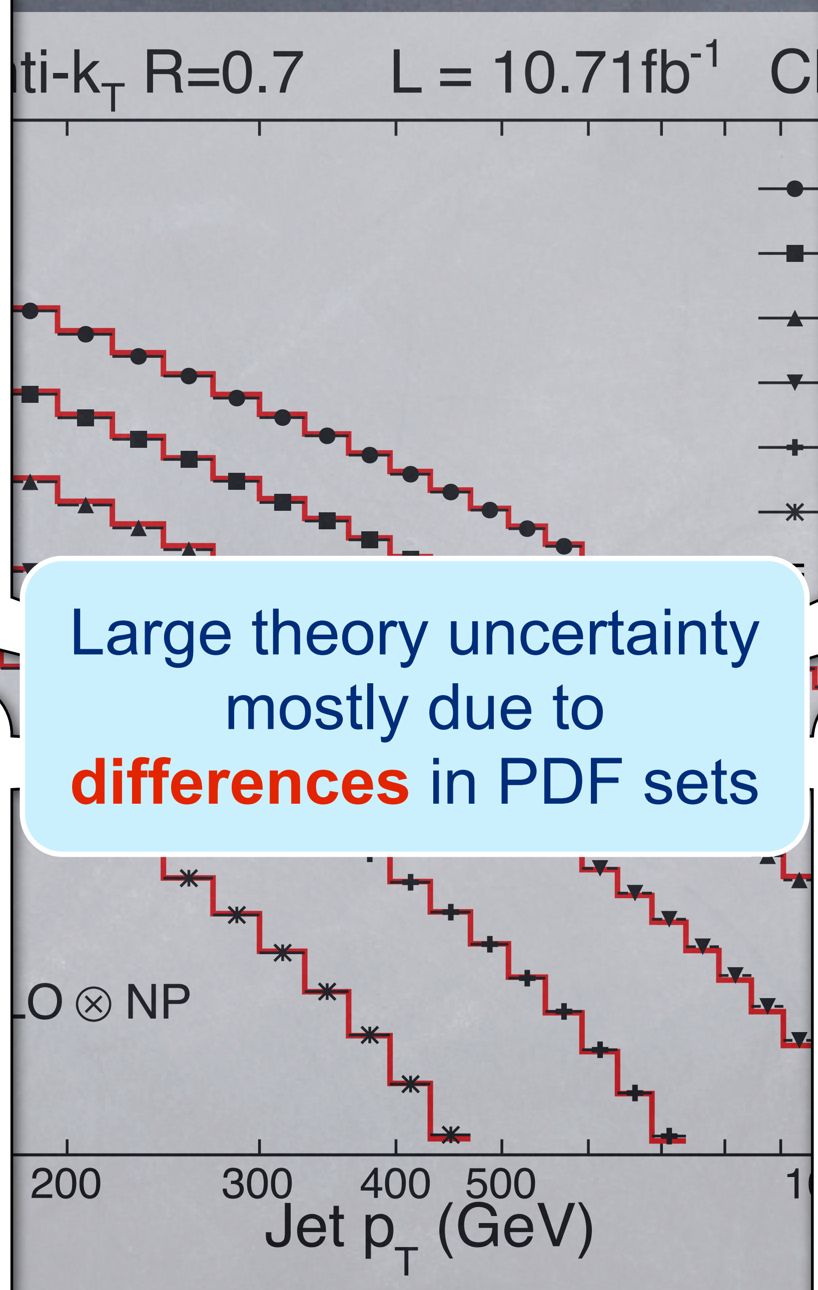

Large theory uncertainty mostly due to **differences** in PDF sets

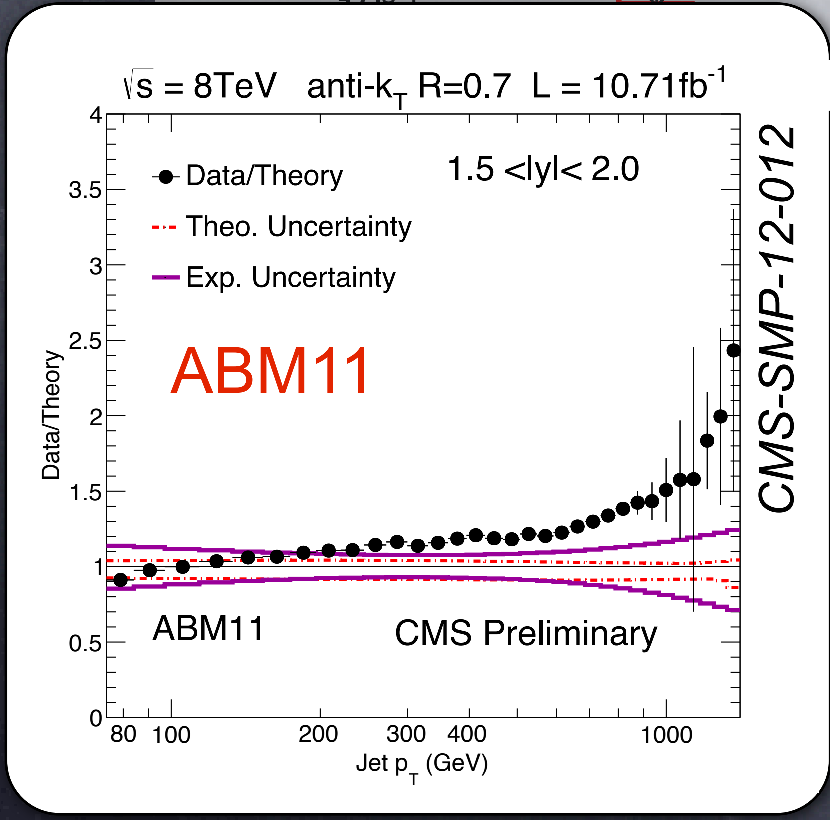

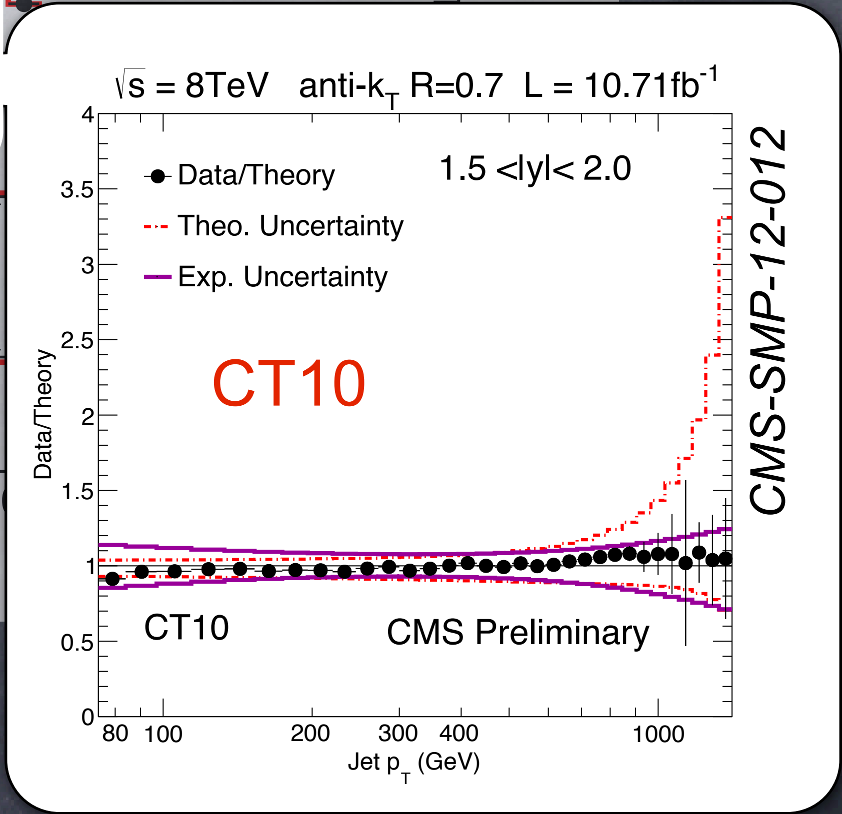

Ultimate QCD tests: di-jet production

Production of two jets used to study further particularities of QCD

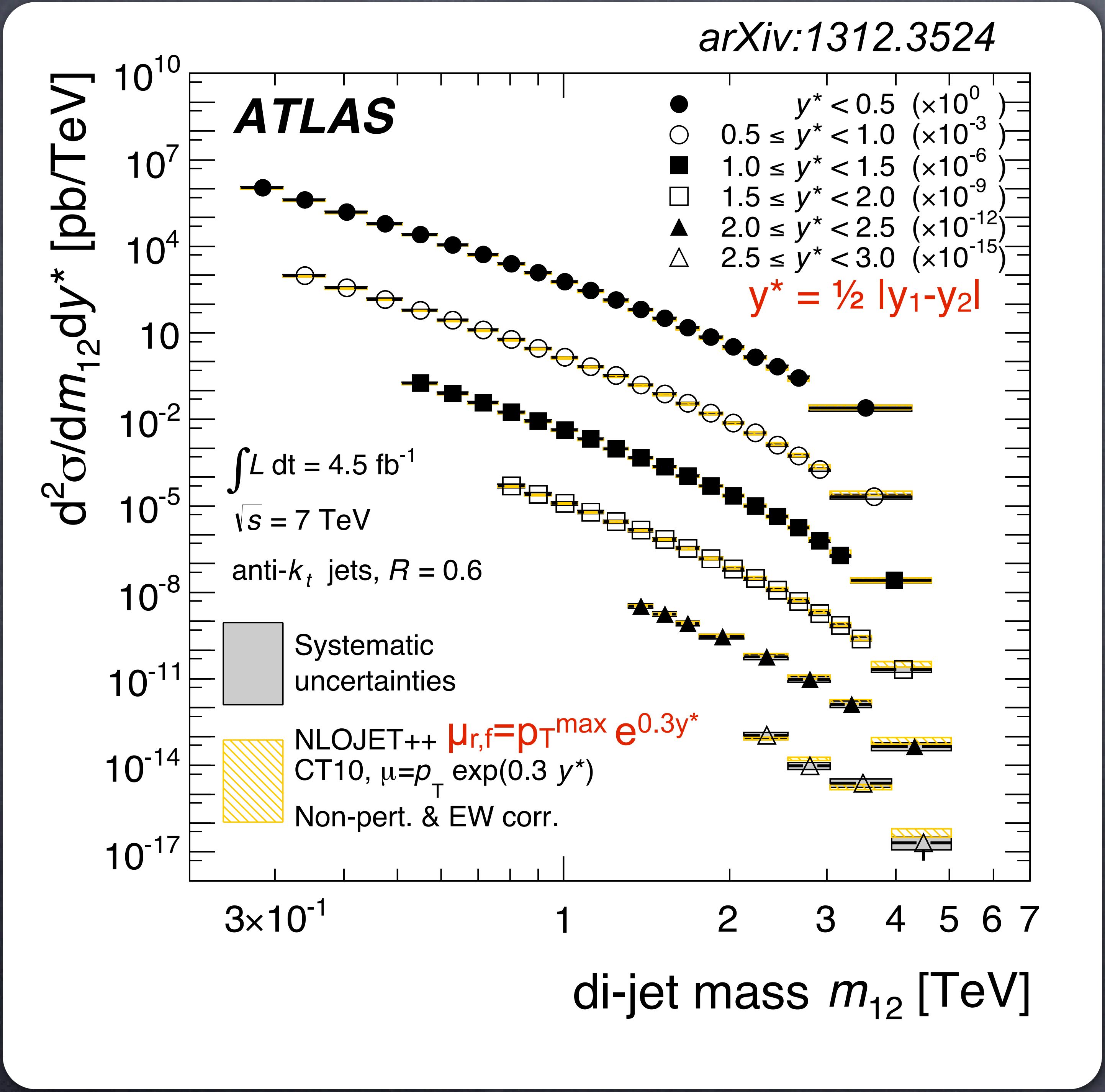

QCD performs well over few orders of magnitude

Compatibility of data and theory can be quantified

Estimate compatibility of data and theory (SM)

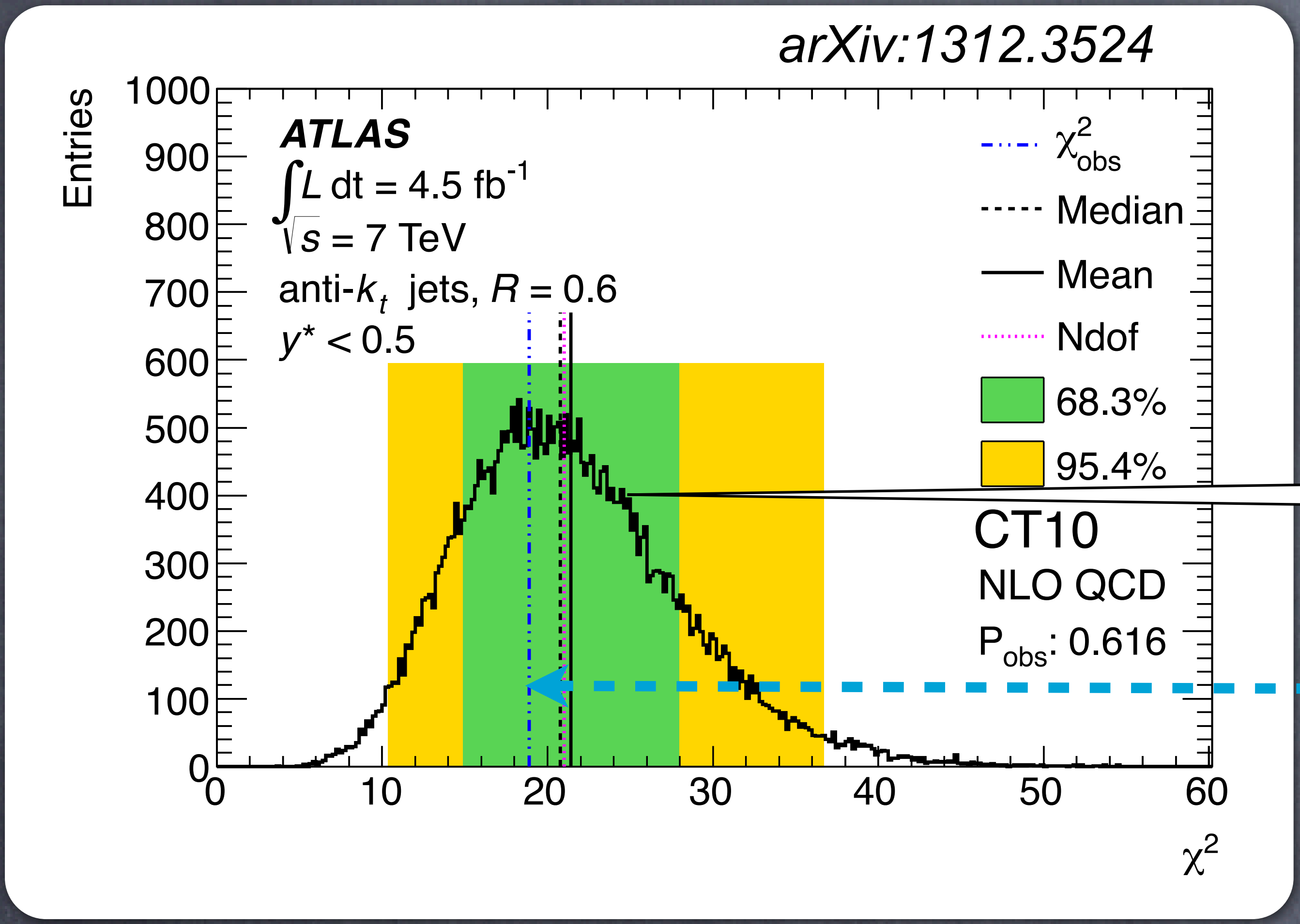

Frequentist method:

χ^2: theory compared to 'pseudo-data' generated using theory prediction, accounts for statistic and systematic correlations of measurements

χ_{obs}^2: theory compared to data

Compatibility measure:
observed probability P_{obs}
fraction of pseudo-data with $\chi^2 > \chi^2_{obs}$

(if P_{obs}<0.05 theory is considered as not describing the data)

Test particularities of the theory in each kinematic range

Compatibility of di-jet production and NLO QCD

Different input details of NLO QCD (PDFs, scales) are investigated

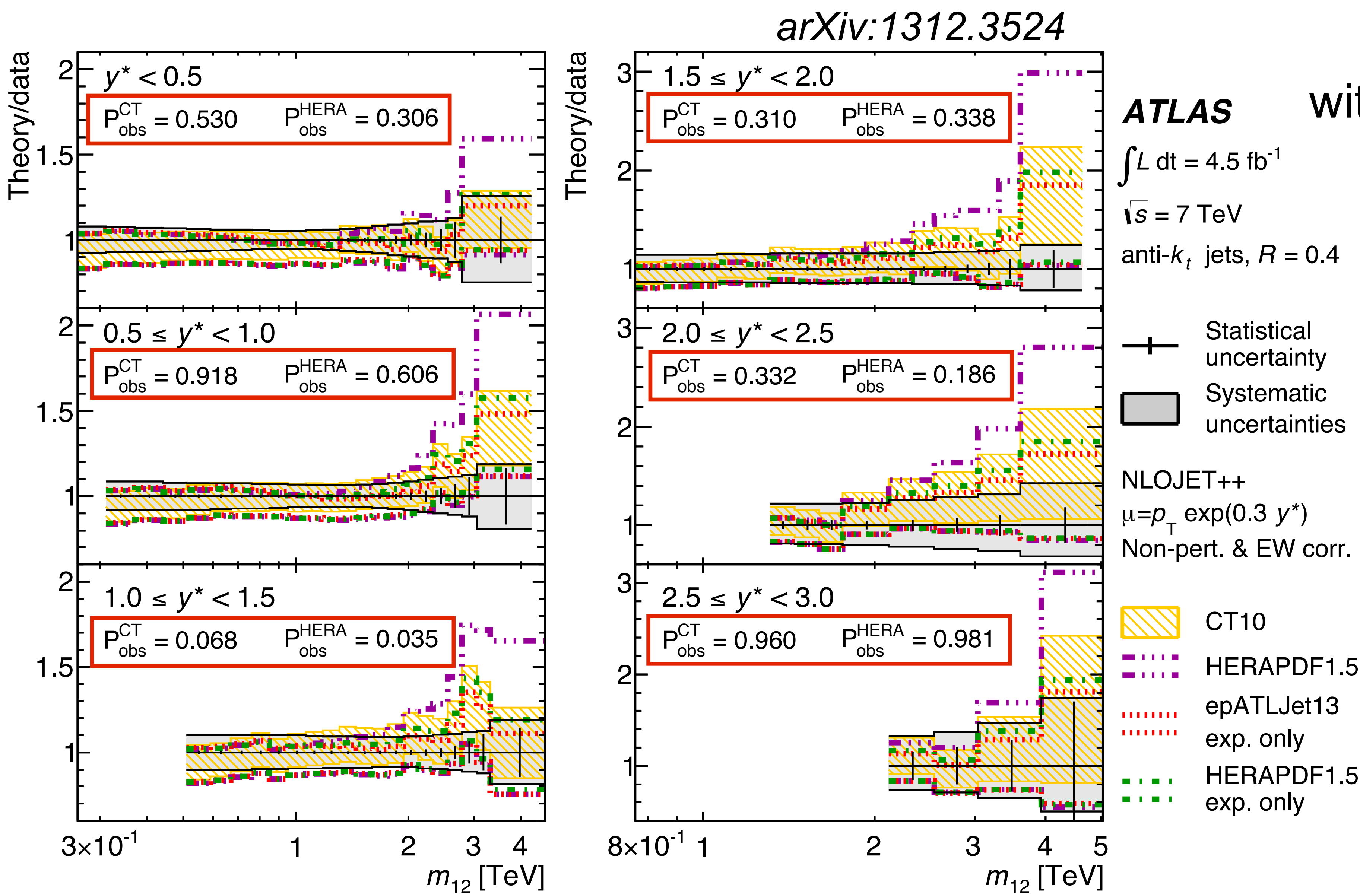

Data vs NLO QCD with different PDF(α_S)

dominant experimental uncertainty due to jet energy calibration

dominant theory uncertainty due to PDFs

experimental precision higher than theory accuracy

Data are used to estimate possible contributions from the models beyond SM

Search for new physics in di-jet production at the LHC

Examples of new phenomena appearing in jet final states:

- Quark compositeness, excited quarks,...
- New interactions from massive particles exchange

New physics at a scale $\Lambda > m_{12}$ is effectively modeled as a contact interaction (CI) characterized by a 4-fermion coupling:

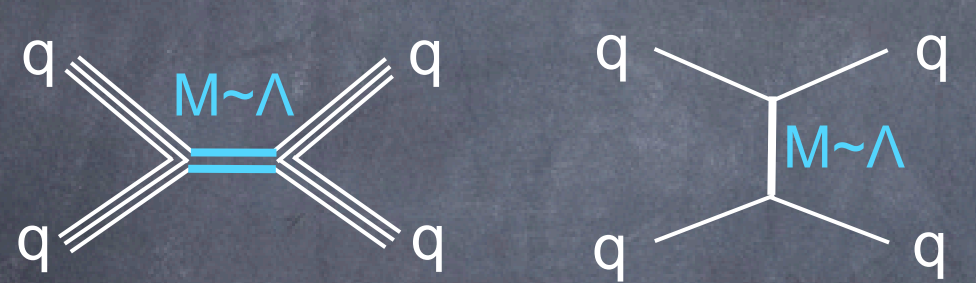

new phenomena should alter m_{12} distribution from SM expectation

Investigate compatibility of data and theory (SM + CI) using di-jet cross section measurements.

Apply frequentist method

signal

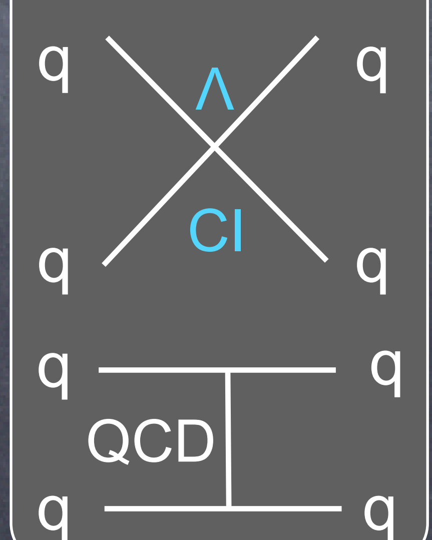

background

Compatibility of data and theory (SM + CI)

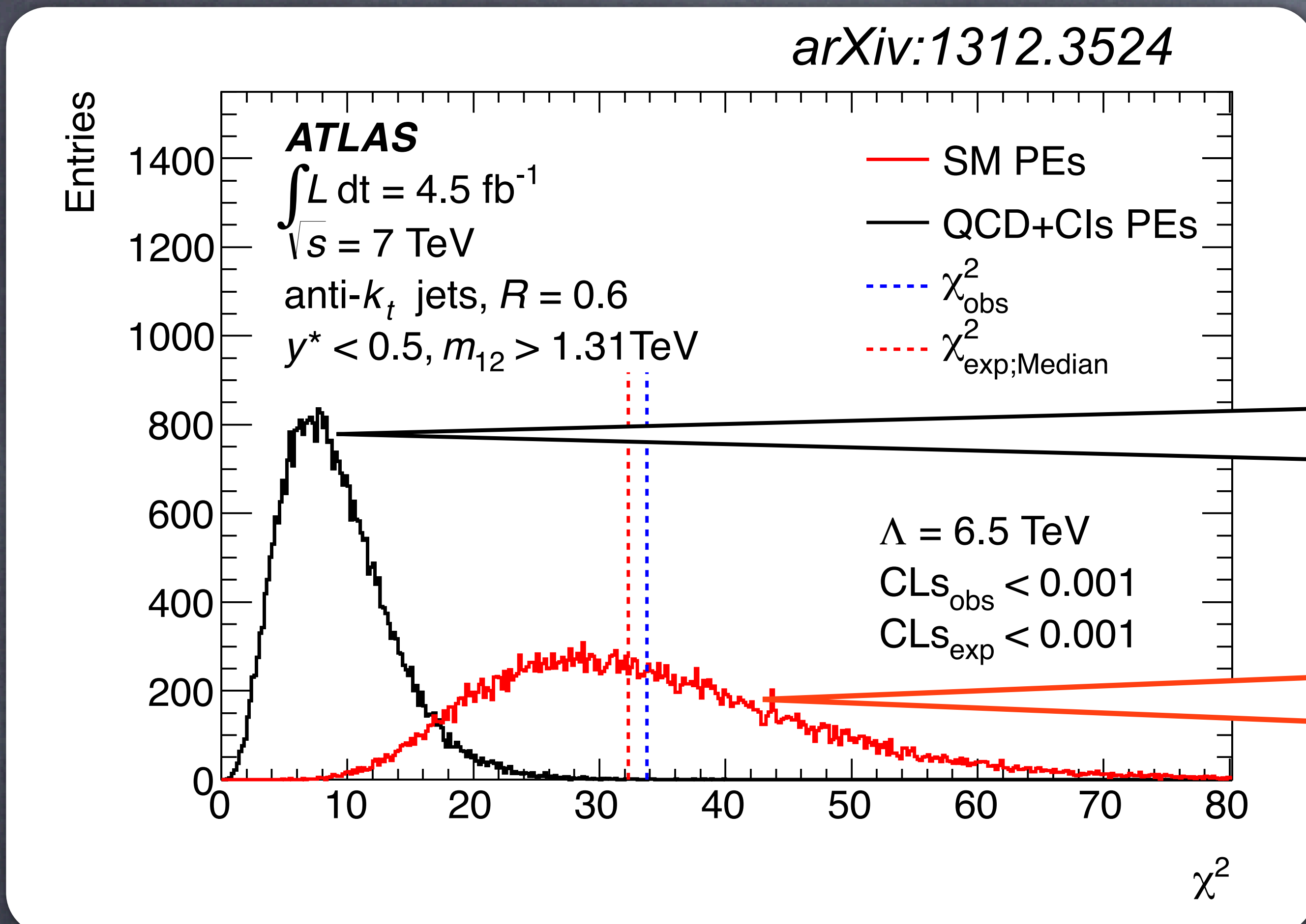

1) χ^2 (background): 'pseudo -data' generated using SM prediction confronted with theory (SM+CI). Median - expected χ^2

2) χ^2 (signal+background): 'pseudo-data' using SM+CI prediction confronted with theory (SM+CI)

Compatibility measures: observed probabilities
p_{s+b} : (QCD+ CI),
p_b : compatibility with QCD
$p_{s+b}/(1-p_b)<0.05$ theory excluded

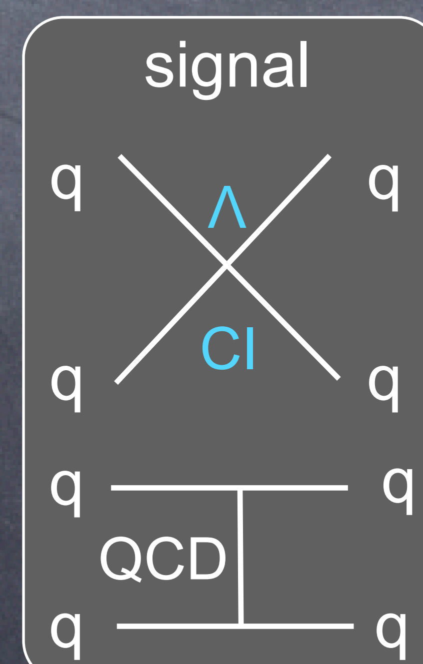

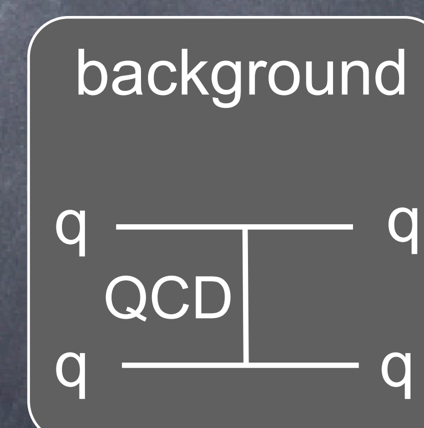

Search for CI in di-jet production at the LHC

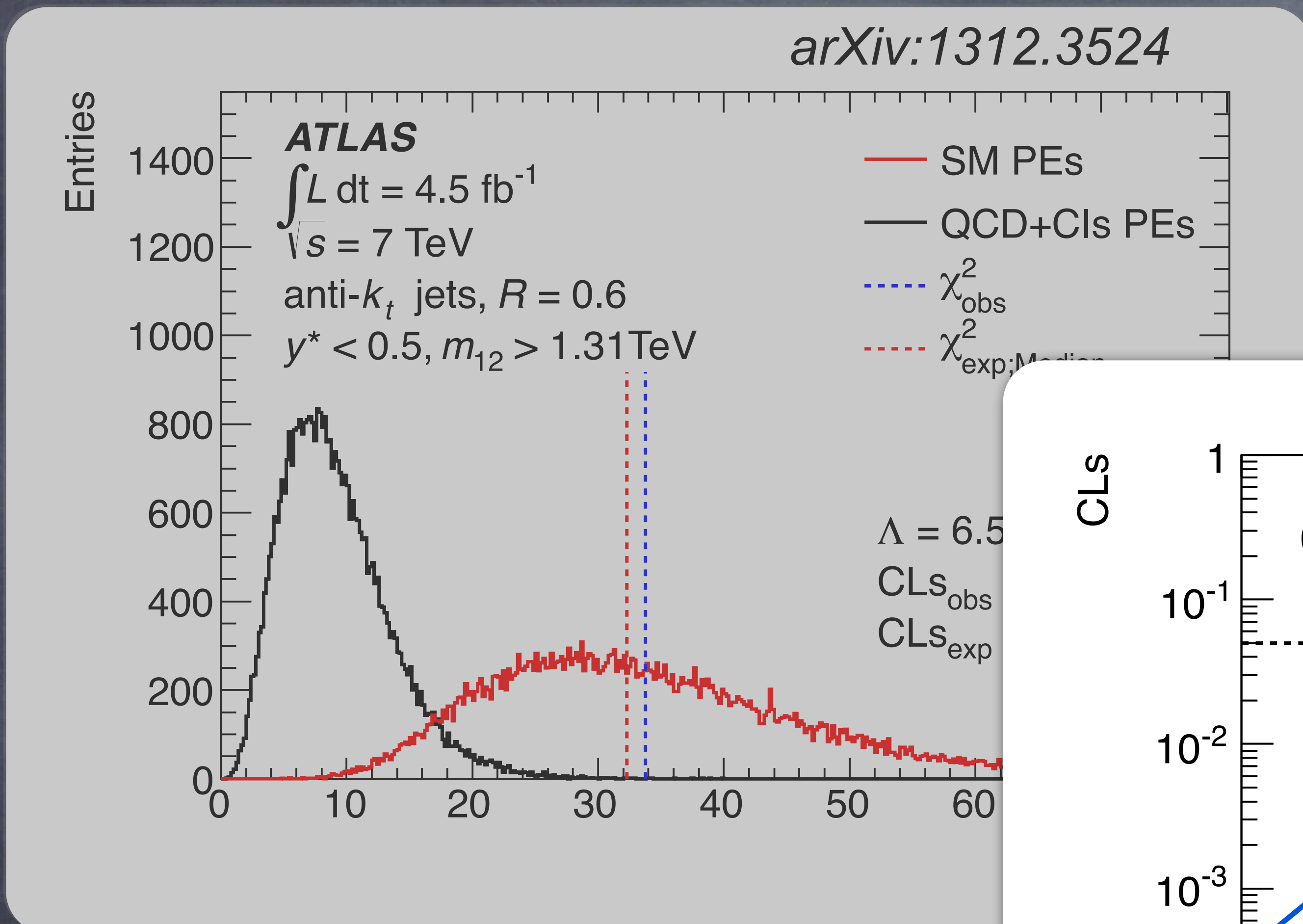

Di-jet cross section measurements
(m_{12} >1.31 TeV, y*< 0.5)
used to set limits on QCD+CI model
(NLO QCD +CI via CIJET)

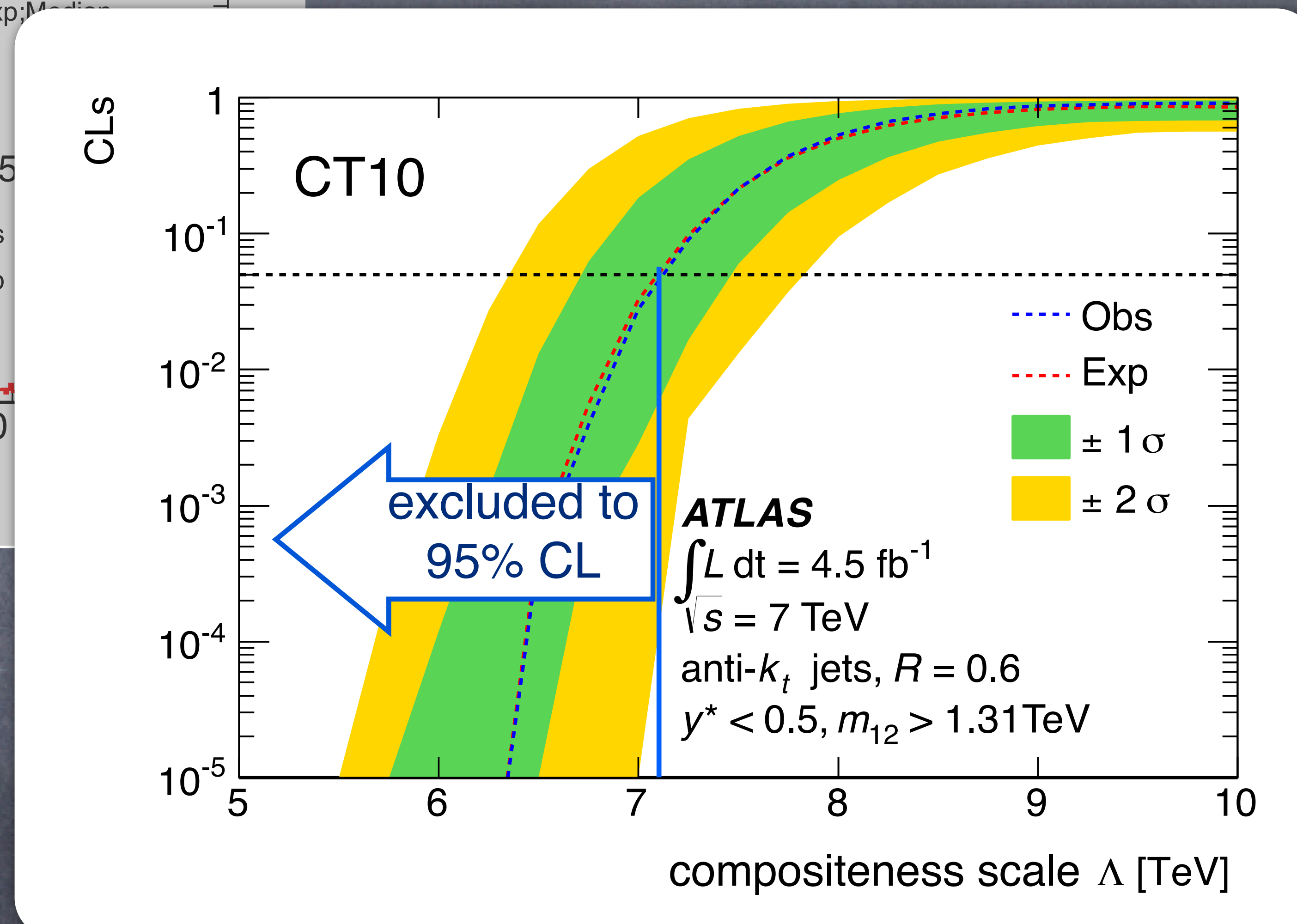

Compatibility measures:
p_{s+b} : (QCD+ CI),
p_b : compatibility with QCD
$p_{s+b}/(1-p_b)<0.05$ theory excluded

Obtained limits Λ < 6.6 -7.3 TeV depends on used PDFs in QCD model

Searches for new phenomena with di-jets

Di-jet angular distribution wrt beam direction sensitive to underlying parton process

CI models: strong peak in the angular distributions in $\chi_{dijet} = e^{|y_1 - y_2|}$, uniform for QCD

several CI models tested

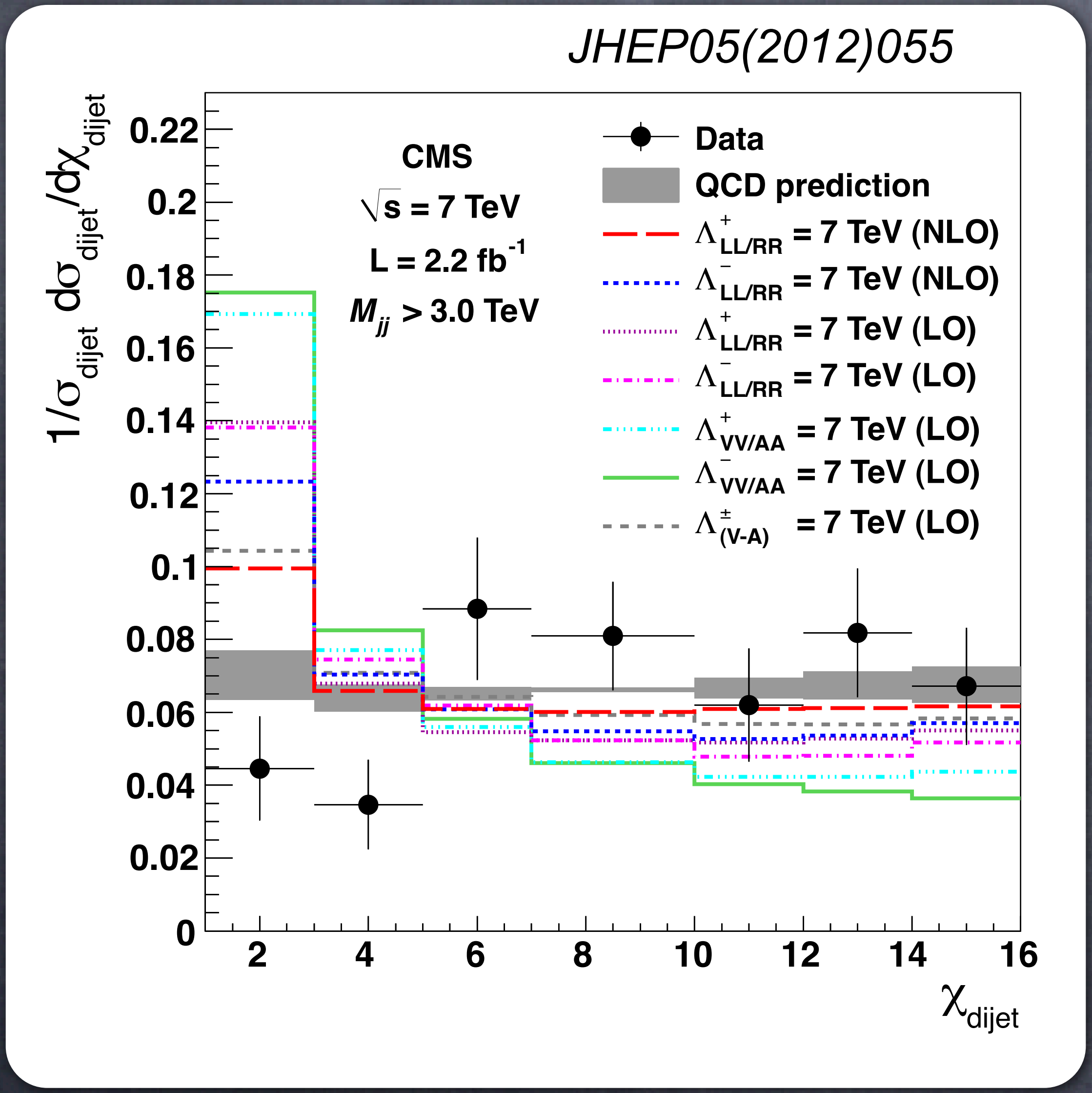

signal: NLO (LO) CI + NLO QCD
background: NLO QCD

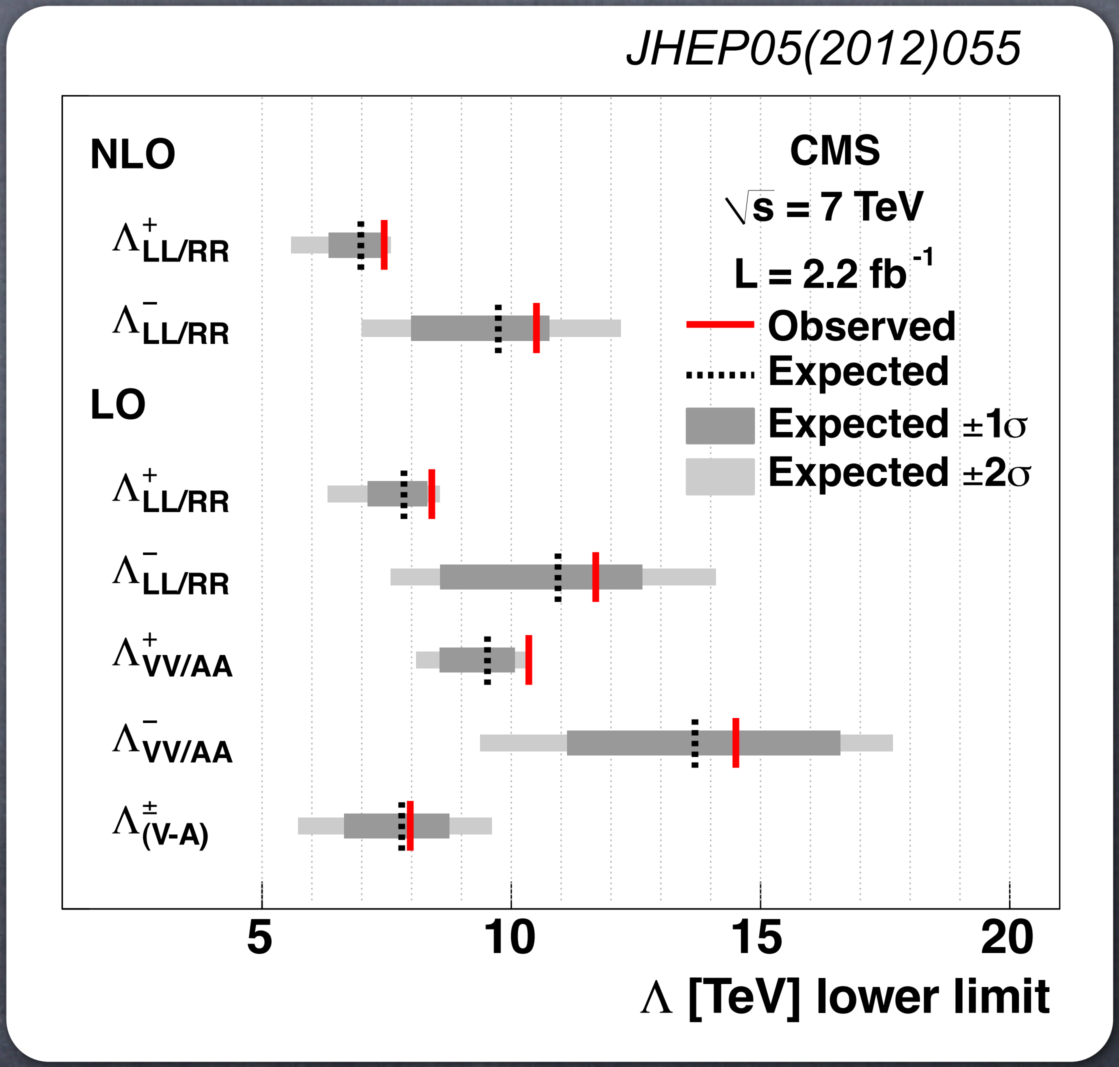

Lower limits for CI scale 7.5 - 14.5 TeV

New phenomena with jet-containing final states

new phenomena can also appear as resonances in di-jet mass spectrum

CMS-PAS-EXO-12-059

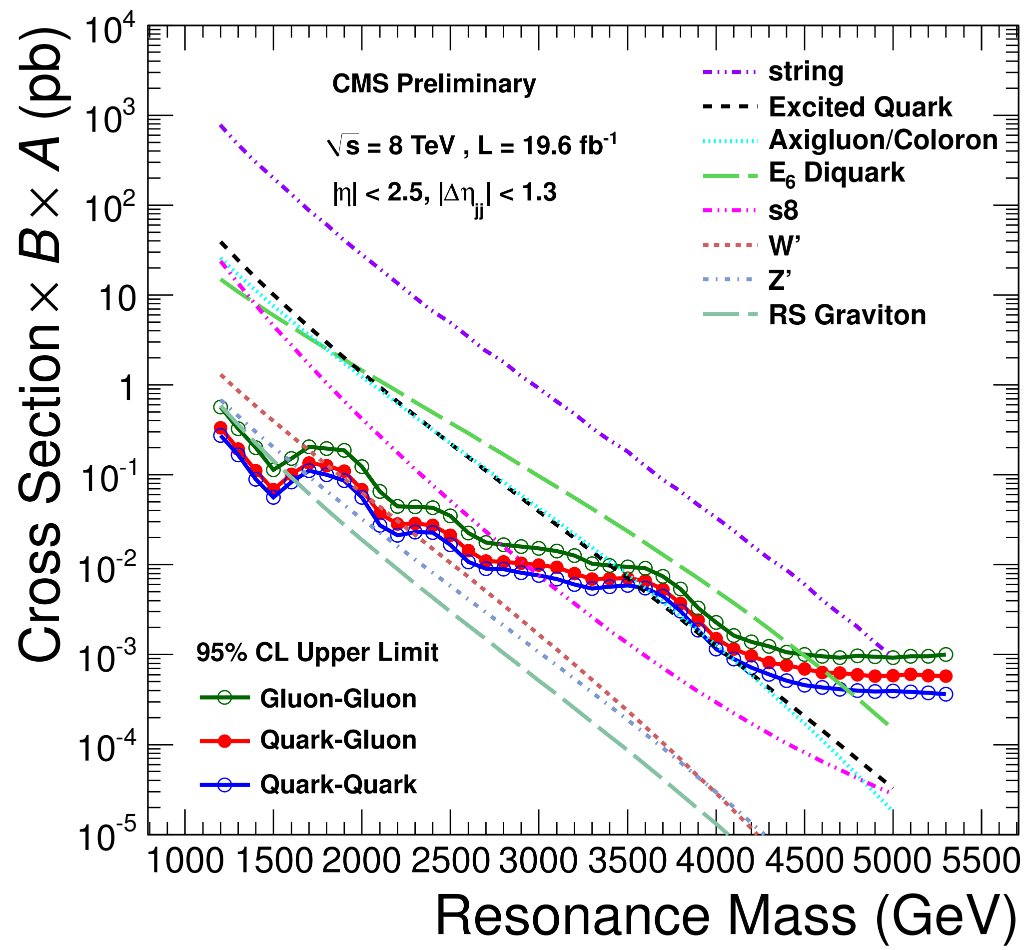

large angular and mass range is explored limits set on a variety of hypotheses

search for quantum black holes in lepton+ jet final states

arXiv:1311.2006

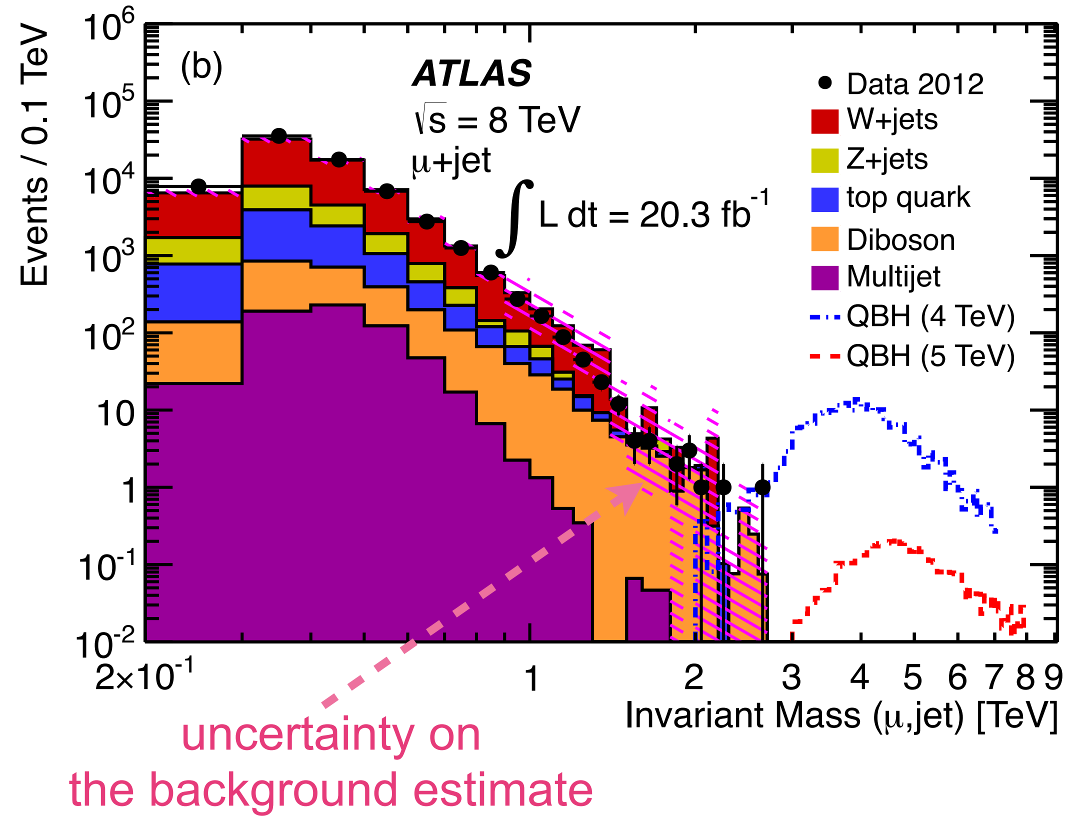

systematic uncertainties dominated by extrapolation of the background to high-mass range, PDF, choice of MC.

Limit M_{th} (QBH) > 5.3 TeV

Searches at high mass are often limited by QCD precision

2) LHC data improving QCD precision

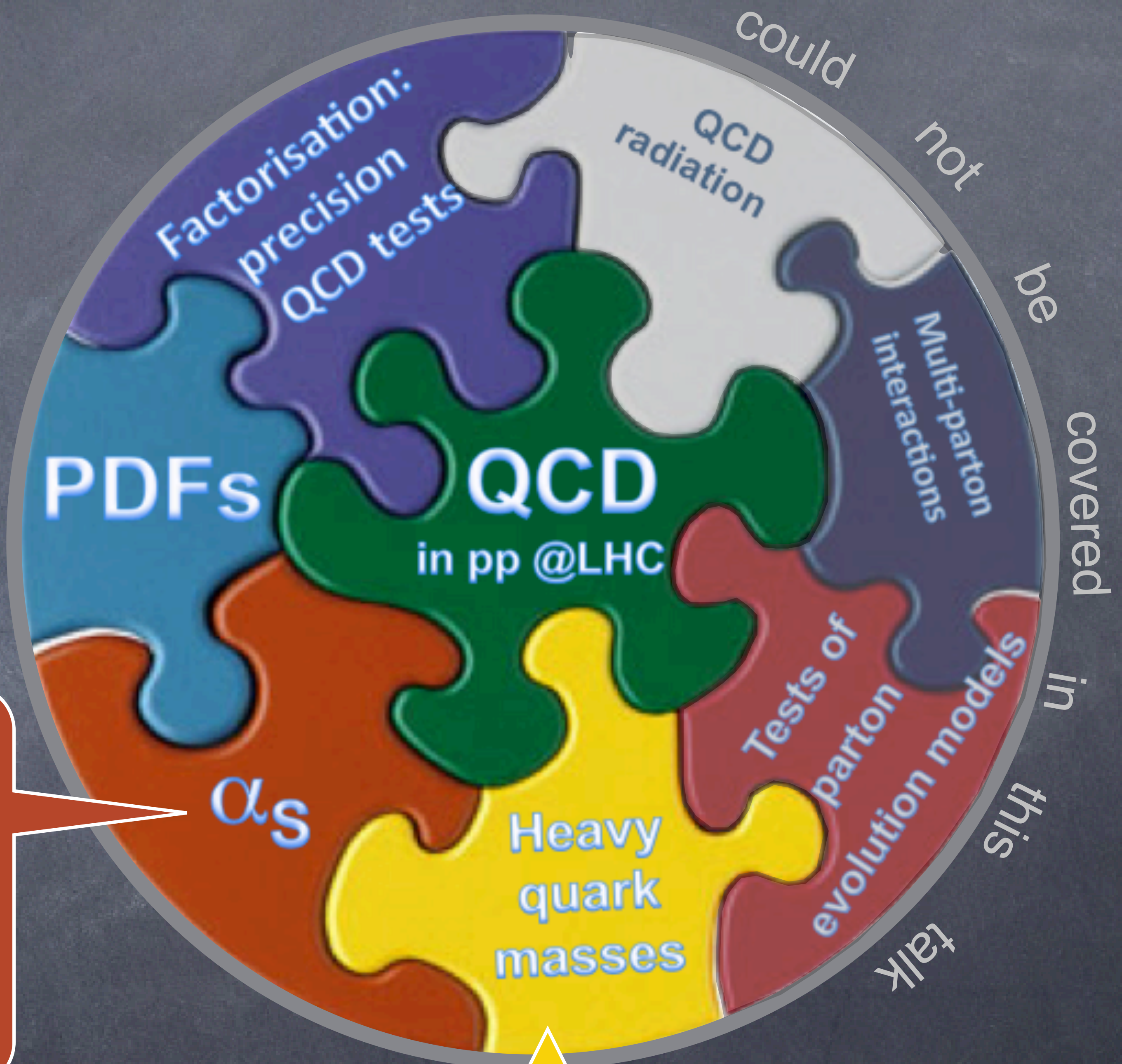

Fundamental QCD parameter

Determined using jet and top-pair production at the LHC

top-pair production:
unambiguously defined top-quark mass

Determination of strong coupling α_s

Non-Abelian nature of QCD ⇒ RGE predict asymptotic freedom
(strong force becomes weaker at short distances or large momentum transfer)
'Strength' α_s (Q) is not predicted, has to be extracted from experiment.

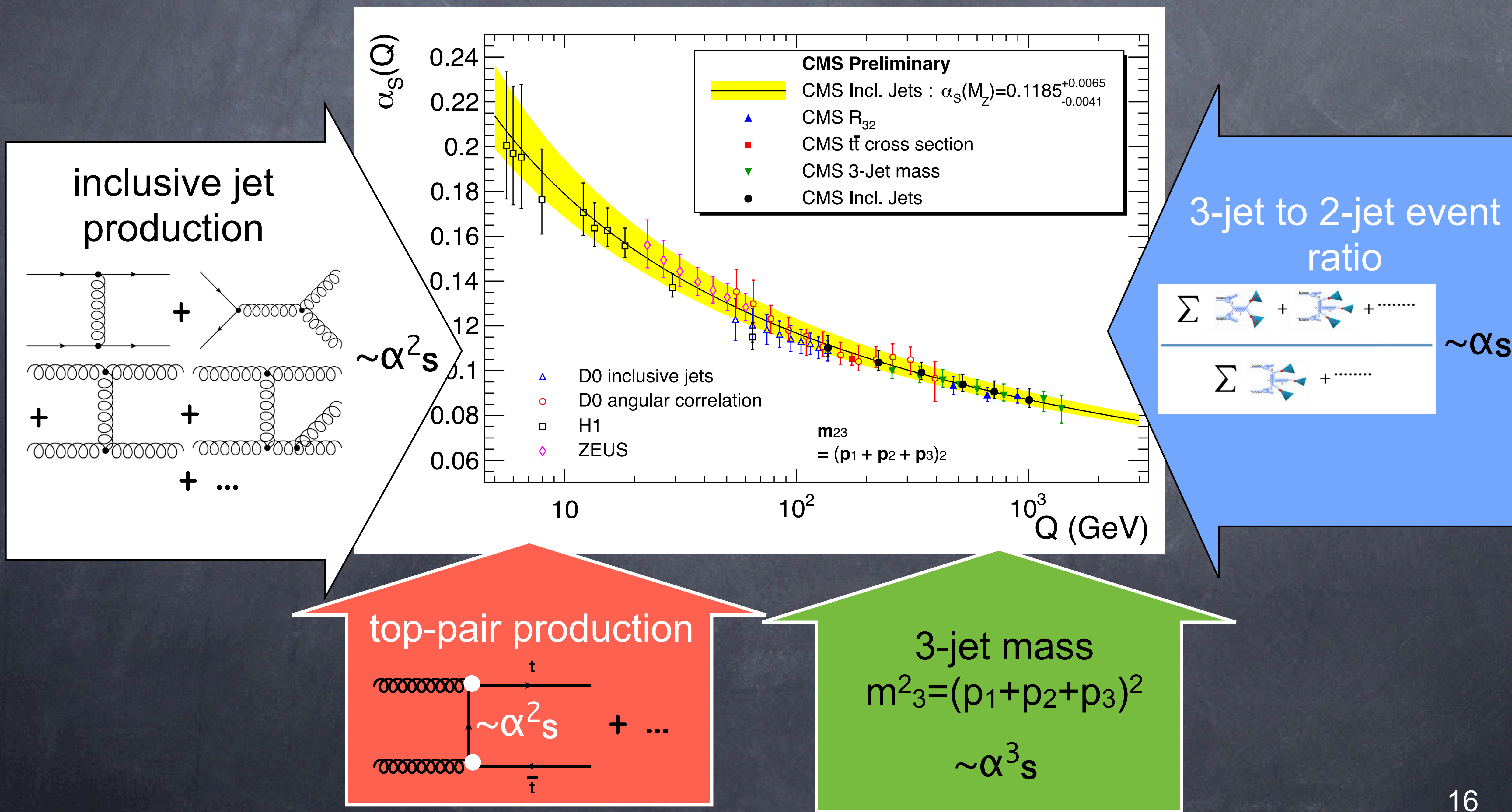

Determination of strong coupling α_S : inclusive jets

Confront measurement to NLO QCD ⊗ PDFs (α_S) in each kinematic bin

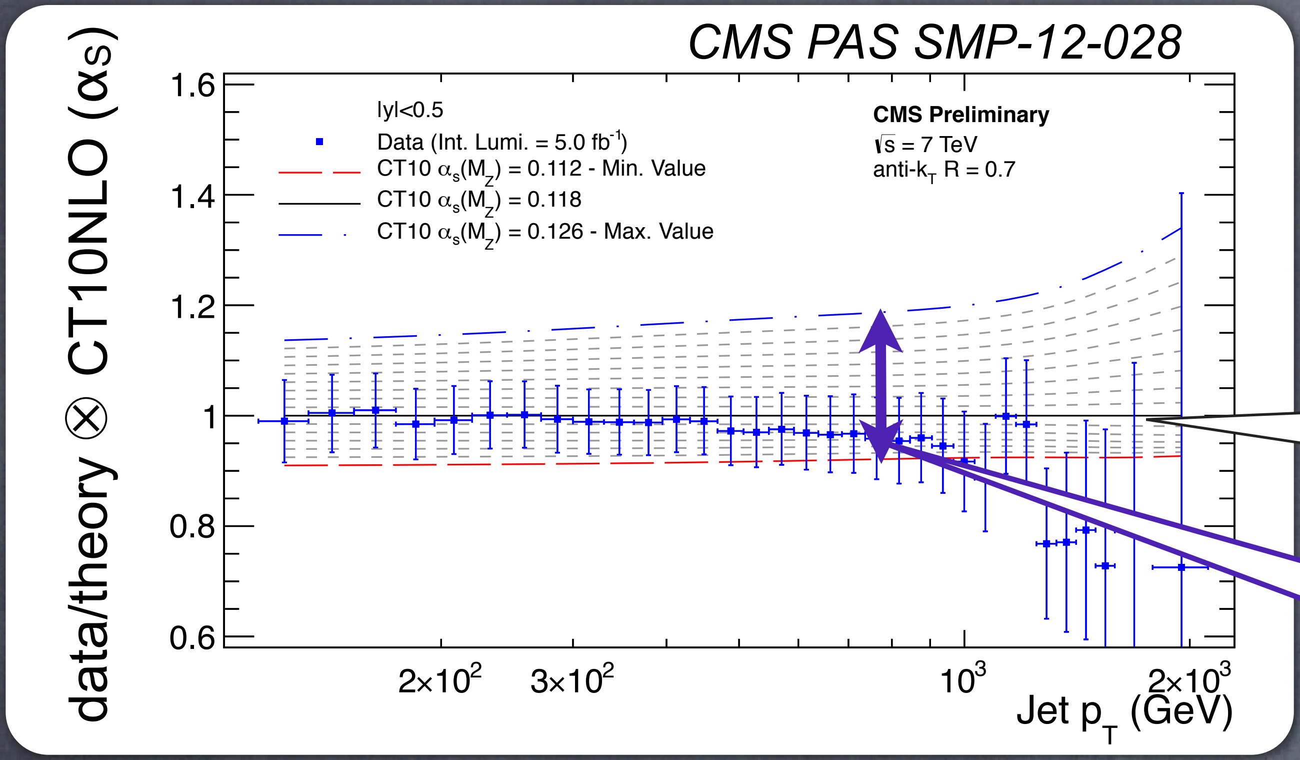

data: inclusive jet cross section

$\sqrt{s}$=7 TeV (5 fb^{-1}) *Phys. Rev. D 87 (2012) 12002*

corrected for electroweak effects

(Dittmeier et at JHEP 2011, 095 (2012))

prediction using central value of α_S for CT10NLO

α_S variation in CT10NLO

Determine α_S from a minimum of χ^2 of data vs theory for each variation

Determination of strong coupling α_S : inclusive jets

Confront measurement to NLO QCD ⊗ PDFs (α_S) in each kinematic bin

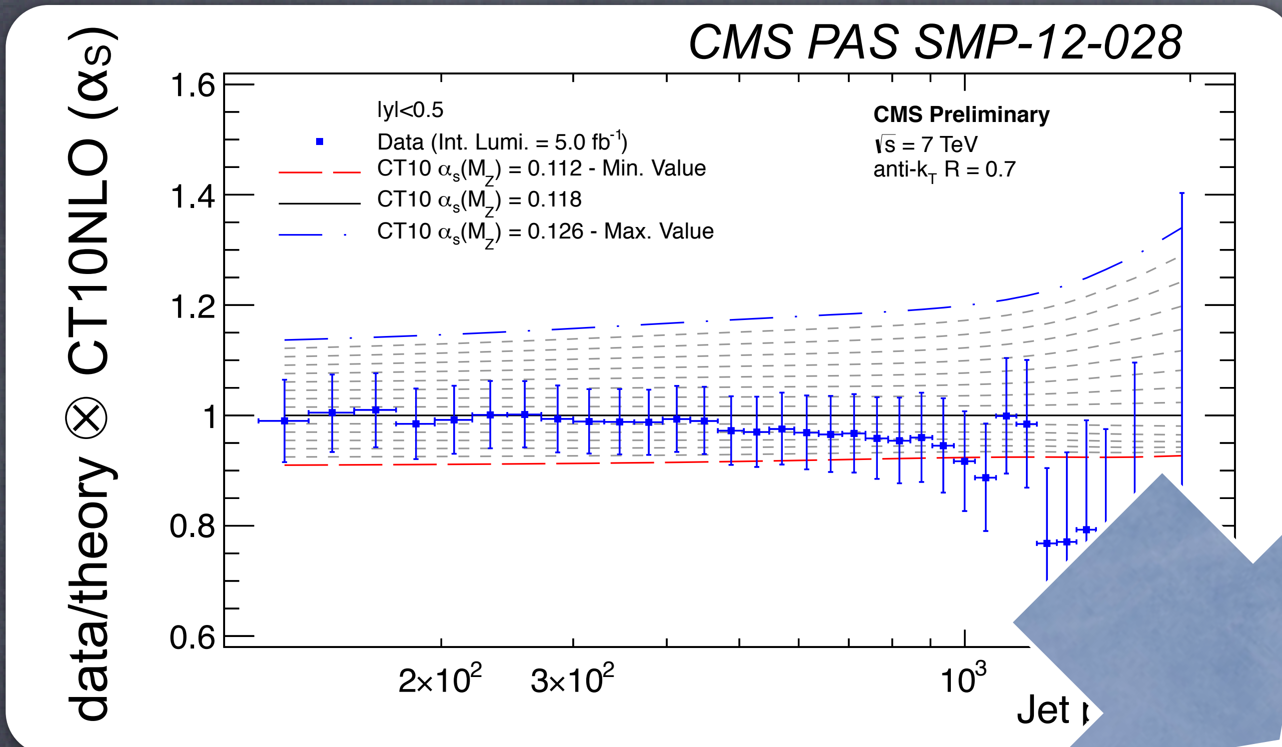

data: inclusive jet cross section

$\sqrt{s}$=7 TeV (5 fb^{-1}) *Phys. Rev. D 87 (2012) 12002*

corrected for electroweak effects

(Dittmeier et at JHEP 2011, 095 (2012))

Similar results obtained with different PDFs

Using CT10NLO, full y range:

$$\alpha_S(m_Z) = 0.1185 \pm 0.0019_{exp} \pm 0.0028_{PDF} \pm 0.0004_{NP} {}^{+0.0055}_{-0.0022}\ \text{(scale)}$$

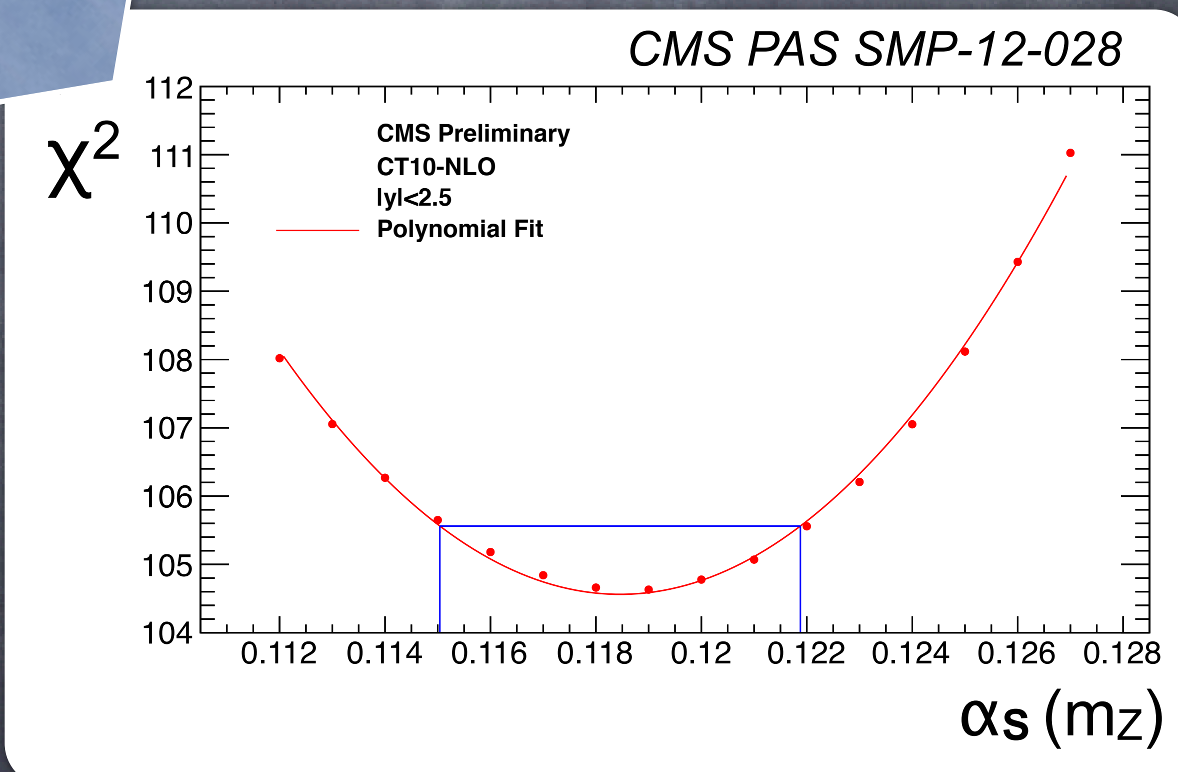

Analysis performed in 6 p_T bins

⇛ running of $\alpha_S = \alpha_S(Q^2)$

Determination of strong coupling α_S : R_{32}

Ratio of 3/2 inclusive jet cross sections

$$R_{32} = \frac{\sigma_3}{\sigma_2} = \frac{\sigma_{pp\to n\ jets+X;\, n\geq 3}}{\sigma_{pp\to n\ jets+X;\, n\geq 2}} =$$

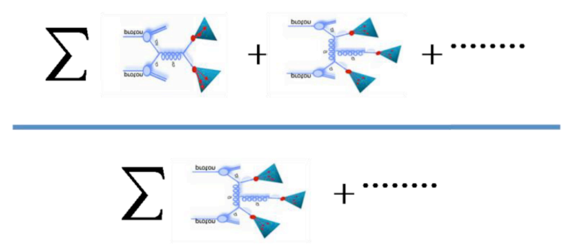

$\sim \alpha_S$

Advantage: cancellation or reduction of uncertainties: experiment and theory (partial cancellation of NP effects, PDFs, scale choice, EWK effects)

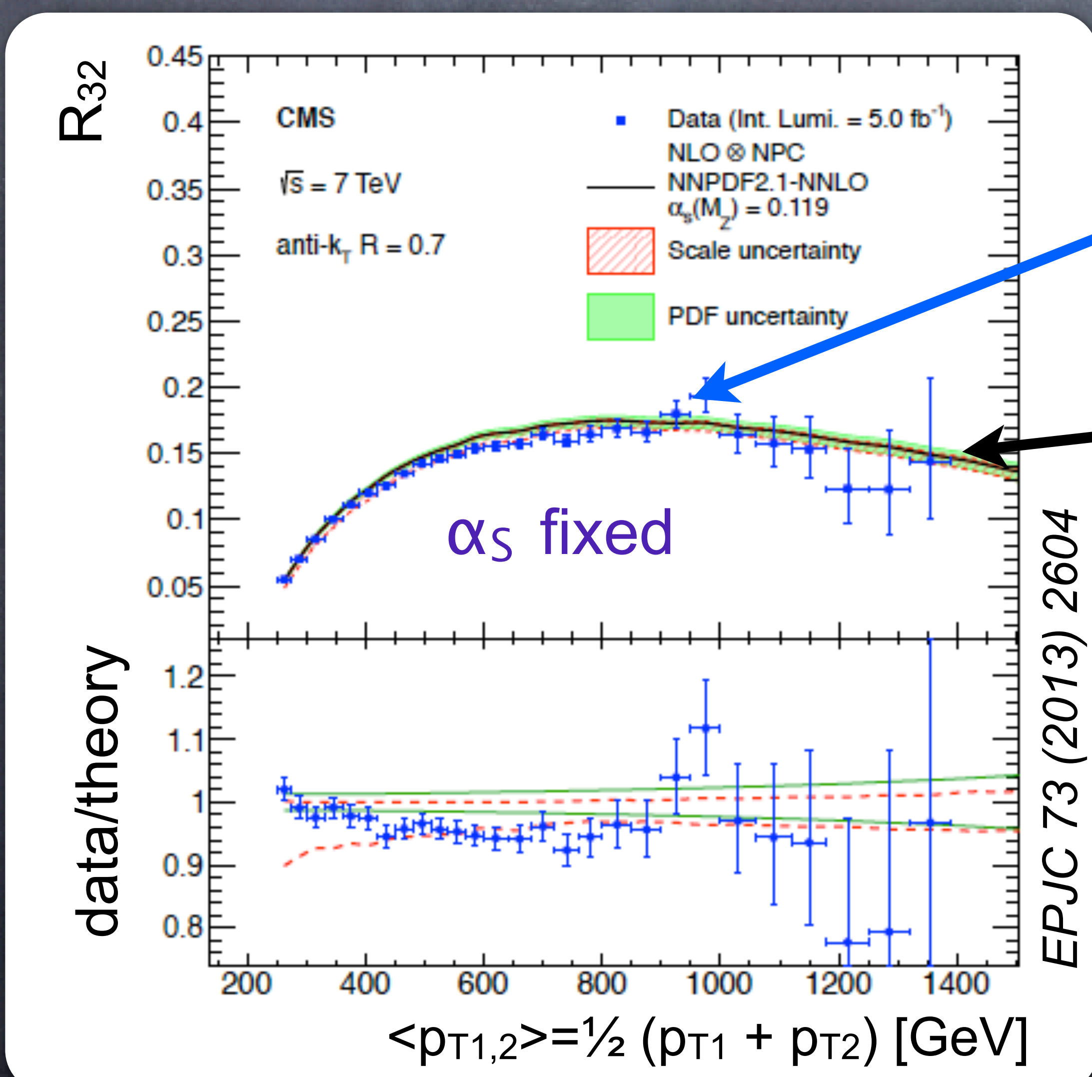

Measured ratio R_{32}

$\sqrt{s}$=7 TeV (5 fb^{-1}) *Eur. Phys. J. C 73 (2013) 2604*

QCD@NLO central value of α_S in PDF

(NLOJet++ via FastNLO)

corrected for MPI and hadronisation

scales $\mu_r=\mu_f=Q=\langle p_{T1,2}\rangle=\frac{1}{2}(p_{T1}+p_{T2})$

Determination of strong coupling α_S : R_{32}

now vary α_S in PDF, use different PDF sets

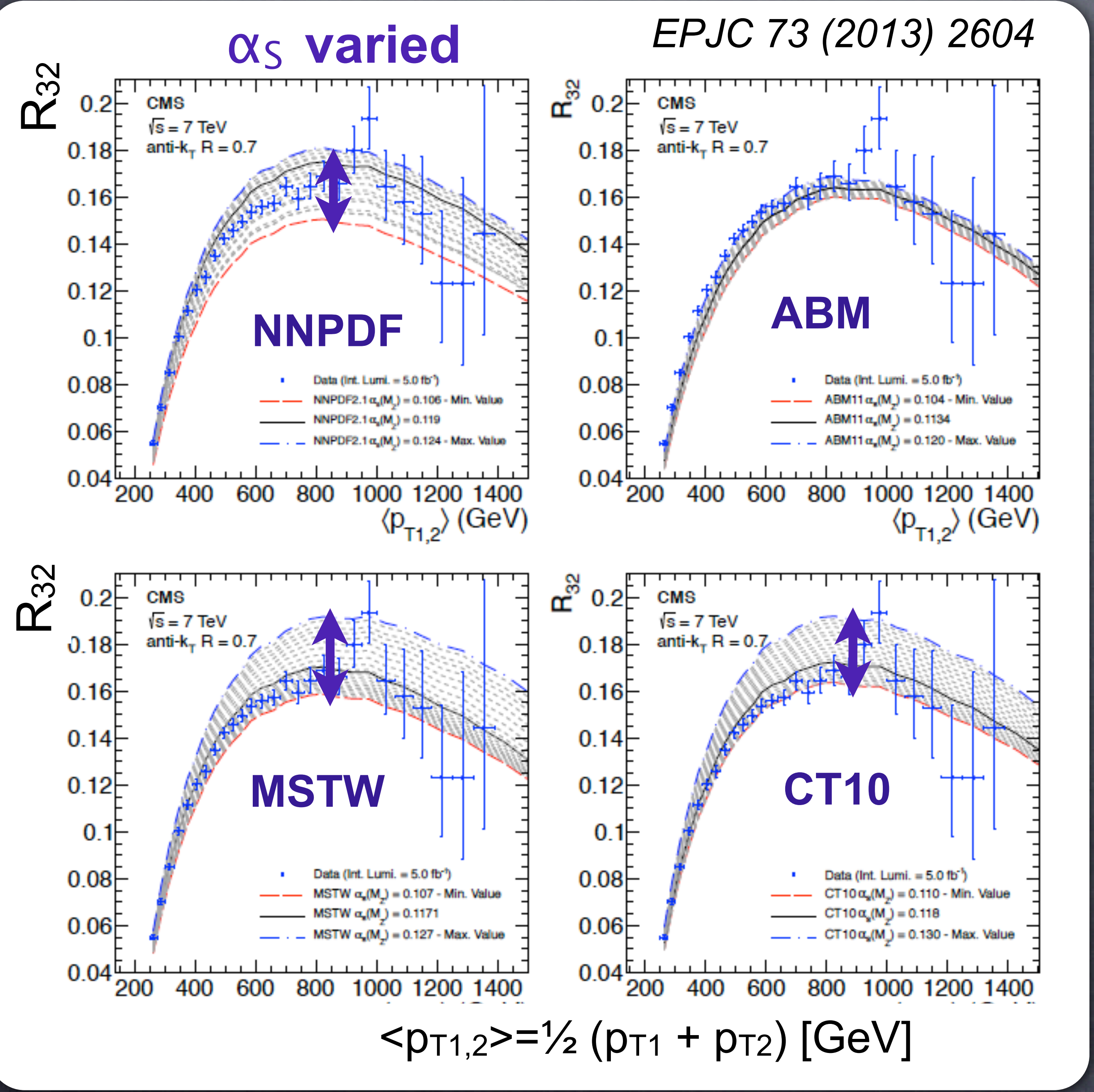

α_S determined by minimizing χ^2 between the data and the theory

Using NNPDF2.1NNLO:

$\alpha_S(m_Z)$= 0.1148 ± 0.0014_{exp} ± 0.0018_{PDF} ± 0.0050(theory)

Difference in results obtained using PDFs at NLO vs NNLO is negligible: demonstration of reduced dependence of R_{32} on details of the PDF evolution

Analysis performed in 3 Q bins
⇛ running of α_S=$\alpha_S(Q^2)$

Determination of strong coupling α_S : 3-jet mass

3-jet production process probes α^3_S

Advantage: reach highest available scales

CMS-SMP-12-027

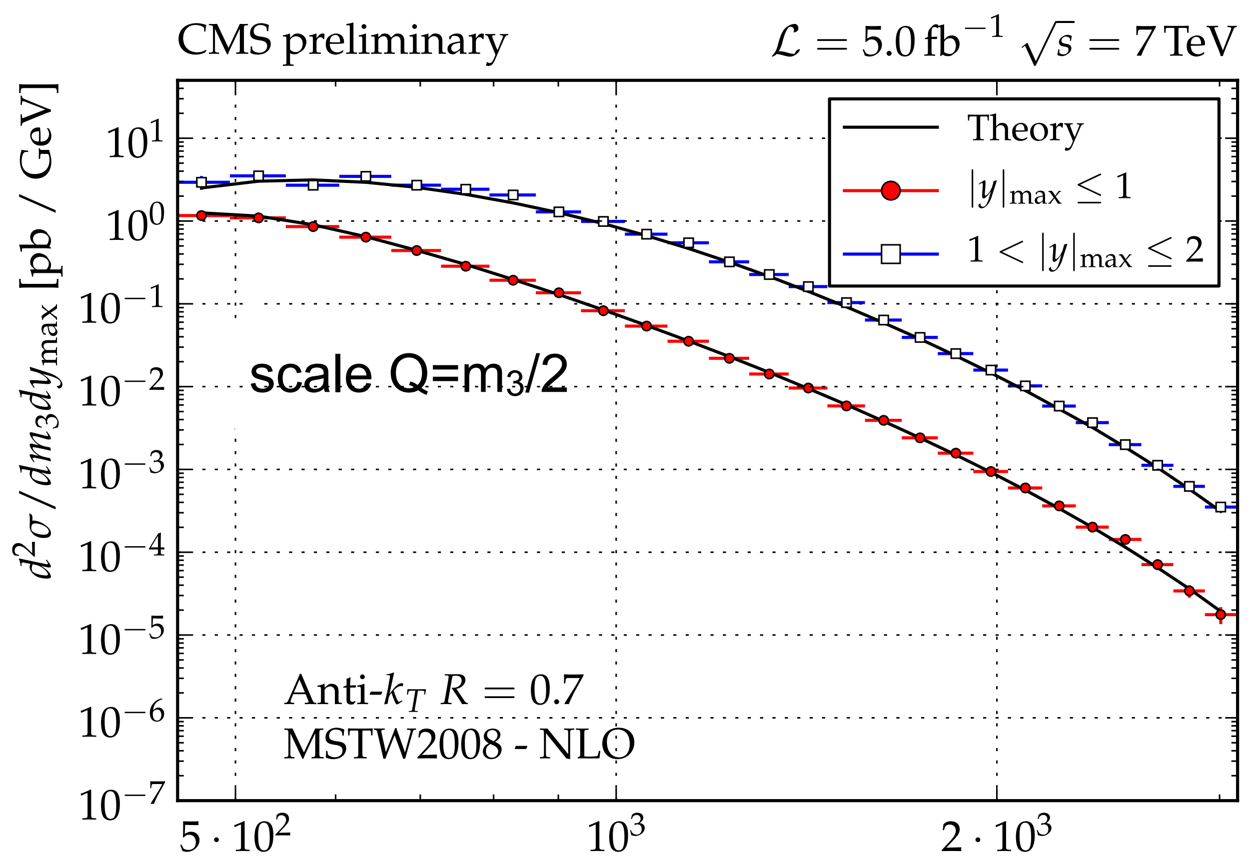

$m^2_3=(p_1+p_2+p_3)^2$, *p_i -4momentum of the i-leading jet*

Determination of strong coupling α_S : 3-jet mass

3-jet production process probes α^3_S

Advantage: reach highest available scales

CMS-SMP-12-027

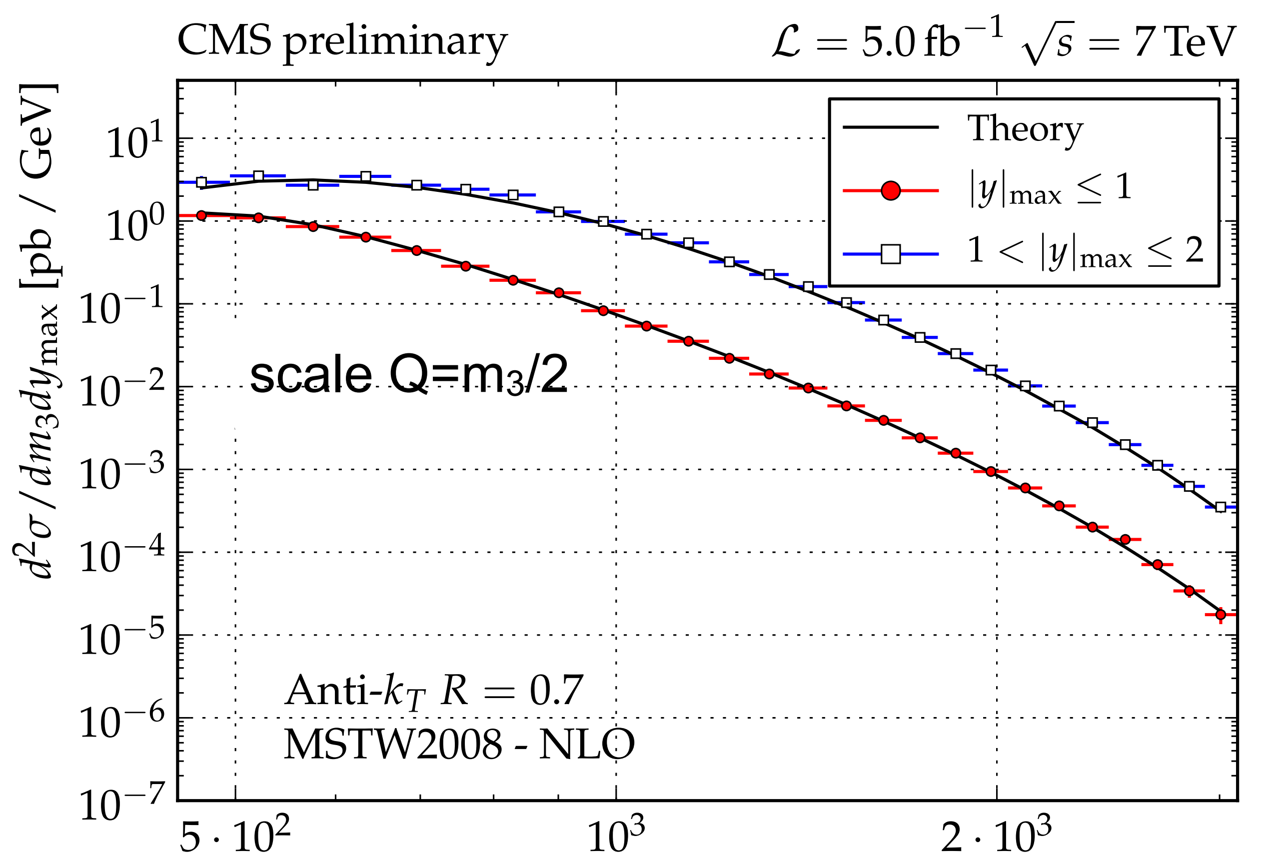

$m^2_3=(p_1+p_2+p_3)^2$, *p_i -4momentum of the i-leading jet*

Use different PDFs (α_S)

determine α_S from comparing data and theory in central rapidity

CMS-SMP-12-027

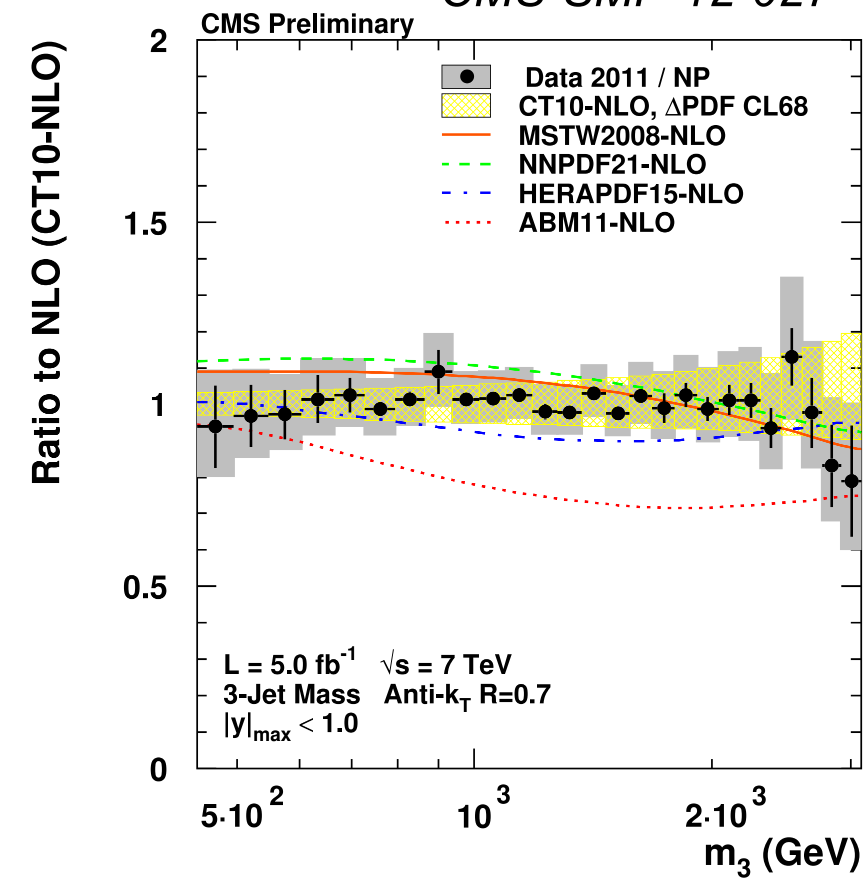

Using MSTW08NLO $\alpha_S(m_Z)$= 0.1160 $^{+0.0025}_{-0.0023}$ (exp +PDF +NP) $^{+0.0068}_{-0.0021}$ (scale)

Determination of strong coupling α_s : top production

Top-quark pair production in pp collisions probes gluon distribution, top mass and α_s

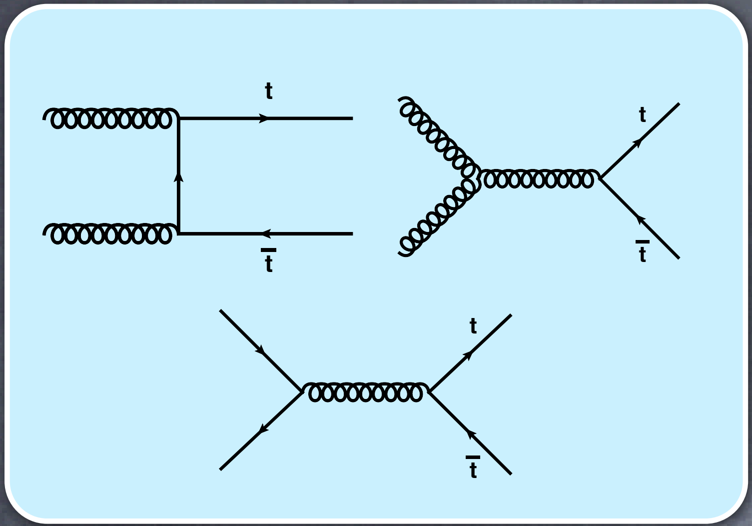

for a fixed g(x)

Constrain m_t or α_s using precise measurements and NNLO calculation

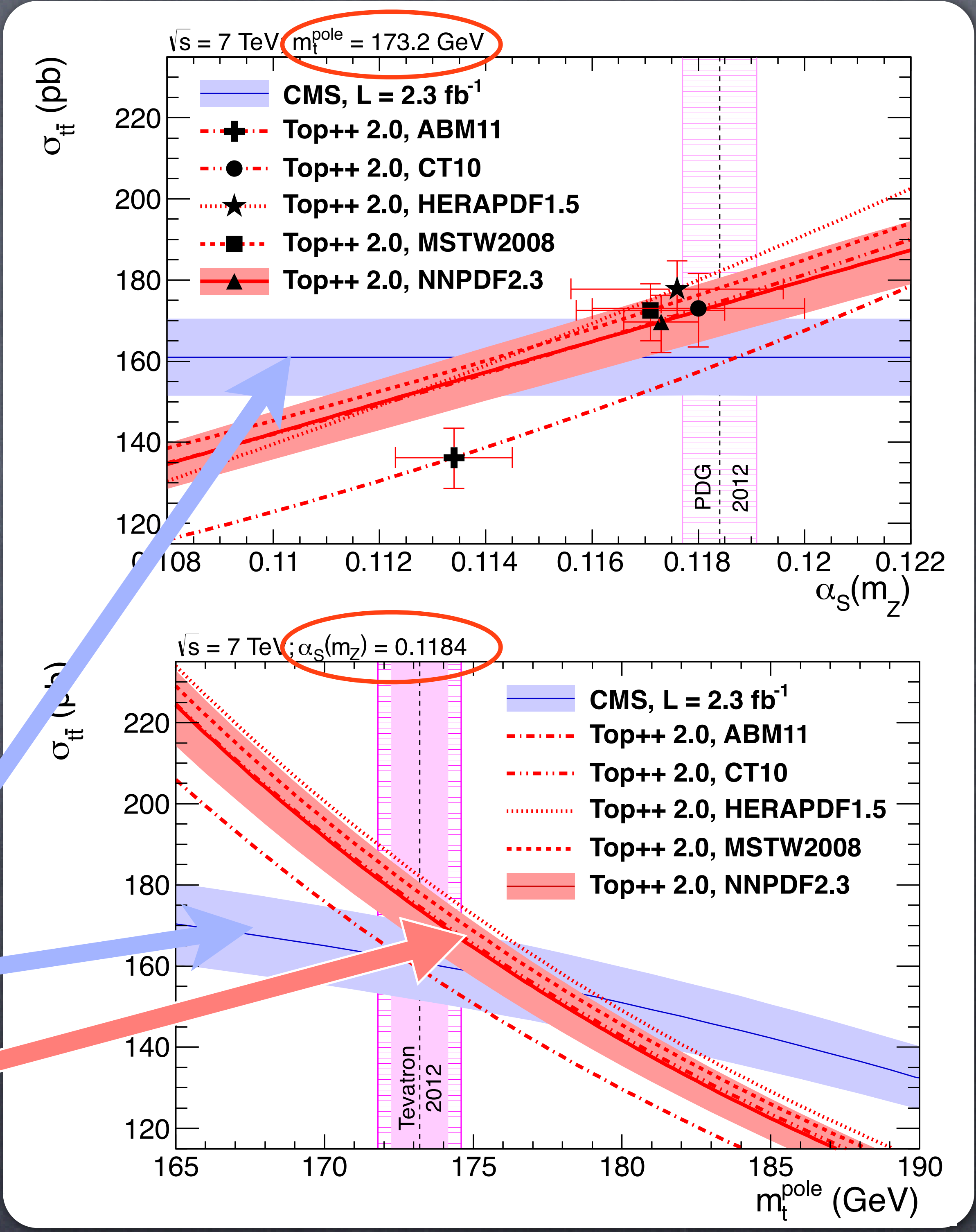

fix m_t → determine α_s

fix α_s → determine m_t

Determination of strong coupling α_S : top production

Top-quark pair production in pp collisions probes gluon distribution, top mass and α_S

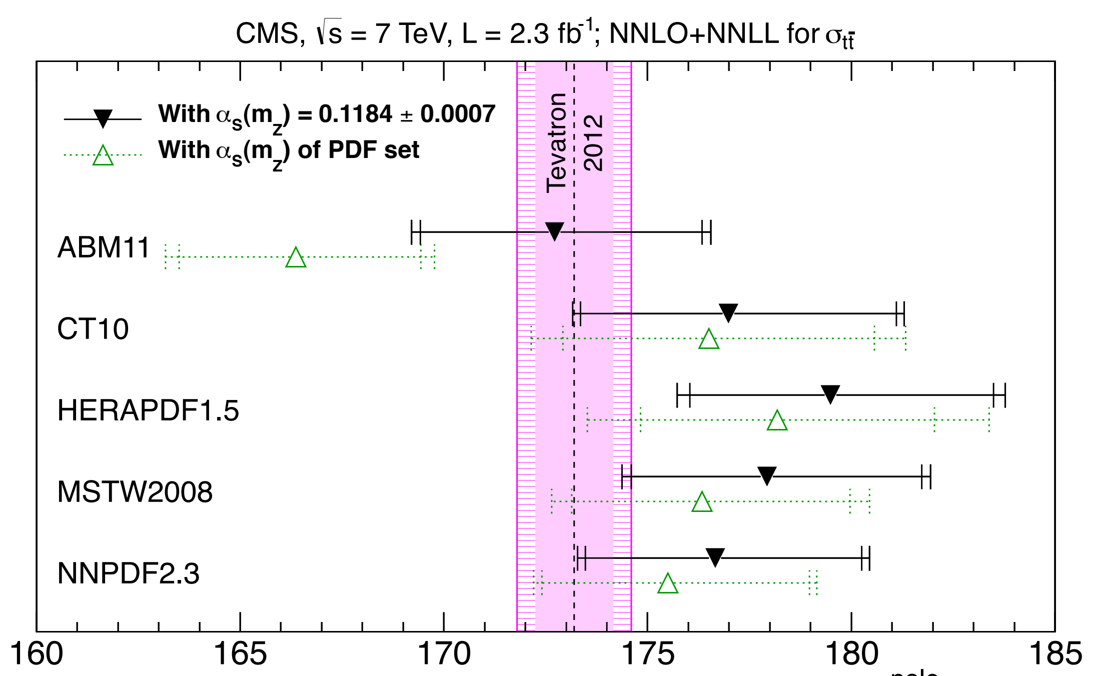

Phys. Lett. B728 (2013) 496

Unambiguously defined top pole mass

m_t^{pole} (NNPDF)=$176.7^{+3.8}_{-3.4}$ GeV

consistent with direct measurements

Determined at NNLO

$\alpha_S(m_Z) = 0.1151^{+0.0033}_{-0.0032}$ (using NNPDF)

consistent with world average

theory uncertainty (scale variation) <1%

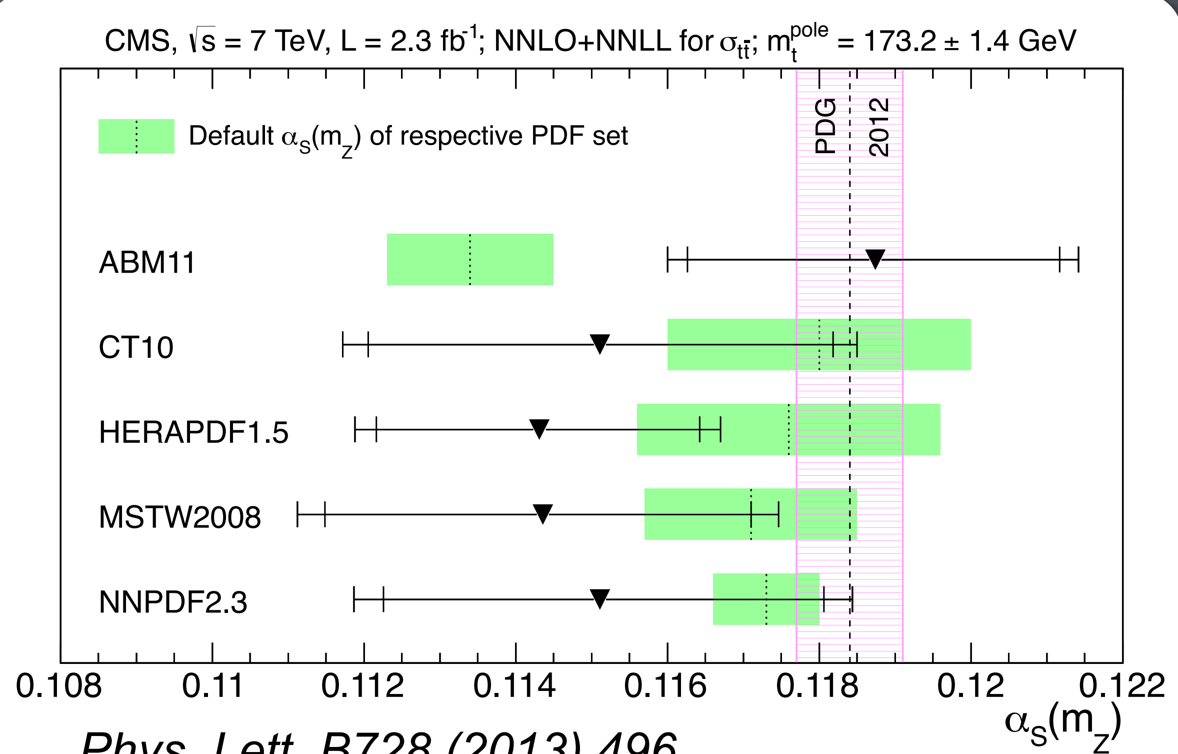

Phys. Lett. B728 (2013) 496

more details in the afternoon talks by G. Cortiana and S. Naumann-Emme

Determination of strong coupling α_S: summary

Running of α_S measured up to 1.4 TeV, in good agreement with QCD expectation

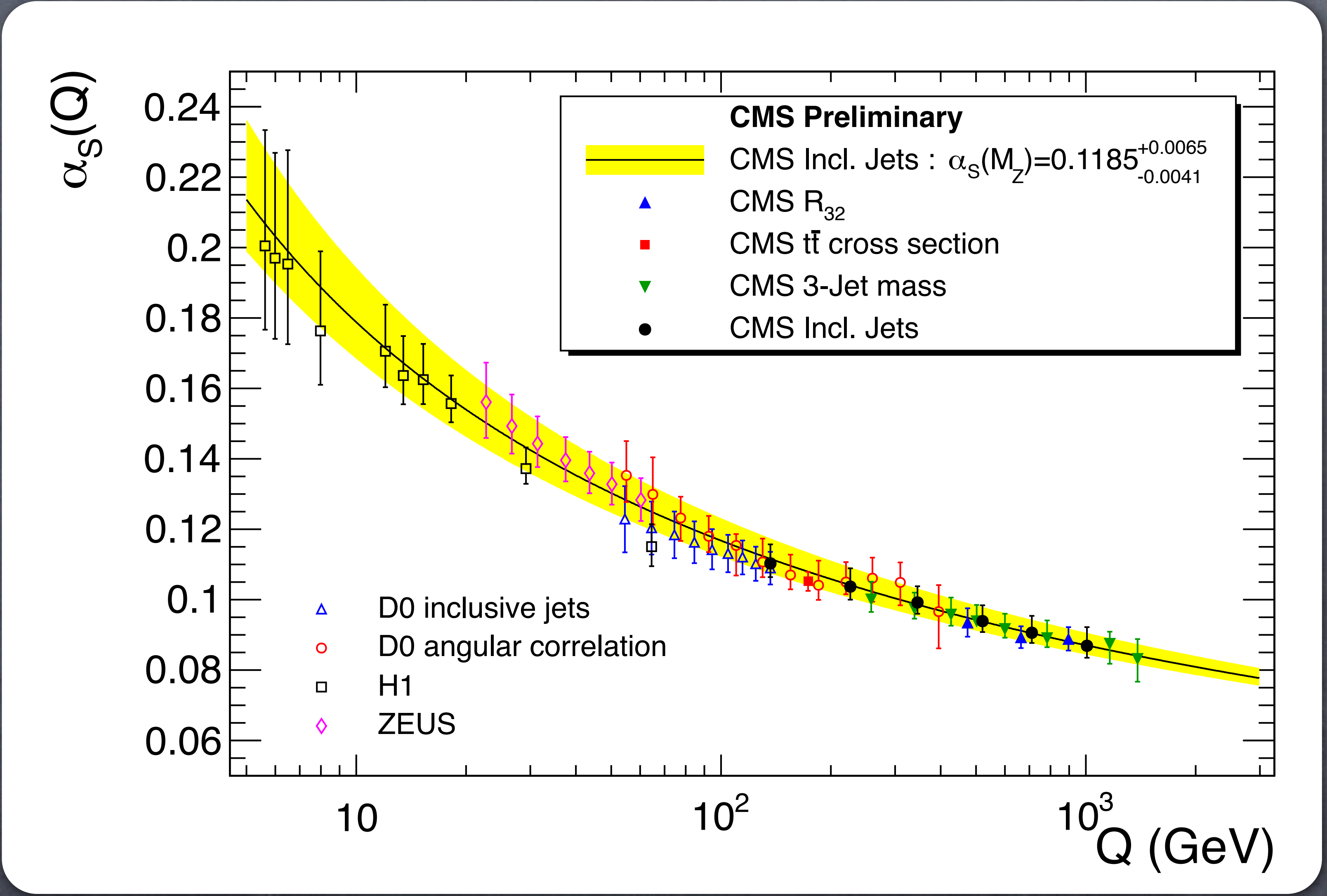

Different methods use PDF as external input, partially account for PDF/α_S correlation

Results compatible with the world average, precision limited by missing higher orders in QCD and PDF uncertainties

2) LHC data improving QCD precision

Expected constraints from LHC

➡ *at high x*:

- jet production: gluon, light quarks
- top-pair production: gluon
- prompt photons: gluon

➡ *at medium x:*

W, Z, W+c production: valence, sea

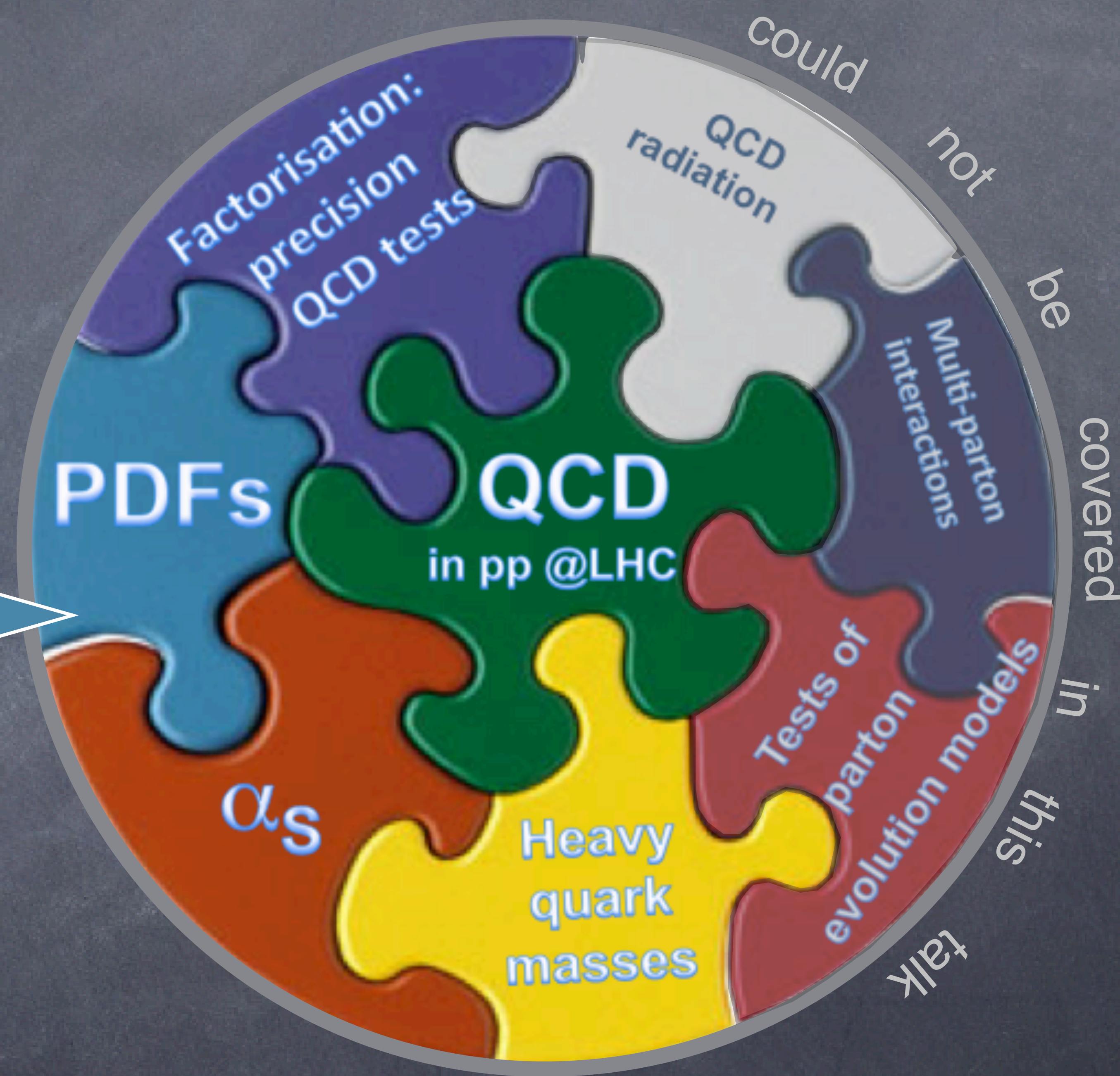

How PDFs are determined

PDF for flavor i: $f_i = f_i(x, Q^2)$
Q^2 dependence predicted by QCD
x-dependence determined from data

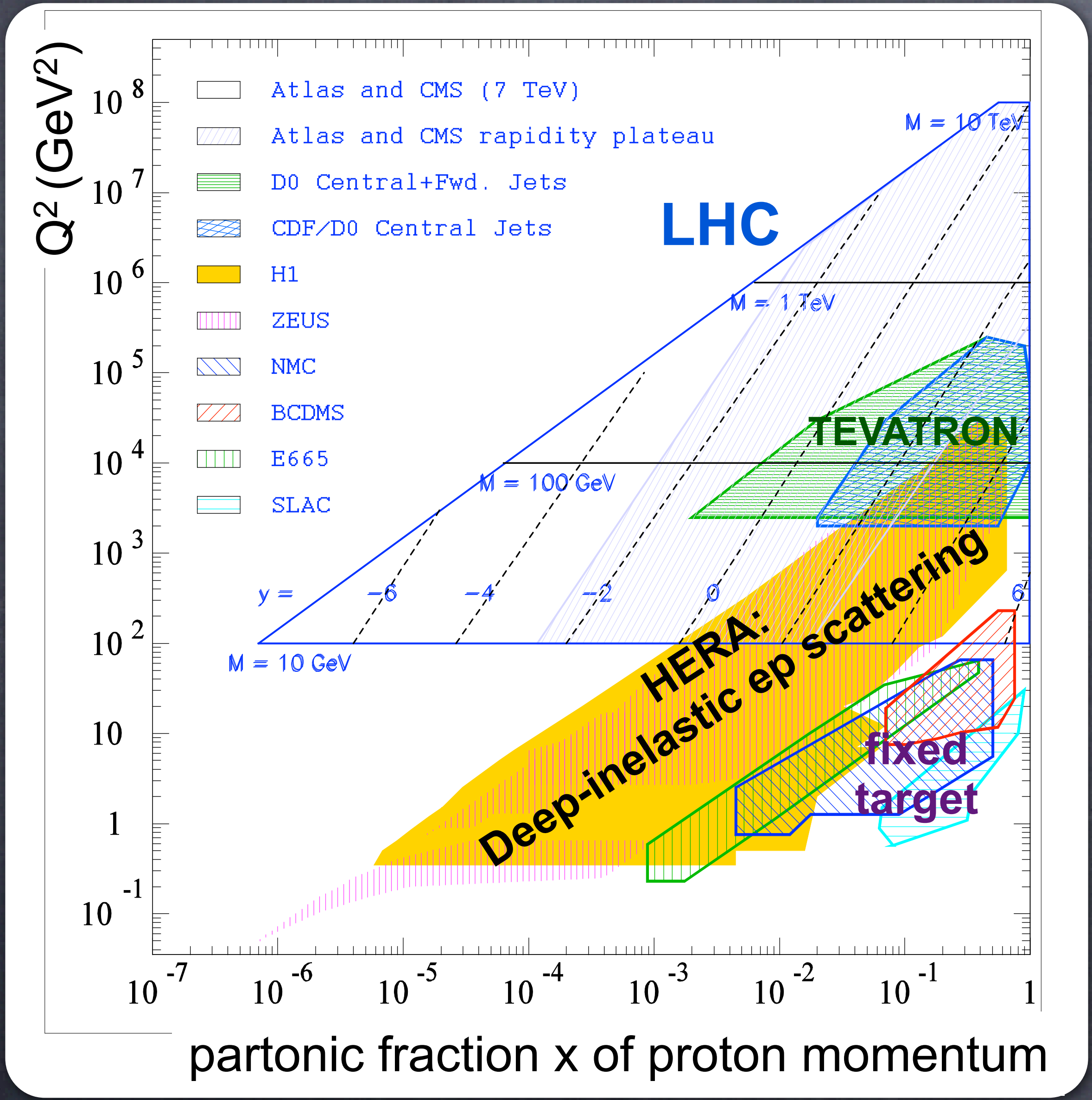

- parameterize PDFs at a scale Q^2_0:
  $f(x) = Ax^B(1-x)^C(1+Dx+Ex^2)$
- evolve these PDFs to $Q^2 > Q^2_0$
- construct expected cross sections
- χ^2- fit to the experimental data

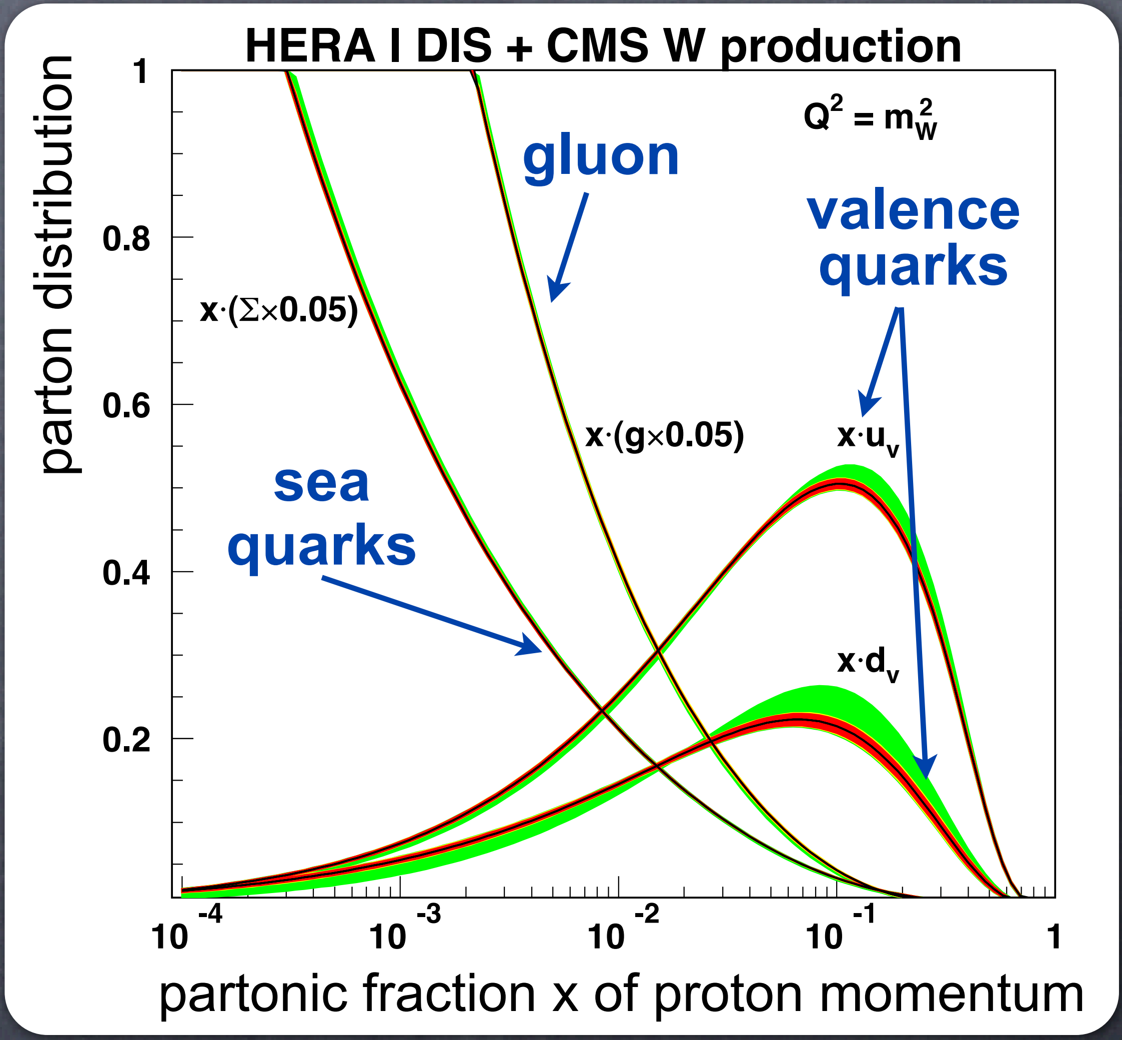

PDFs determined mostly from HERA data, LHC provides further constraints

Include LHC data in PDF fit using HERAFitter

Unique tool to test impact of the measurements on e.g. PDFs **during data analysis**

experimental input

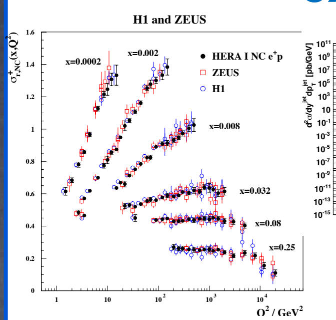

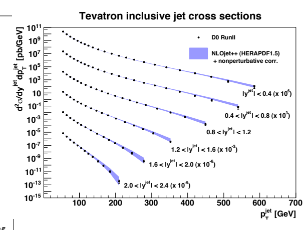

experiments:
HERA, Tevatron, LHC, fixed target

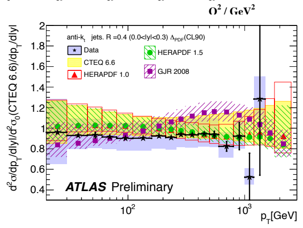

processes:
NC, CC DIS, jets, diffraction, heavy quarks (c,b,t)
Drell-Yan, W production

theoretical calculations/tools

Heavy quark schemes:	MSTW, CTEQ, ABM
Jets, W, Z production:	fastNLO, Applgrid
Top production	NNLO (Hathor)
QCD Evolution	DGLAP (QCDNUM)
	k_T factorisation
Alternative tools	NNPDF reweighting
Other models	Dipole model

+ Different error treatment models
+ Tools for data combination (HERAaverager)

HERAFitter

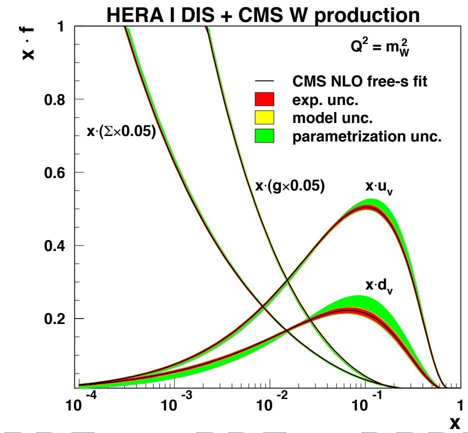

PDF or uPDF or DPDF

$\alpha_S(M_Z), m_c, m_b, m_t, f_s, ..$

Theory predictions

Benchmarking

Comparison of schemes

open-source QCD framework

developed by experimentalists and theorists

strong contribution from ATLAS and CMS members

https://www.herafitter.org/HERAFitter

ATLAS and CMS results shown on following slides are obtained using HERAFitter

LHC jet measurements in PDF determination

inclusive jet production probes gluon and quark distributions
sensitivity of the data to parton distributions quantified by correlation coefficients

e.g. central rapidity:

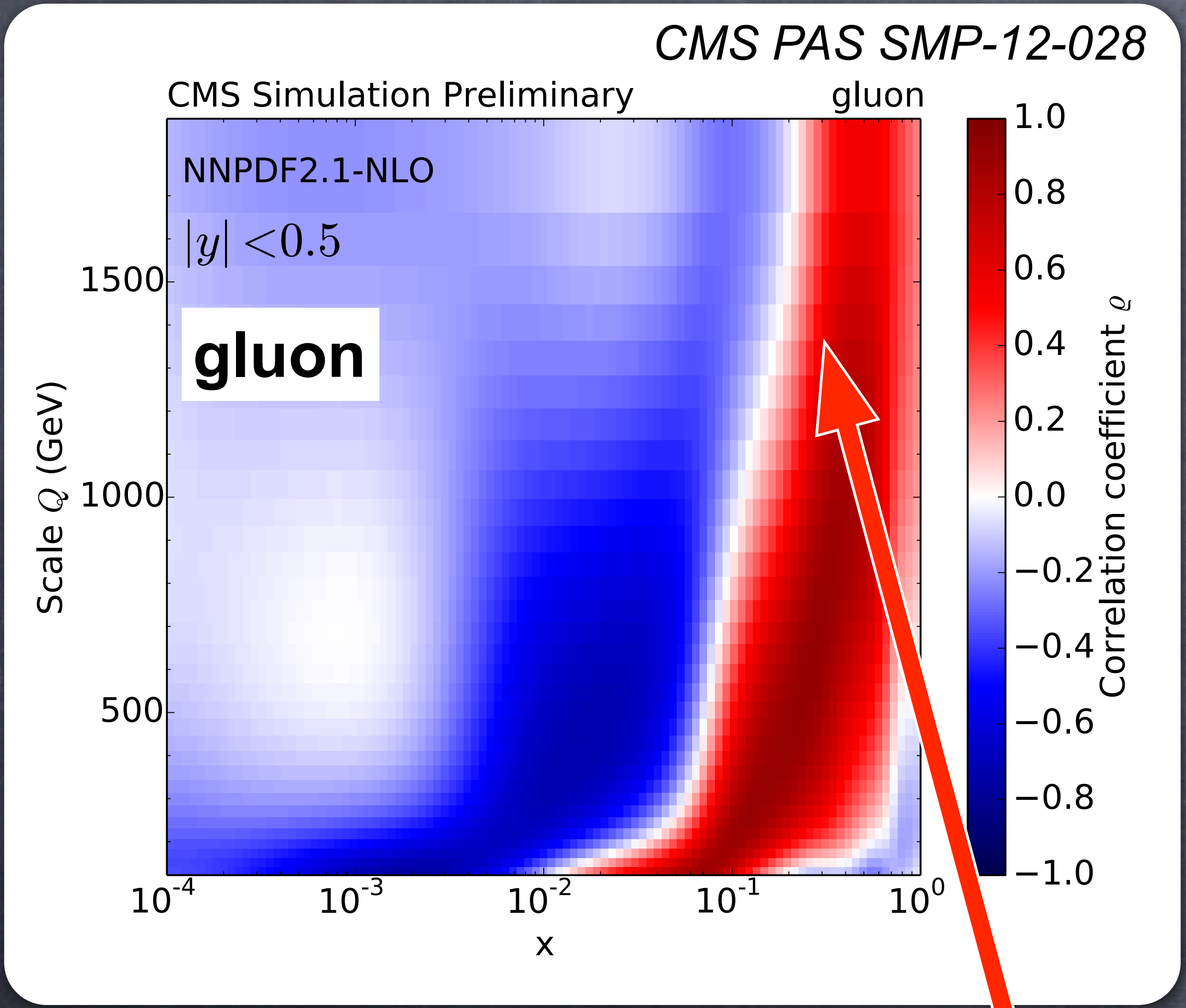

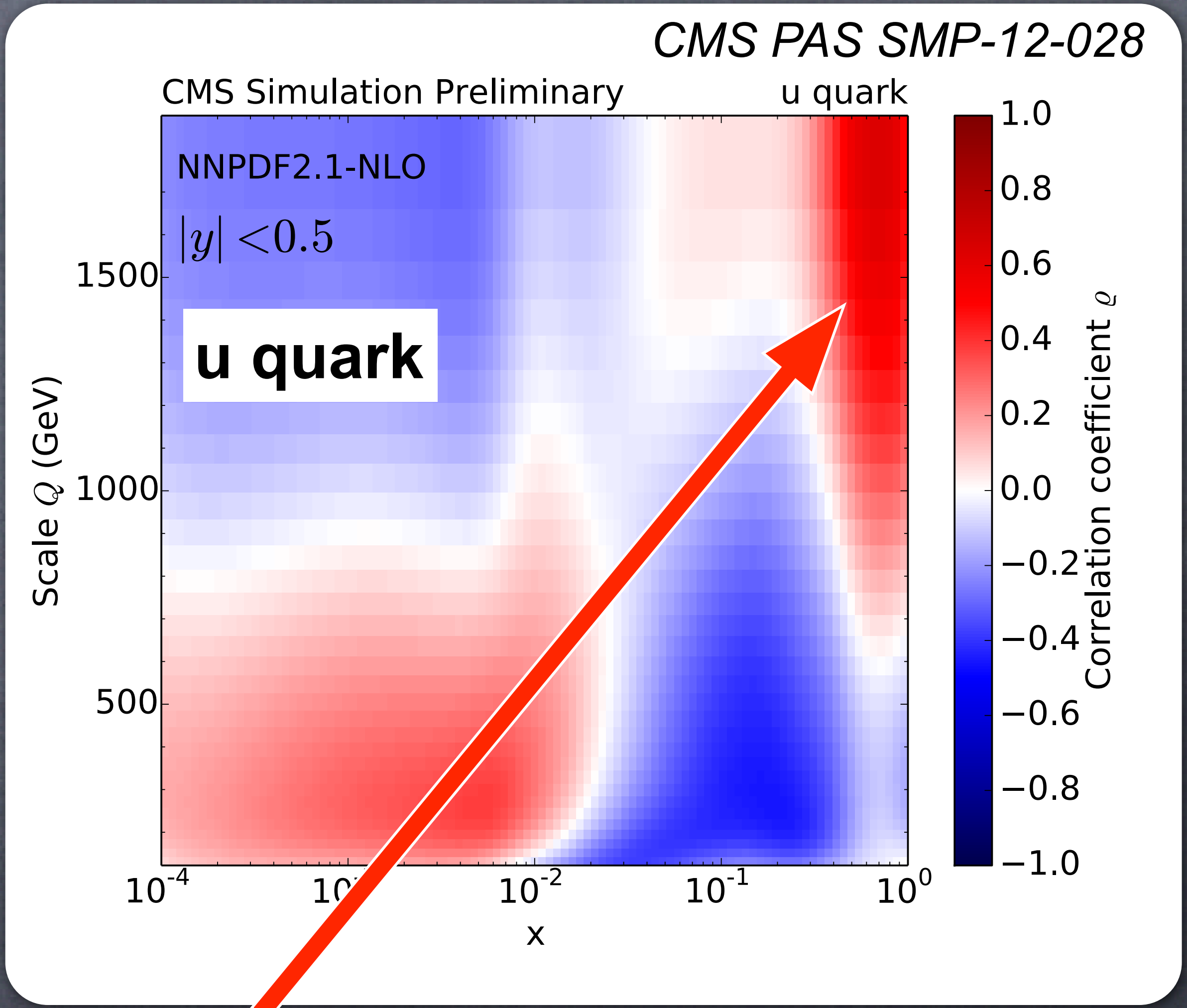

strong correlation

expect an impact of the measurement on gluon at medium x, quarks at high x

LHC inclusive jet measurements improve PDFs

QCD analysis at NLO using HERAFitter

- Deep Inelastic Scattering in ep collisions (HERA I *[JHEP 1001:109 (2010)]*)
- CMS inclusive jet production at √s=7 TeV (L= 5 fb^{-1}) *[Phys. Rev. D 87 (2012) 12002]*

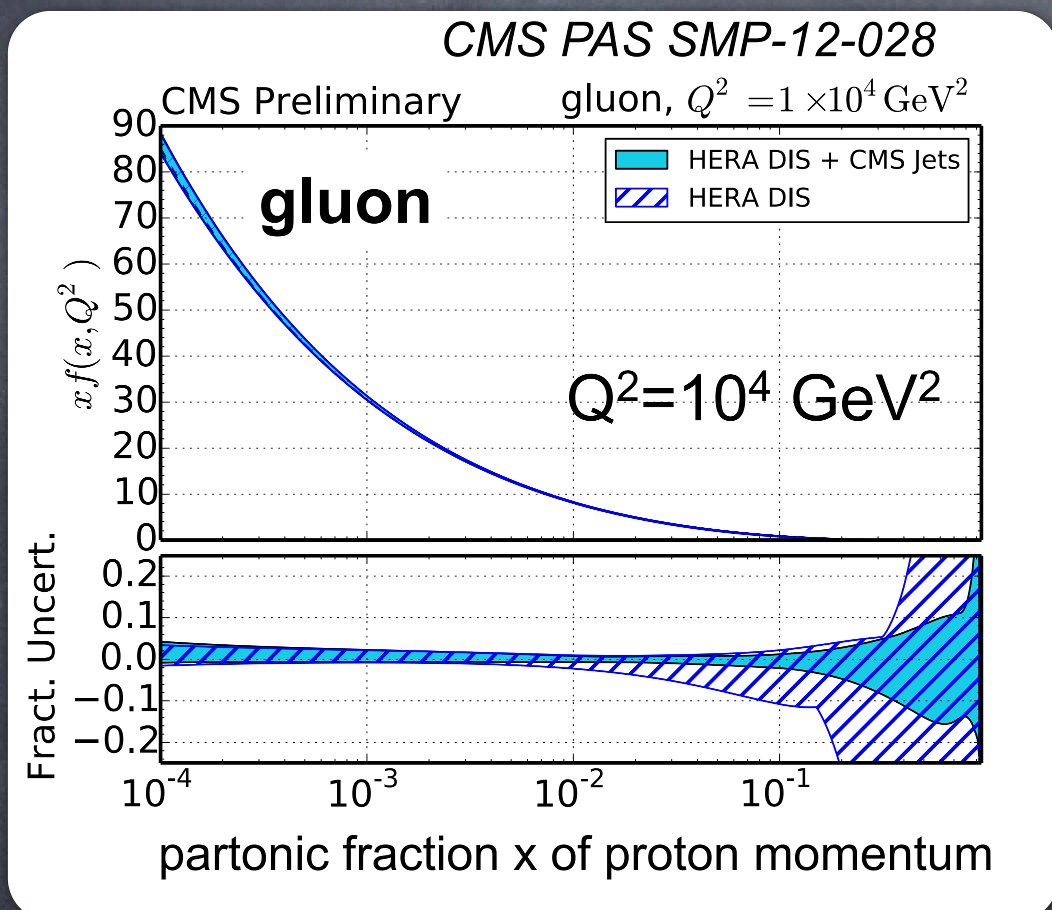

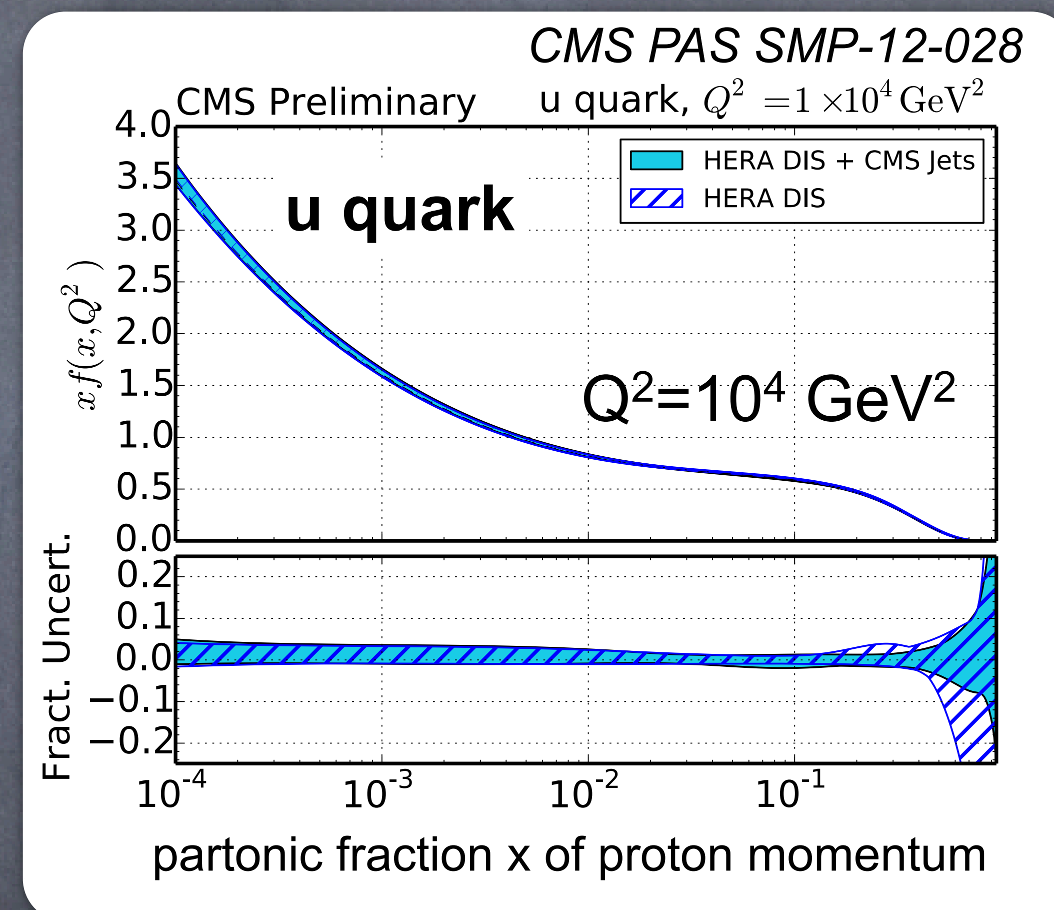

Improved constraints on the gluon and light quark distributions at high x

Simultaneous determination of PDF and $\alpha_S(m_Z) = 0.1192^{+0.0017}_{-0.0015}$ (exp)

uncertainty accounts for the experimental uncertainties of the data and the NP uncertainties

Inclusive jet production at different energies

QCD analysis at NLO using HERAFitter

- Deep Inelastic Scattering in ep collisions (HERA I *[JHEP 1001:109 (2010)]*)
- ATLAS inclusive jet production at $\sqrt{s}$=7 TeV (L=37pb^{-1}) and $\sqrt{s}$=2.76 TeV (L=0.20 pb^{-1})

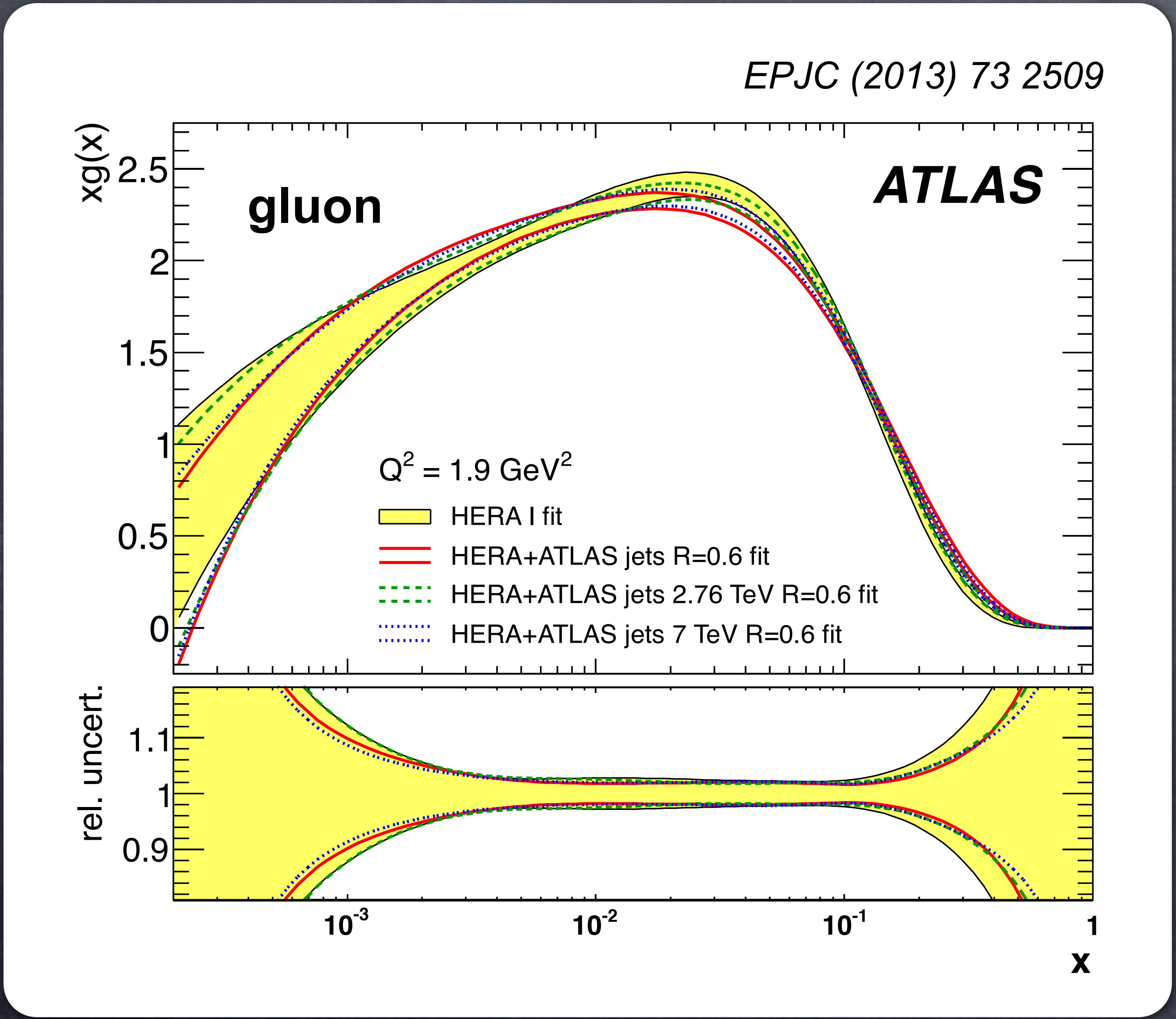

correlations of experimental uncertainties between two jet measurements accounted for

increased sensitivity to PDF

Error reduction at high x
Harder gluon distribution

PDF constraints using electroweak bosons at LHC

Measurements of Drell-Yan production probe bi-linear combination of PDFs

$$W^+ \approx 0.95(u\bar{d} + c\bar{s}) + 0.05(u\bar{s} + c\bar{d})$$
$$W^- \approx 0.95(d\bar{u} + s\bar{c}) + 0.05(d\bar{c} + s\bar{u})$$

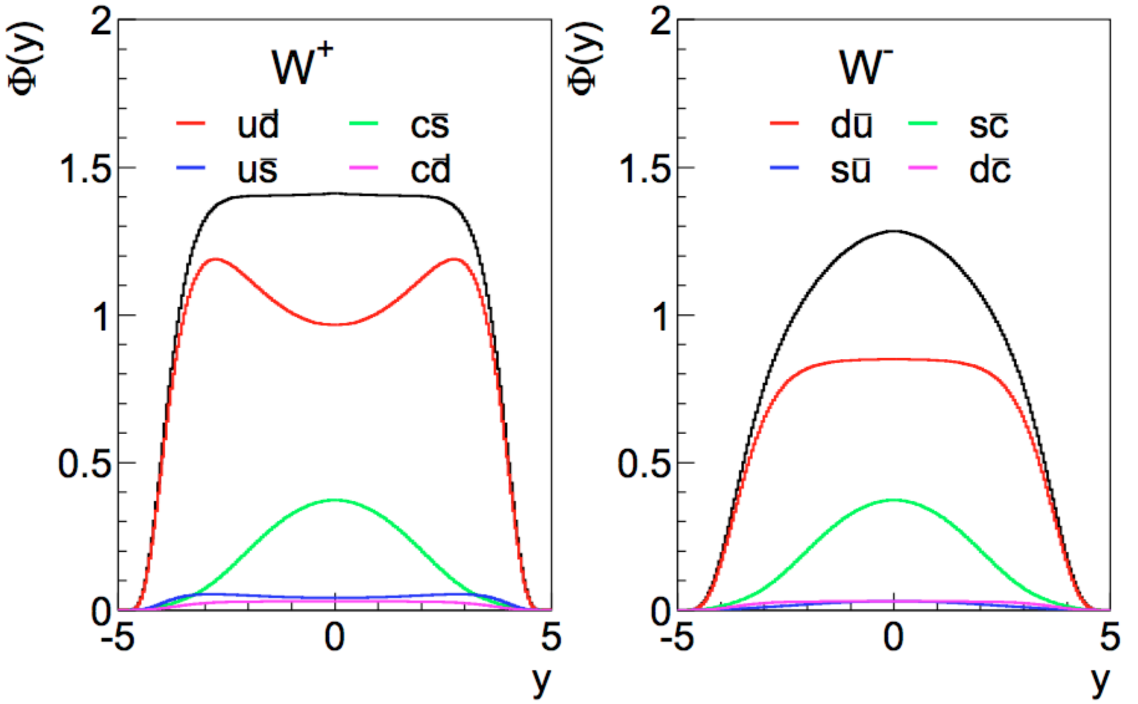

$$Z \approx 0.29(u\bar{u} + c\bar{c}) + 0.37(d\bar{d} + s\bar{s} + b\bar{b})$$
$$\gamma^* \approx 0.44(u\bar{u} + c\bar{c}) + 0.11(d\bar{d} + s\bar{s} + b\bar{b})$$

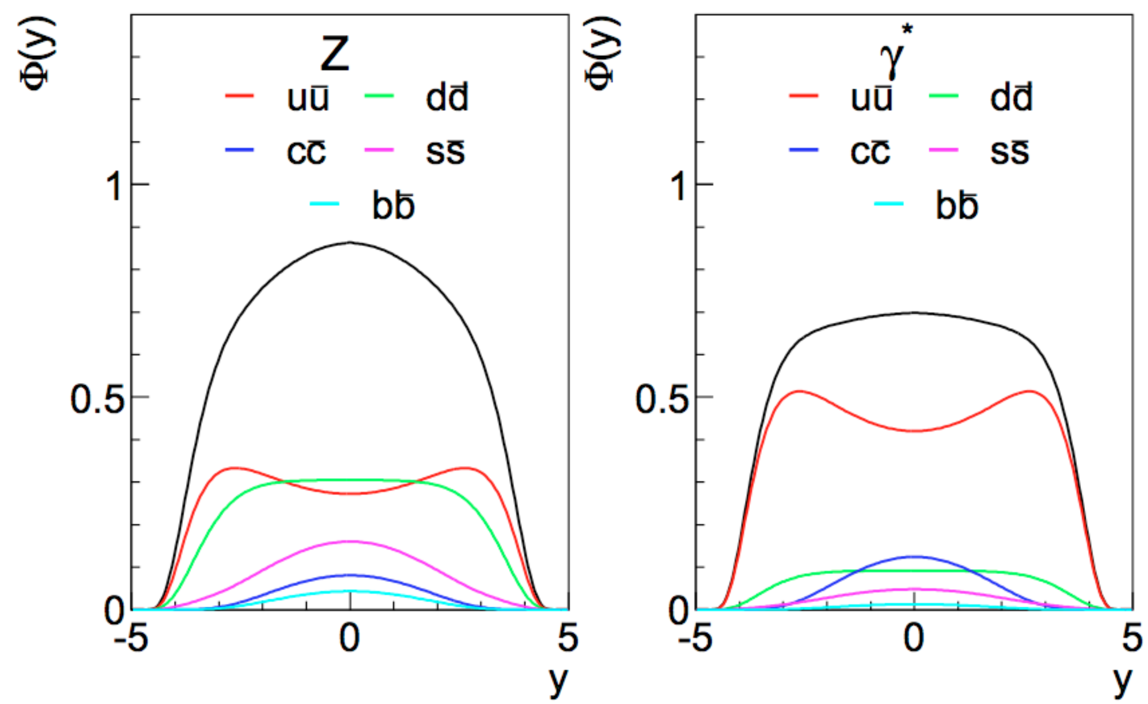

NB: LO with suppressed strangeness

...courtesy A.Glazov/V.Radescu

differential cross sections for W and Z production provide important information on light quarks and the sea decomposition
(particularly interesting is strange-quark distribution, which is poorly known)

Asymmetry in W± production at LHC improves PDFs

Lepton asymmetry in W production in pp collisions: $$A_W = \frac{W^+ - W^-}{W^+ + W^-} \approx \frac{u_v - d_v}{u_v + d_v + 2u_{sea}}$$

QCD analysis at NLO using W± charge asymmetry at LHC **improves valence**

- Deep Inelastic Scattering in ep collisions (HERA I *[JHEP 1001:109 (2010)]*)
- CMS muon charge asymmetry in W production at 7 TeV (L=4.7 fb^{-1}) *[arXiv:1312.6283]*

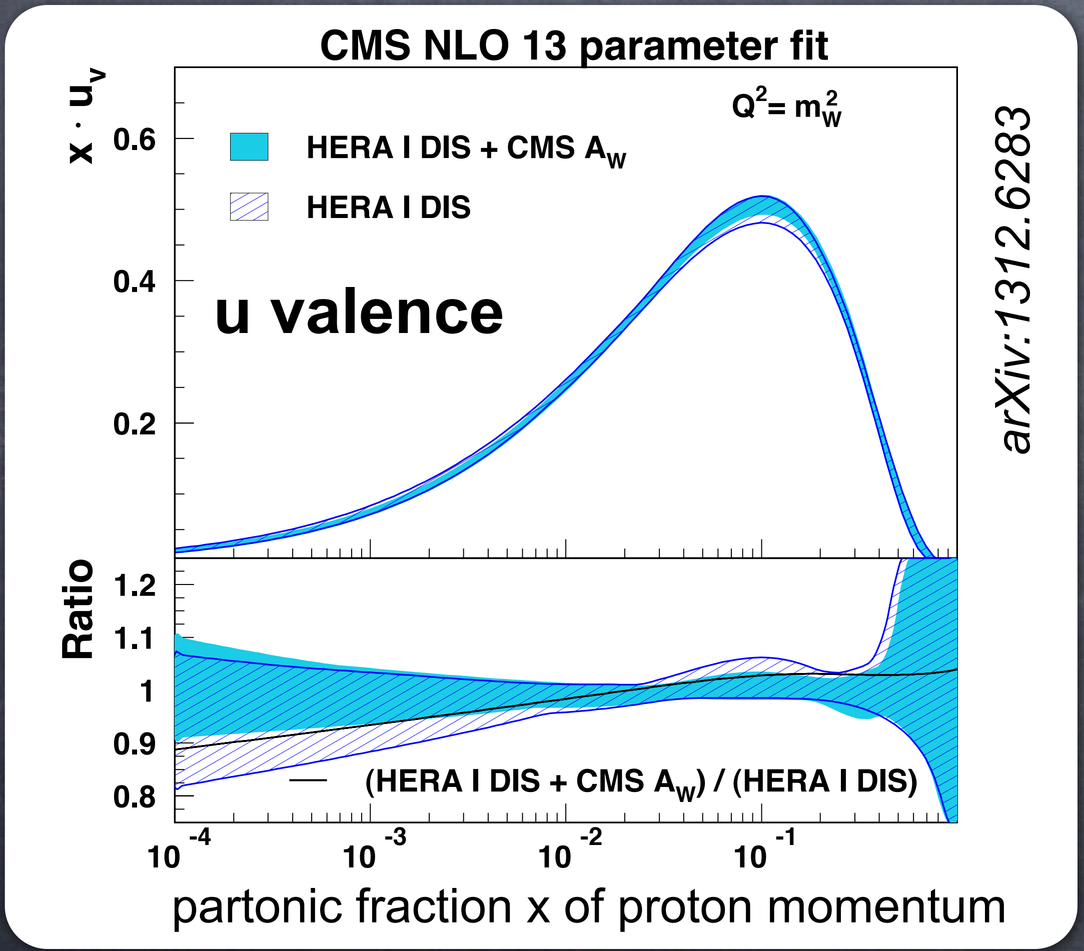

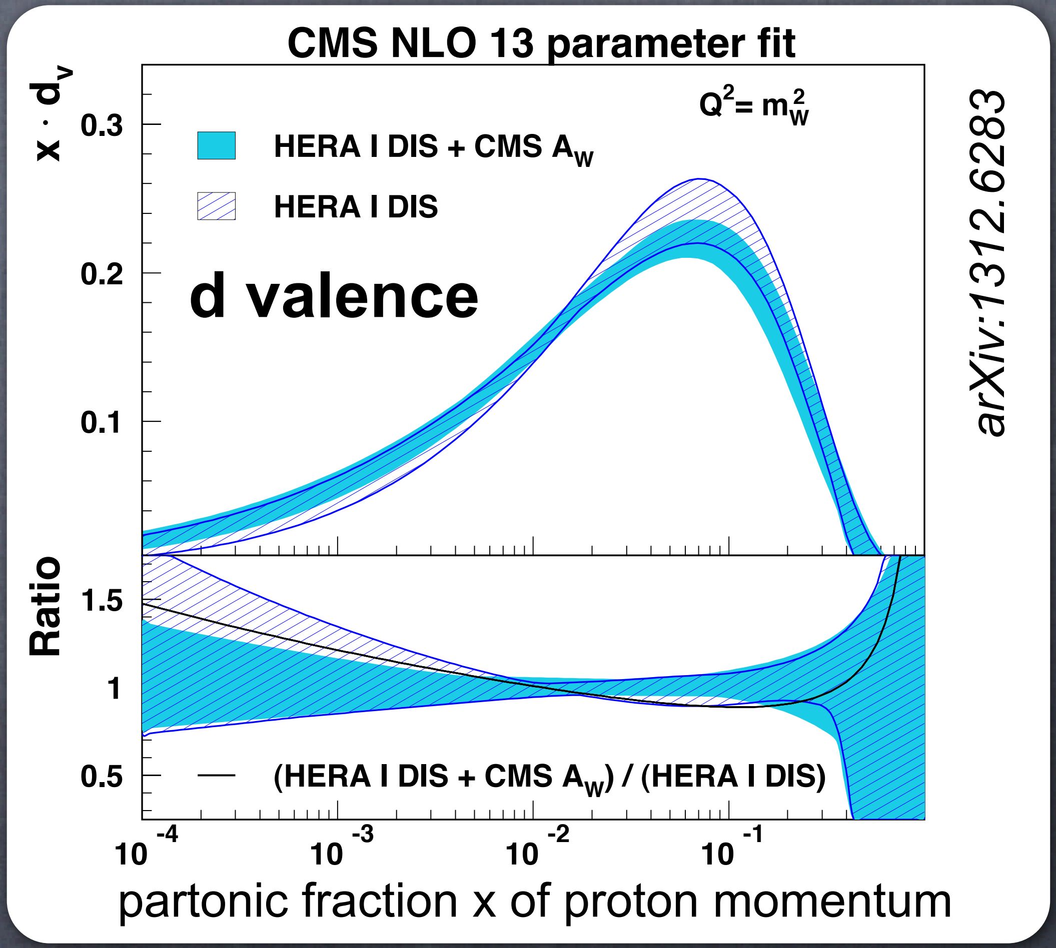

Improvement in the uncertainty of the valence-quark distributions

Strangeness determination using W+c production

In pp collisions, production process of W+c probes strange quark directly at LO

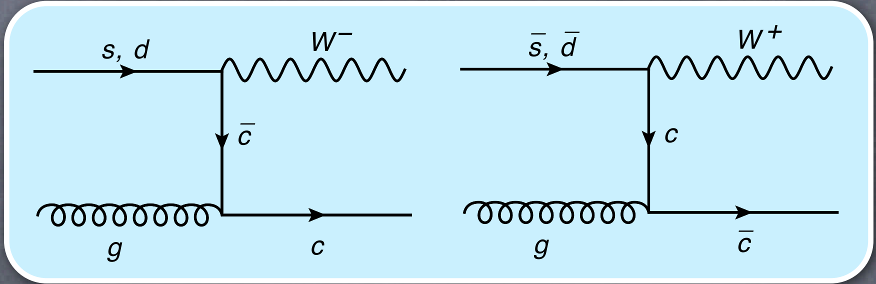

NLO QCD analysis using W+c production at LHC **determines s-quark distribution**

- Deep Inelastic Scattering in ep collisions (HERA I *[JHEP 1001:109 (2010)]*)
- CMS muon charge asymmetry in W production at 7 TeV (L=4.7 fb-1) *[arXiv:1312.6283]*
- CMS associated W+charm production at 7 TeV (L=4.7 fb-1) *[arXiv:1310.1138]*

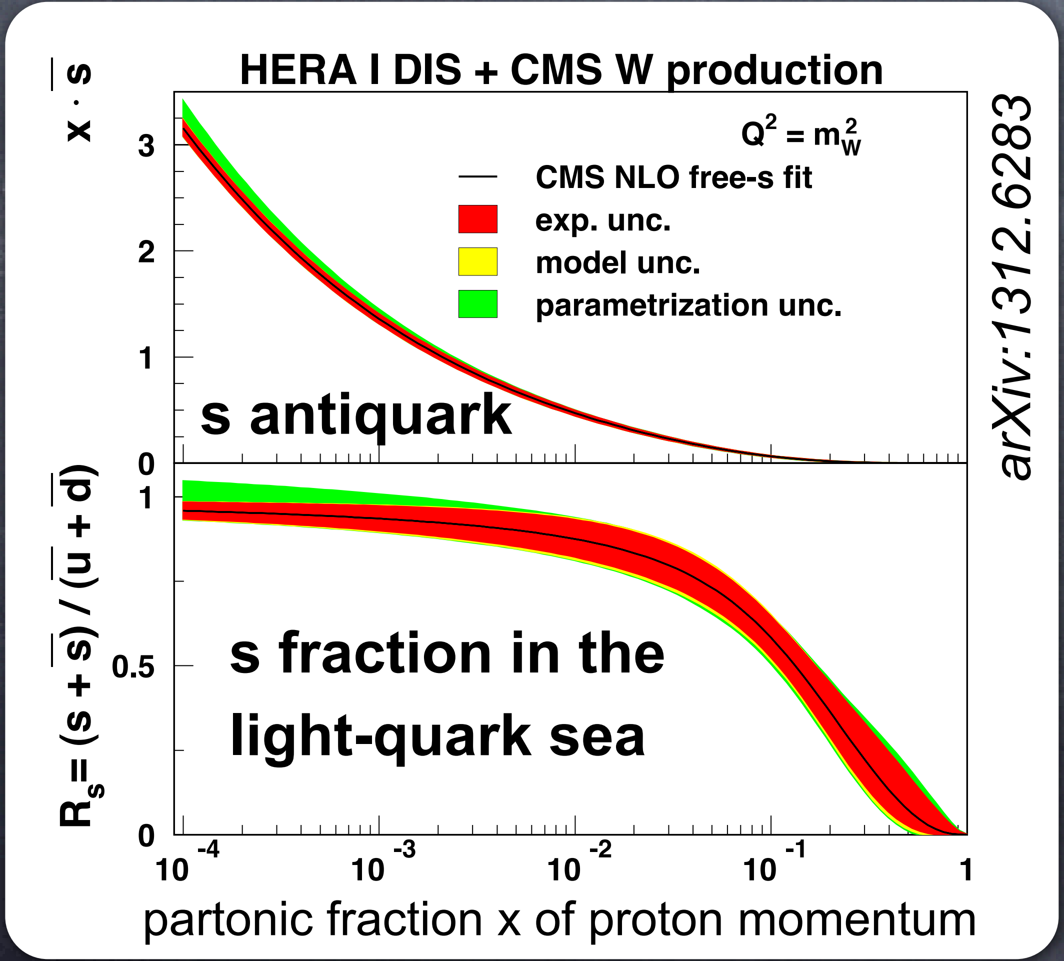

s-quark distribution agrees well with CT10 and NNPDF

strangeness suppression in good agreement with results of neutrino scattering experiments

Strangeness determination using W+c production

Fiducial cross sections of W+c jet, W+D confronted to aMC@NLO

Estimate constraints on s-quark minimizing χ^2 in comparing measurement with NLO $\otimes$ HERAPDF1.5 (r_s)

arXiv:1402.6263

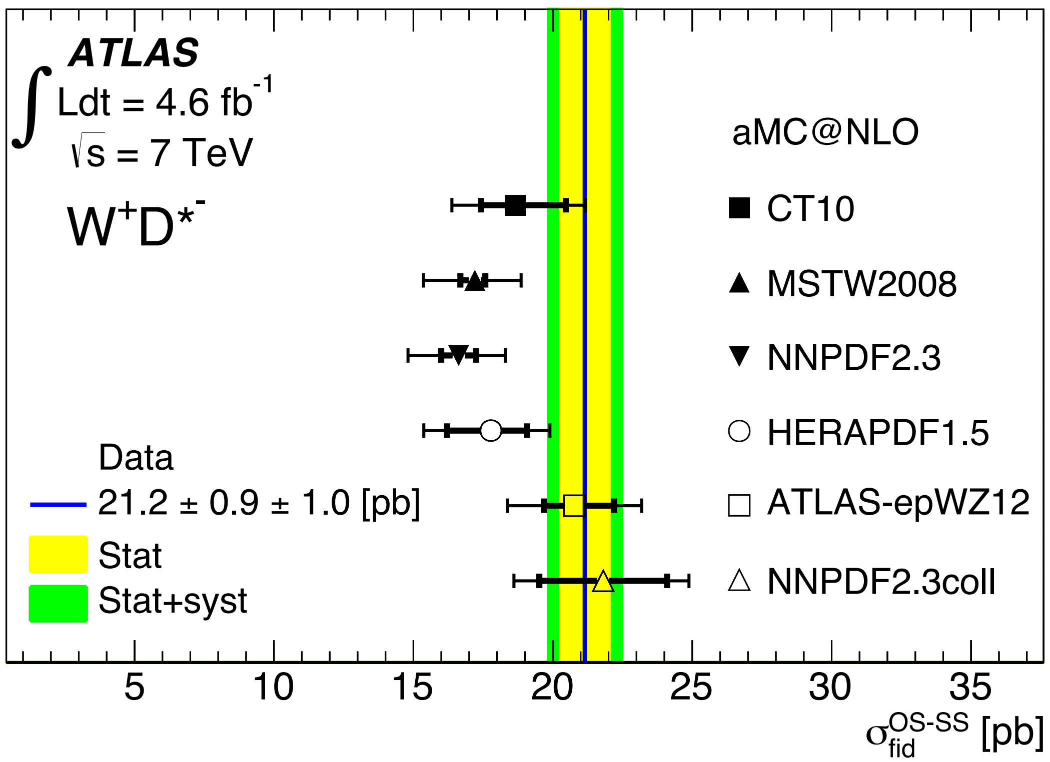

arXiv:1402.6263

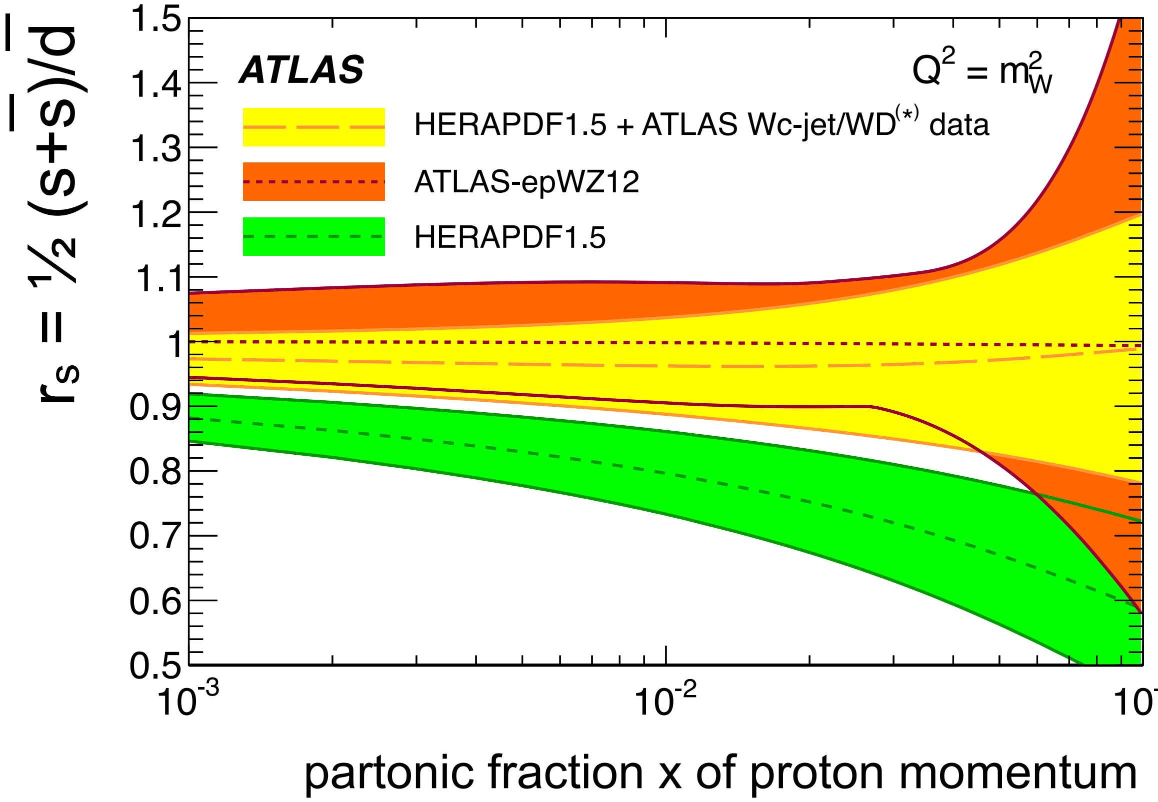

Results in agreement with flavour-symmetric sea ($\bar{s}=\bar{d}$).
Somewhat enhanced strange distribution with respect to results neutrino scattering

Strangeness determination using W+c production

Fiducial cross sections of W+c jet, W+D confronted to aMC@NLO

Estimate constraints on s-quark minimizing χ^2 in comparing measurement with NLO $\otimes$ HERAPDF1.5 (r_s)

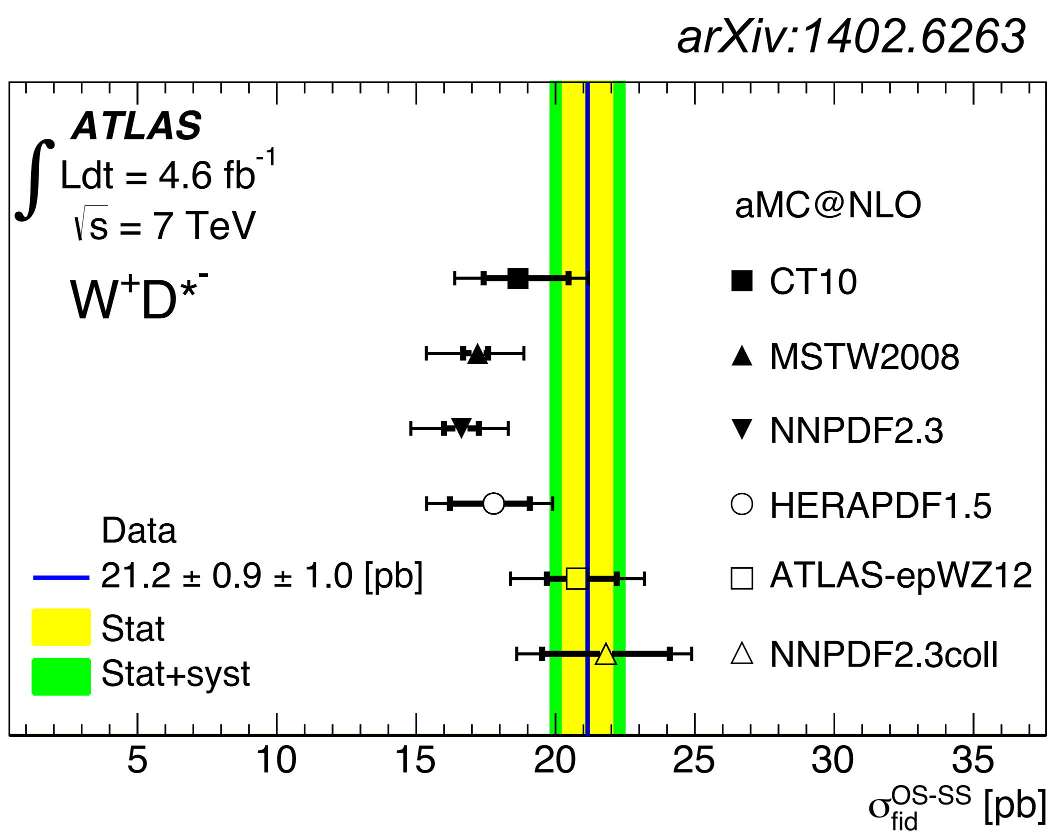

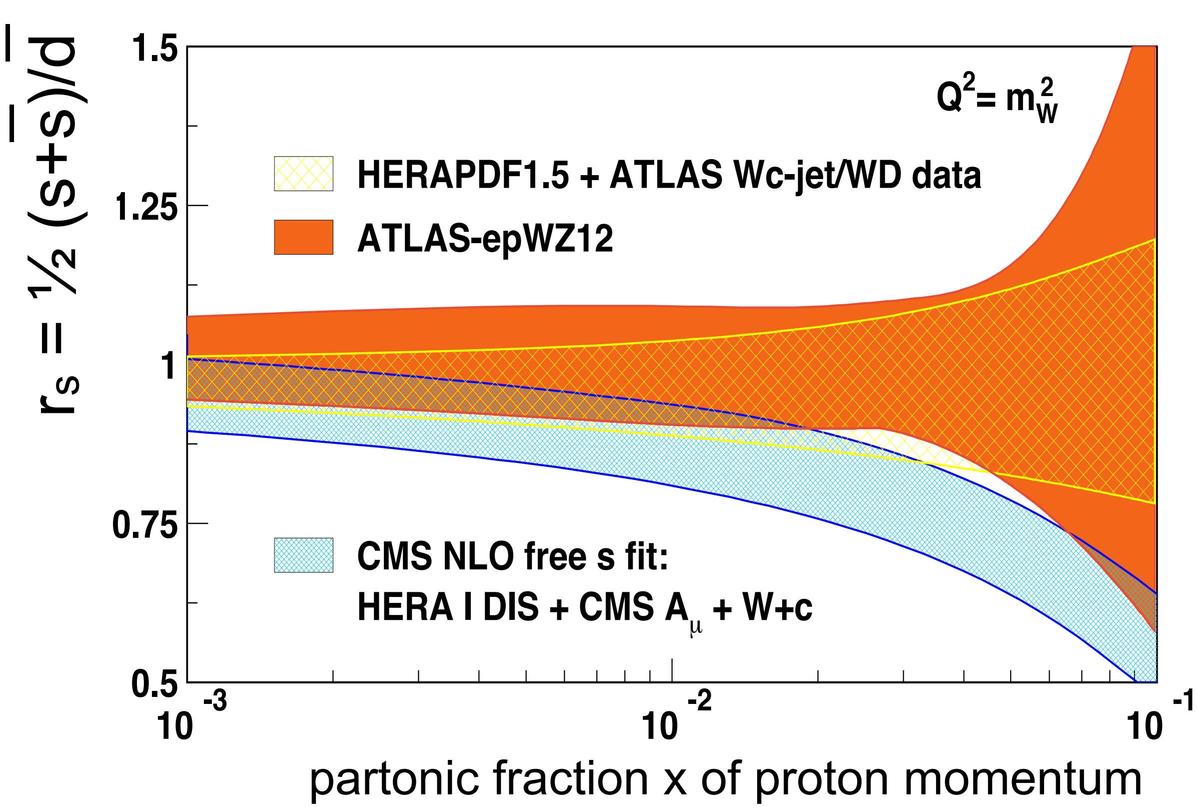

ATLAS observes somewhat enhanced strange distribution but is in agreement with CMS result within uncertainties

Summary

• QCD passes stringent tests with the precise LHC data up to highest scales
• Interpretation of the measurements limited by missing higher order calculations, uncertainties and correlations of strong coupling and PDFs

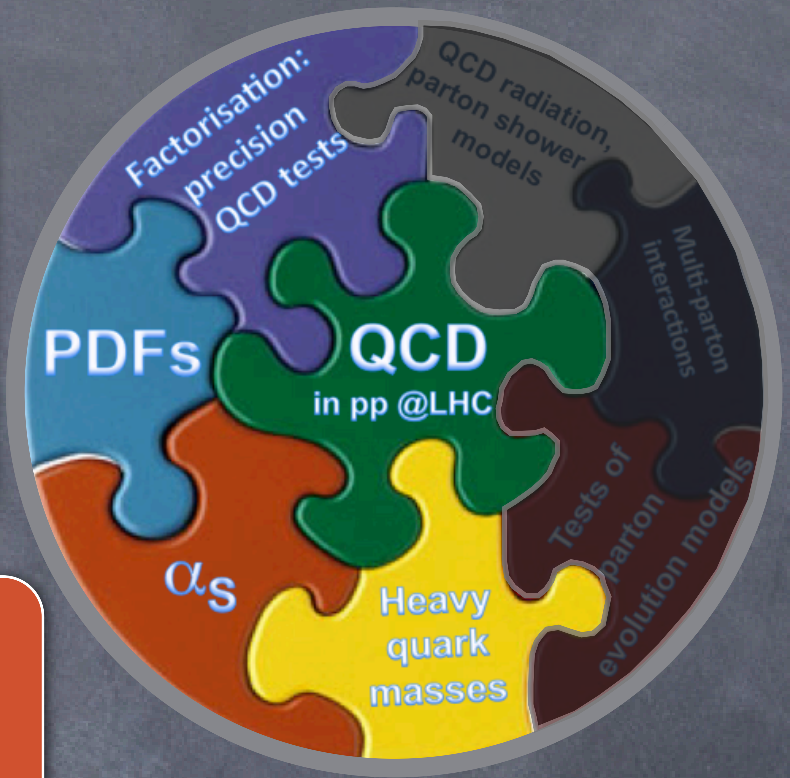

• Precise measurements of (multi) jet and top production used to determine α_S with very small experimental error.
• Running of α_S measured up to 1.4 TeV, in good agreement with renormalisation group equations of QCD

• Inclusion of the LHC measurements into the QCD analysis has started, followed up by relevant developments in the theory and analysis tools.
• We observe improvements in the gluon and valence distributions and for the first time decompose the light sea using only hadron collider data.

QCD analyses at the LHC continue to be prepared for high-energy running

Outlook

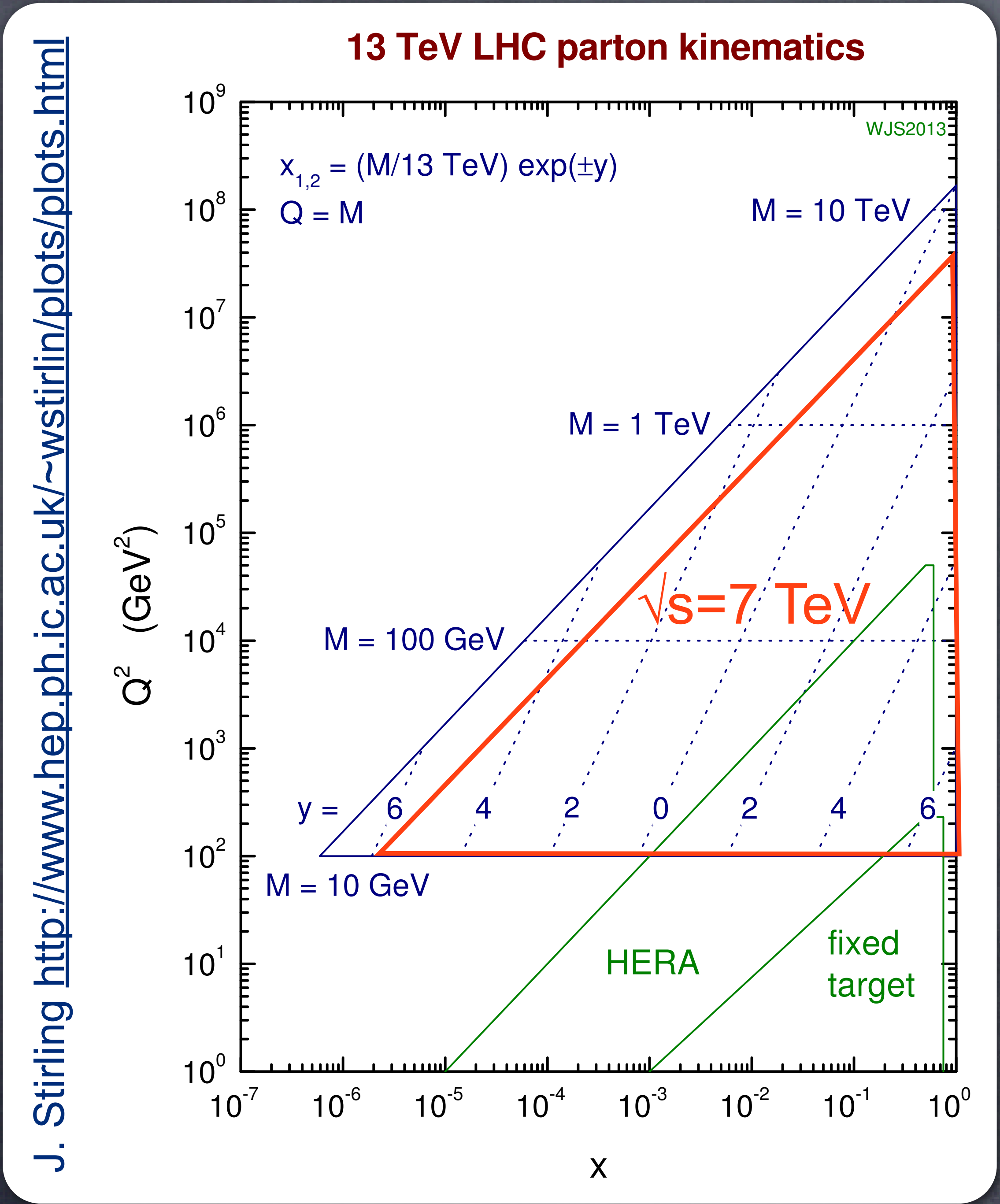

Kinematic plane of the LHC at 13(14) TeV
very similar to that at 7(8) TeV
very similar x coverage at high M

Expect similar limitations by QCD precision

Improvements in experimental precision demands better understanding of QCD

Back up slides

How well do we know PDFs

g(x) by different PDF groups:

- uncertainties have to be improved
- differences have to be understood

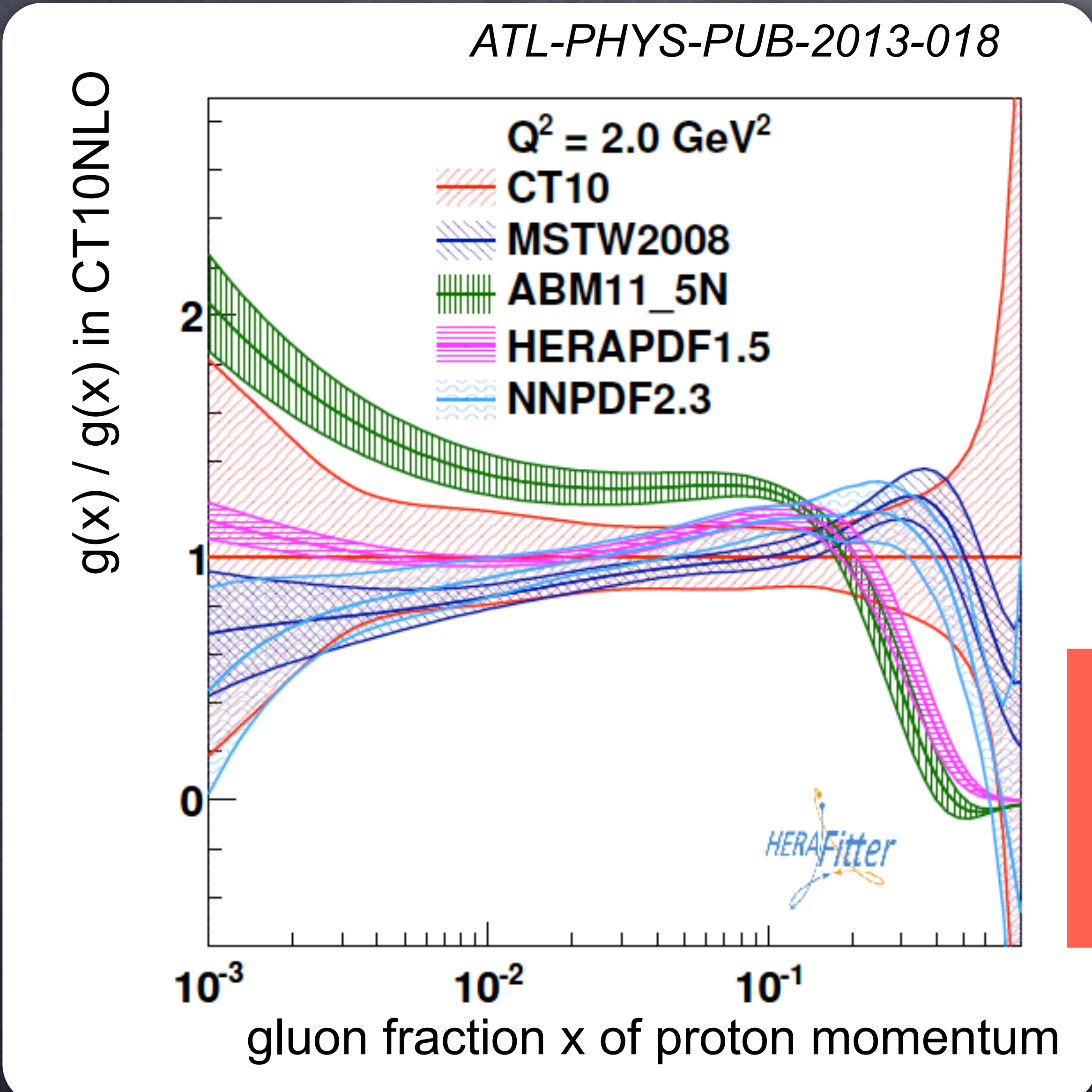

Origin of the large spread arise from differences in phenomenological analysis of PDF determination, treatment of heavy quarks in the proton and consistency of experimental data sets used in PDF analysis

		σ (8 TeV)	uncertainty
NNLL QCD +NLO EW	gg→H	19.5 pb	14.7%
	VBF	1.56 pb	2.9%
NNLO QCD +NLO EW	WH	0.70 pb	3.9%
	ZH	0.39 pb	5.1%
NLO QCD	ttH	0.13 pb	14.4%

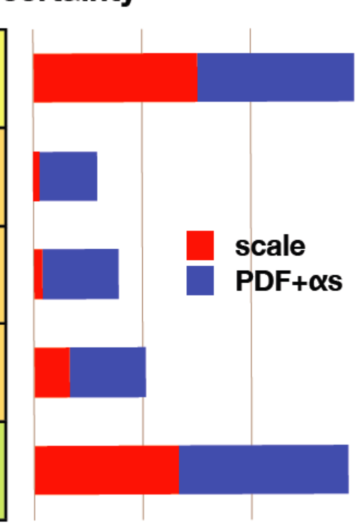

Correlations between PDF and cross sections

The NNPDF Collaboration provides PDF sets in the form of an ensemble of replicas, which sample variations in the PDF parameter space allowed within uncertainties.

Evaluating means and variance using the replicas, obtain predictions and uncertainties for PDF-dependent observables.

correlation coefficient

number of replicas in NNPDF ensemble

inclusive jet cross section

parton distribution for flavour i

$$\varrho_i\left[\sigma_{\mathrm{jet}}(x,Q^2), xf_i(x,Q^2)\right] = \frac{N_{\mathrm{rep}}}{(N_{\mathrm{rep}}-1)} \frac{\langle \sigma_{\mathrm{jet}}(x,Q^2)\, x f_i(x,Q^2)\rangle - \langle\sigma_{\mathrm{jet}}\rangle\langle x f_i(x,Q^2)\rangle}{\Delta_{\sigma_{\mathrm{jet}}(x,Q^2)}\,\Delta_{xf_i(x,Q^2)}}$$

uncertainties of measured cross sections

uncertainties of PDFs

General Strategy for a QCD analysis

QCD Factorization: e.g. DIS Structure functions for the exchange of Boson V (γ, Z, $W^{\pm}$)
are expressed as convolution products

$$\underbrace{F_2^V(x,Q^2)}_{\text{determined by using measured cross sections}} = \sum_{i=q,\bar{q},g} \int_x^1 dz \times \underbrace{C_2^{V,i}(\frac{x}{z}, Q^2, \mu_F, \mu_R, \alpha_S)}_{\text{coefficient functions calculable in pQCD}} \times \underbrace{f_i(z, \mu_F, \mu_R)}_{\text{universal PDF}}$$

the *x*-dependence of PDFs is not predicted by perturbative QCD. A general approach:

- parameterize PDFs at a starting scale Q^2_0 : $f(x)=Ax^B(1-x)^C(1+Dx+Ex^2)$

  A: normalization, **B**: small-x behavior, **C:** $x \rightarrow 1$ shape
- evolve these PDFs to $Q^2 > Q^2_0$
- construct structure functions from PDFs and coefficient functions:
  predictions for every data point in (x, Q^2) – plane
- χ^2- fit to the experimental data

QCD Analysis Framework: Parametrization at the Starting Scale

- 13 parameters, ***fixed strange distribution***

at Q^2_0 :

$$
\begin{aligned}
xg(x) &= A_g x^{B_g} \cdot (1-x)^{C_g} - A'_g x^{B'_g} \cdot (1-x)^{C'_g}, \\
xu_v(x) &= A_{u_v} x^{B_{u_v}} \cdot (1-x)^{C_{u_v}} \cdot (1+E_{u_v} x^2), \\
xd_v(x) &= A_{d_v} x^{B_{d_v}} \cdot (1-x)^{C_{d_v}}, \\
x\overline{U}(x) &= A_{\overline{U}} x^{B_{\overline{U}}} \cdot (1-x)^{C_{\overline{U}}}, \\
x\overline{D}(x) &= A_{\overline{D}} x^{B_{\overline{D}}} \cdot (1-x)^{C_{\overline{D}}}.
\end{aligned}
$$

fixed s

$$
\begin{aligned}
x\,\overline{U} &= x\,\bar{u} \\
x\,\overline{D} &= x\,\bar{d} + x\,\bar{s} \\
B_{\overline{U}} &= B_{\overline{D}} \\
A_{\overline{U}} &= A_{\overline{D}}(1-f_s) \\
f_s &= \bar{s}/(\bar{d}+\bar{s}) \equiv 0.31 \pm 0.08
\end{aligned}
$$

Au_v , Ad_v, Ag are determined by QCD sum rules

- 15 parameters, "***free s fit***"

at Q^2_0 :

$$
\begin{aligned}
xg(x) &= A_g x^{B_g} \cdot (1-x)^{C_g} - A'_g x^{B'_g} \cdot (1-x)^{C'_g}, \\
xu_v(x) &= A_{u_v} x^{B_{u_v}} \cdot (1-x)^{C_{u_v}} \cdot (1+E_{u_v} x^2), \\
xd_v(x) &= A_{d_v} x^{B_{d_v}} \cdot (1-x)^{C_{d_v}}, \\
x\overline{U}(x) &= A_{\overline{U}} x^{B_{\overline{U}}} \cdot (1-x)^{C_{\overline{U}}}, \\
\cancel{x\overline{D}(x)} &\cancel{= A_{\overline{D}} x^{B_{\overline{D}}} \cdot (1-x)^{C_{\overline{D}}}.}
\end{aligned}
\quad
\begin{cases}
x\,\bar{d}(x) = A_{\bar{d}}\, x^{B_{\bar{d}}}\, (1-x)^{C_{\bar{d}}} \\
x\,\bar{s}(x) = A_{\bar{s}}\, x^{B_{\bar{s}}}\, (1-x)^{C_{\bar{s}}}
\end{cases}
$$

$A_{\bar{u}} = A_{\bar{d}}$; $B_{\bar{u}} = B_{\bar{d}}$ ensures same normalization for u and d- antiquarks at $x \to 0$

$B_{\bar{s}} = B_{\bar{d}}$ for the central fit, **A_s and C_s are free parameter of the fit**, assumed $s = \bar{s}$

$B_{\bar{s}} \neq B_{\bar{d}}$ fit performed, difference to results of the central fit included in parametrization uncertainty

Strange quark distribution using LHC data

Differential cross sections of W and Z production used for constraints on s-quark

NLO and NNLO analysis using HERAFitter, ***s-quark distribution fitted***

- Deep Inelastic Scattering in ep collisions (HERA I combined *[JHEP 1001:109 (2010)]*)
- ATLAS W and Z production $\sqrt{s}$=7 TeV (35 pb^{-1}) *[Phys. Rev. D 85, 072004 (2012)]*

Phys.Rev.Lett. 109 (2012) 012001

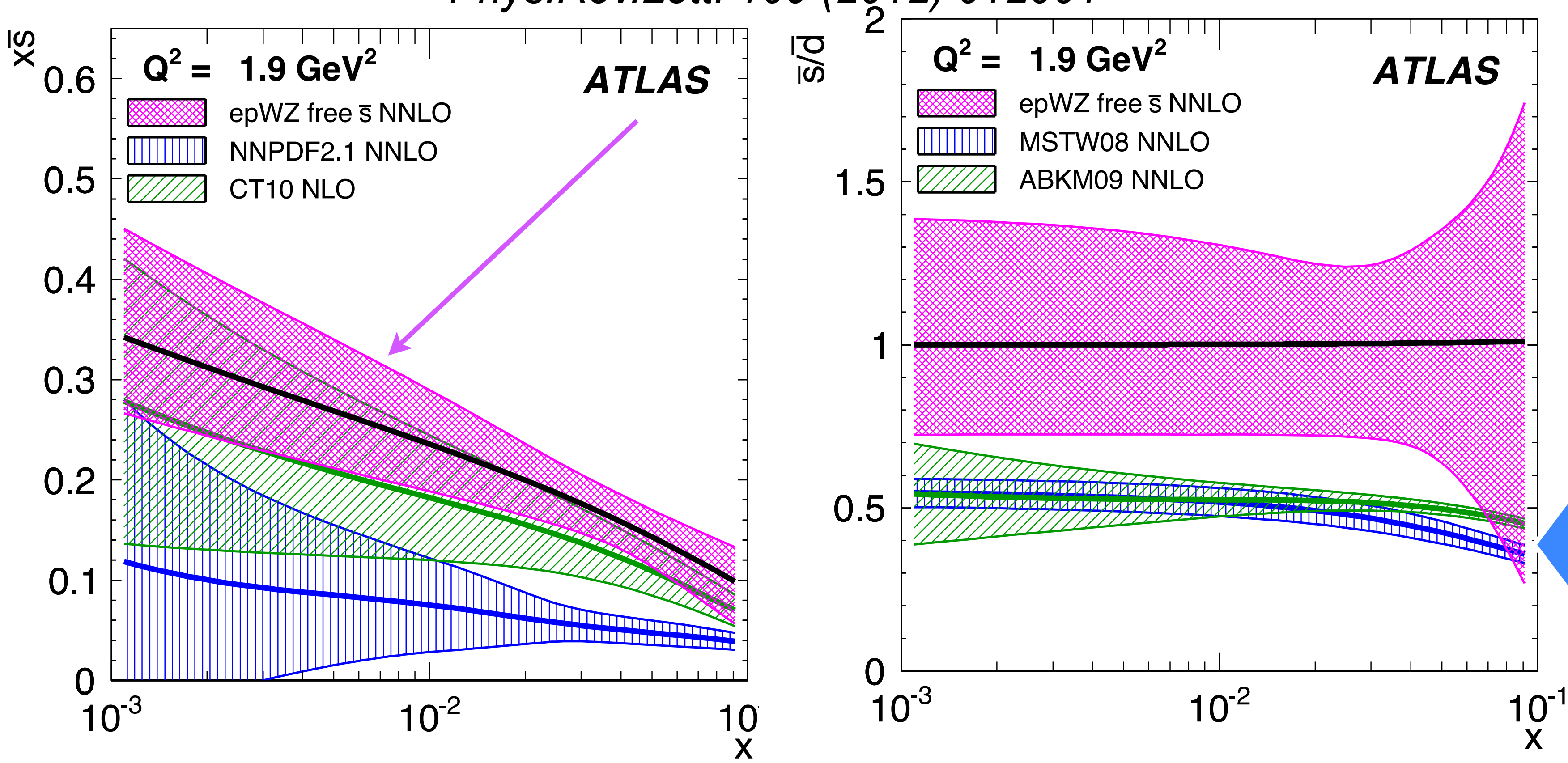

other PDFs use neutrino-scattering data for strangeness determination

Enhanced strangeness observed with respect to results of neutrino scattering experiments, consistent with flavor-symmetric sea ($\bar{s}=\bar{d}$)

LHC measurements of W+c probe strangeness

Associated W+c production in pp collisions probes strange quark in the proton directly at LO

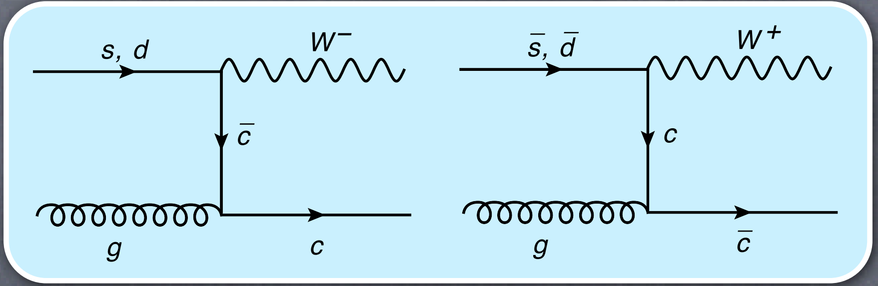

NLO QCD analysis using HERAFitter, ***s-quark distribution determined***

- Deep Inelastic Scattering in ep collisions (HERA I *[JHEP 1001:109 (2010)]*)
- CMS muon charge asymmetry in W production at 7 TeV (L=4.7 fb-1) *[arXiv:1312.6283]*
- CMS associated W+charm production at 7 TeV (L=4.7 fb-1) *[arXiv:1310.1138]*

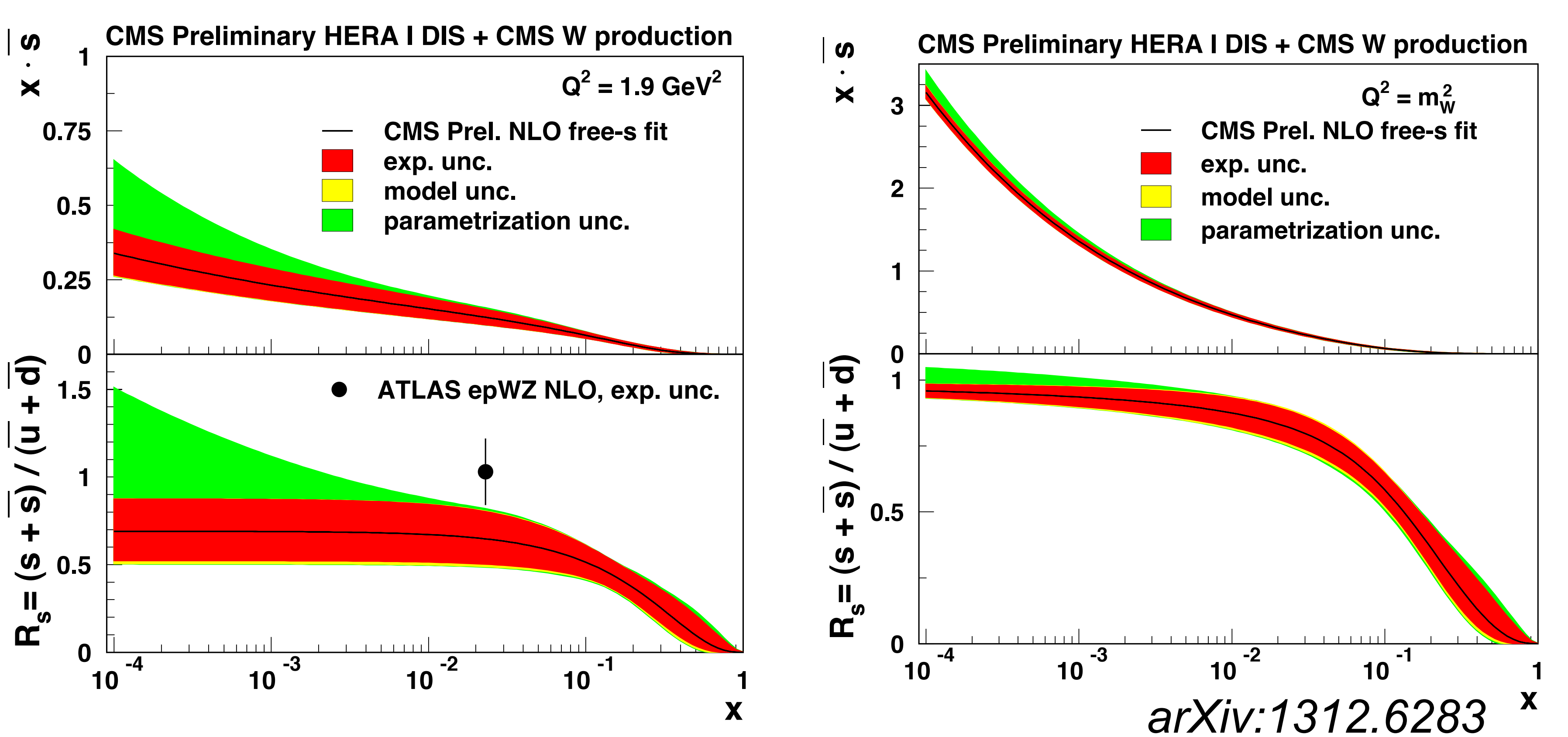

arXiv:1312.6283

at the starting scale, $R_s = r_s = \bar{s}/\bar{d}$

consistent with ATLAS result at NLO for x = 0.023

Strange quark distribution using LHC data

Results agree with the global PDFs

where assumptions on s(x) are based on results of neutrino scattering experiments

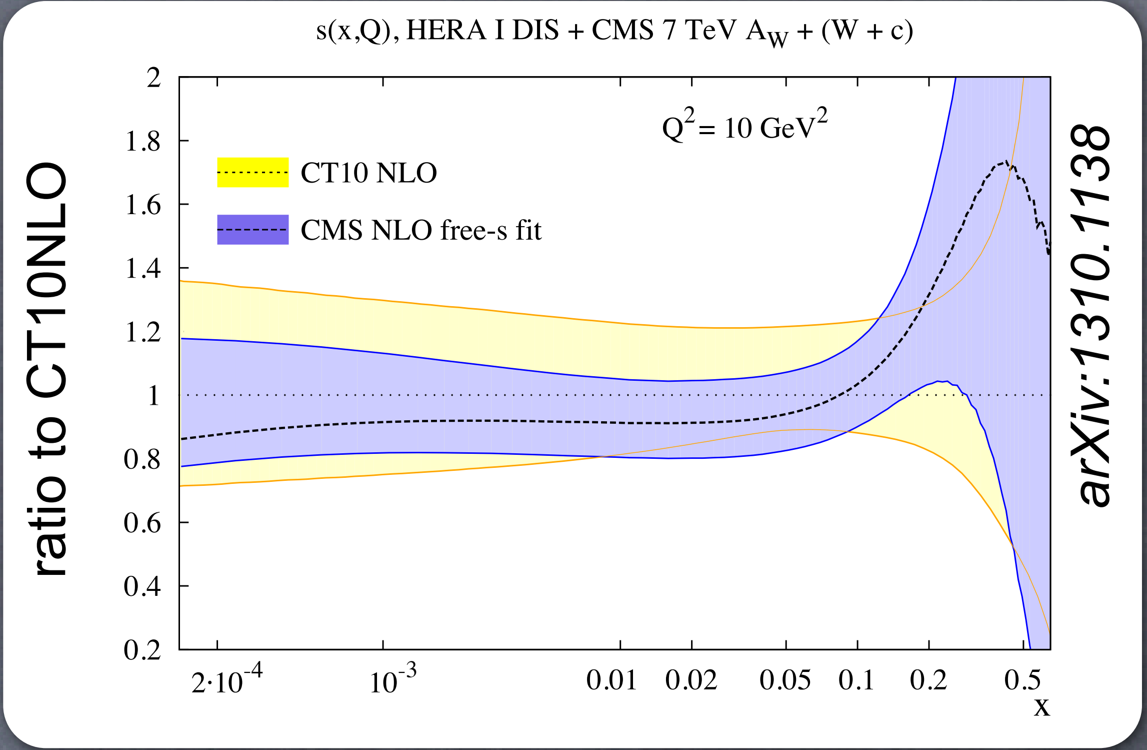

Strangeness suppression factor :

$$\kappa_s(Q^2) = \frac{\int_0^1 (\bar{s}(x,Q^2) + s(x,Q^2))dx}{\int_0^1 (\bar{u}(x,Q^2) + \bar{d}(x,Q^2))dx}$$

Result of the CMS QCD analysis at NLO using W production:

$\kappa_s = 0.52^{+0.12}_{-0.10}(exp.)^{+0.05}_{-0.06}(mod.)^{+0.13}_{-0.10}(par.)$ at Q^2=20 GeV^2

in good agreement with the NOMAD *[Nucl.Phys. B876 (2013) 339, κ_s =0.59 ± 0.019]*

Direct constraints on the strange quark distribution by using collider data only in good agreement with results of neutrino scattering experiments

Sensitivity of prompt photons to proton structure

Prompt photon production at LHC probes the gluon distribution at high x via qg→qγ

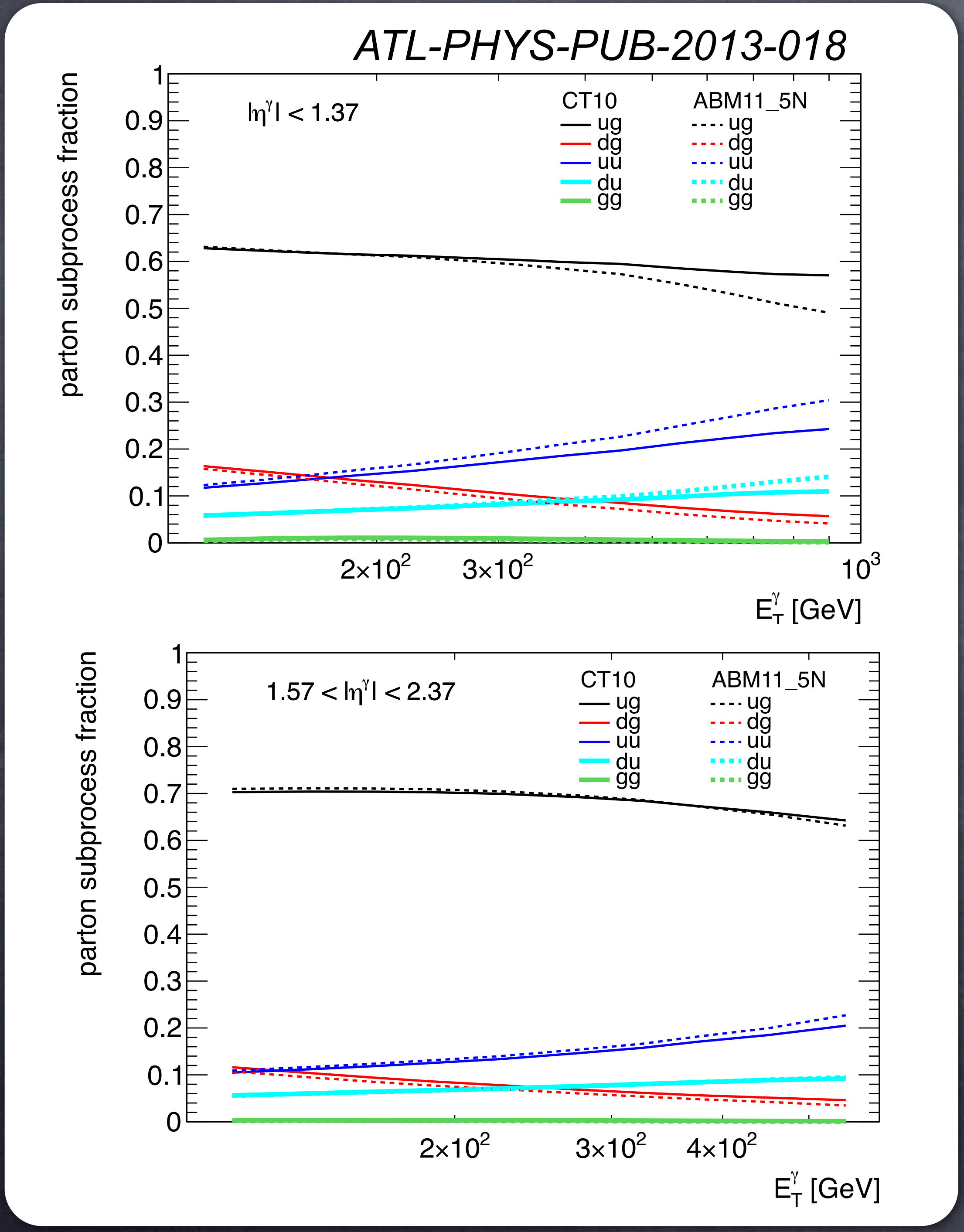

Sensitivity of prompt photons to proton structure

Prompt photon production at LHC probes the gluon distribution at high x via qg→qγ

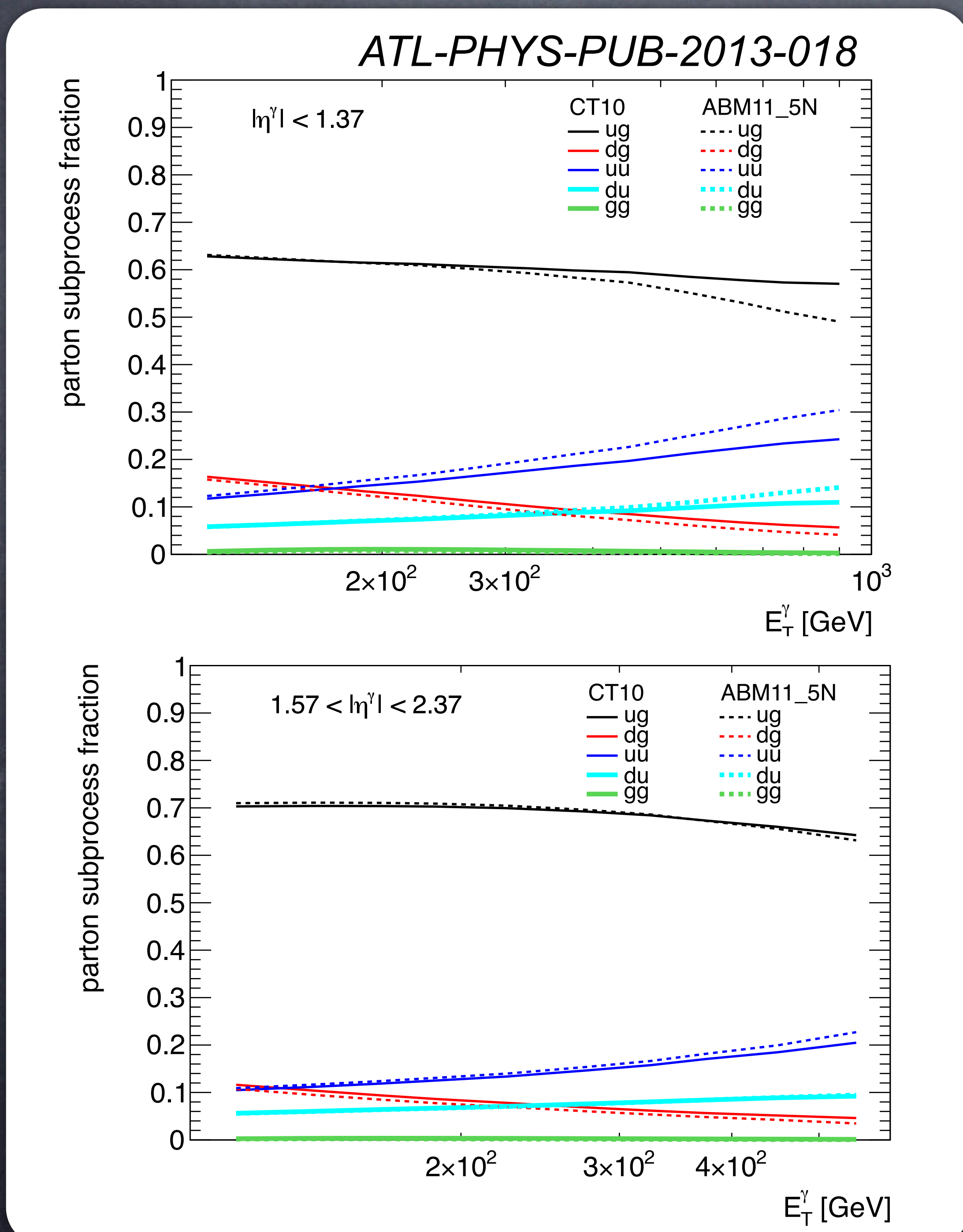

Measured precisely at LHC:

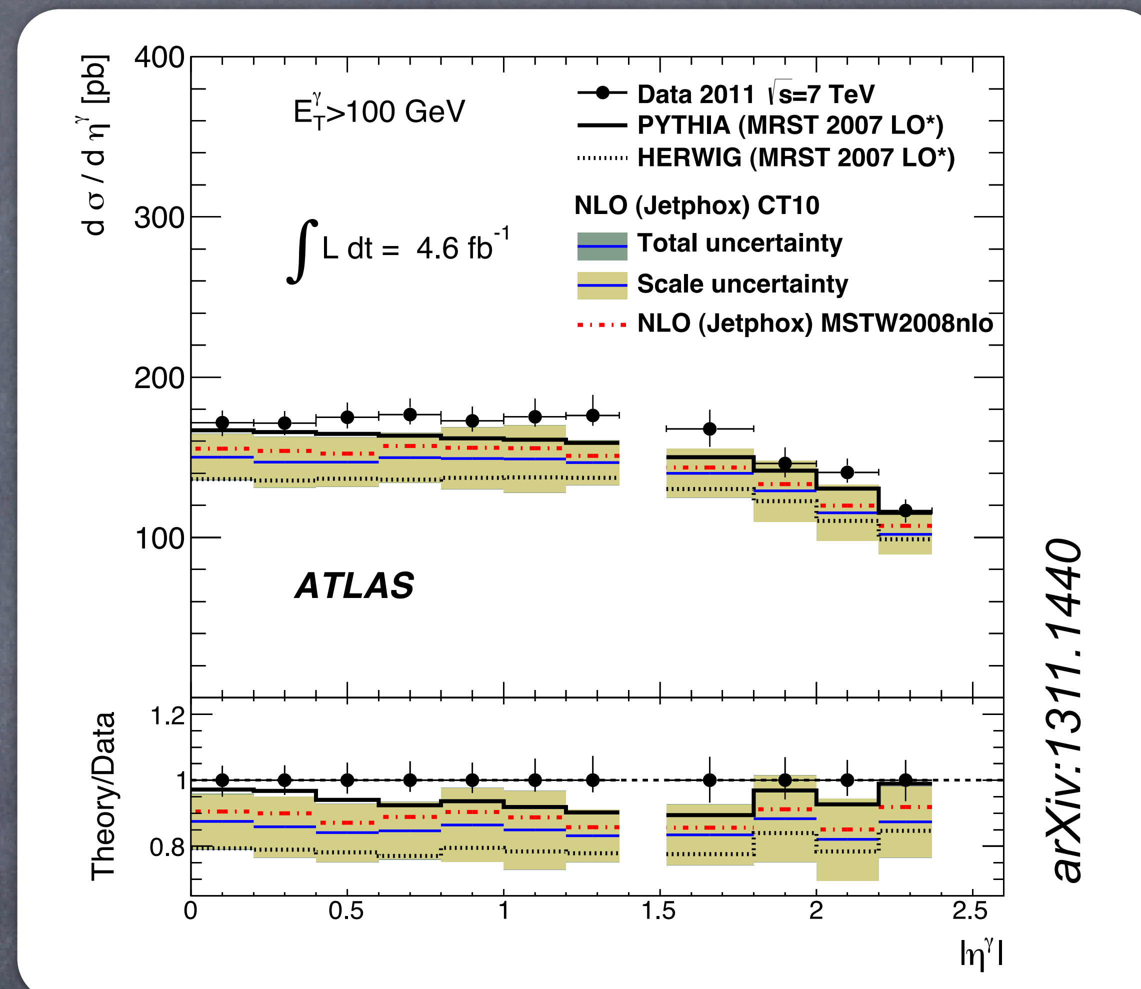

ATLAS √s=7 TeV, L=4.6pb^{-1}

- exp. systematic uncertainty < 7%
- theory uncertainty: 12-20% scale,

  5-15% PDF, 4.5% α_s

Sensitivity of prompt photons to proton structure

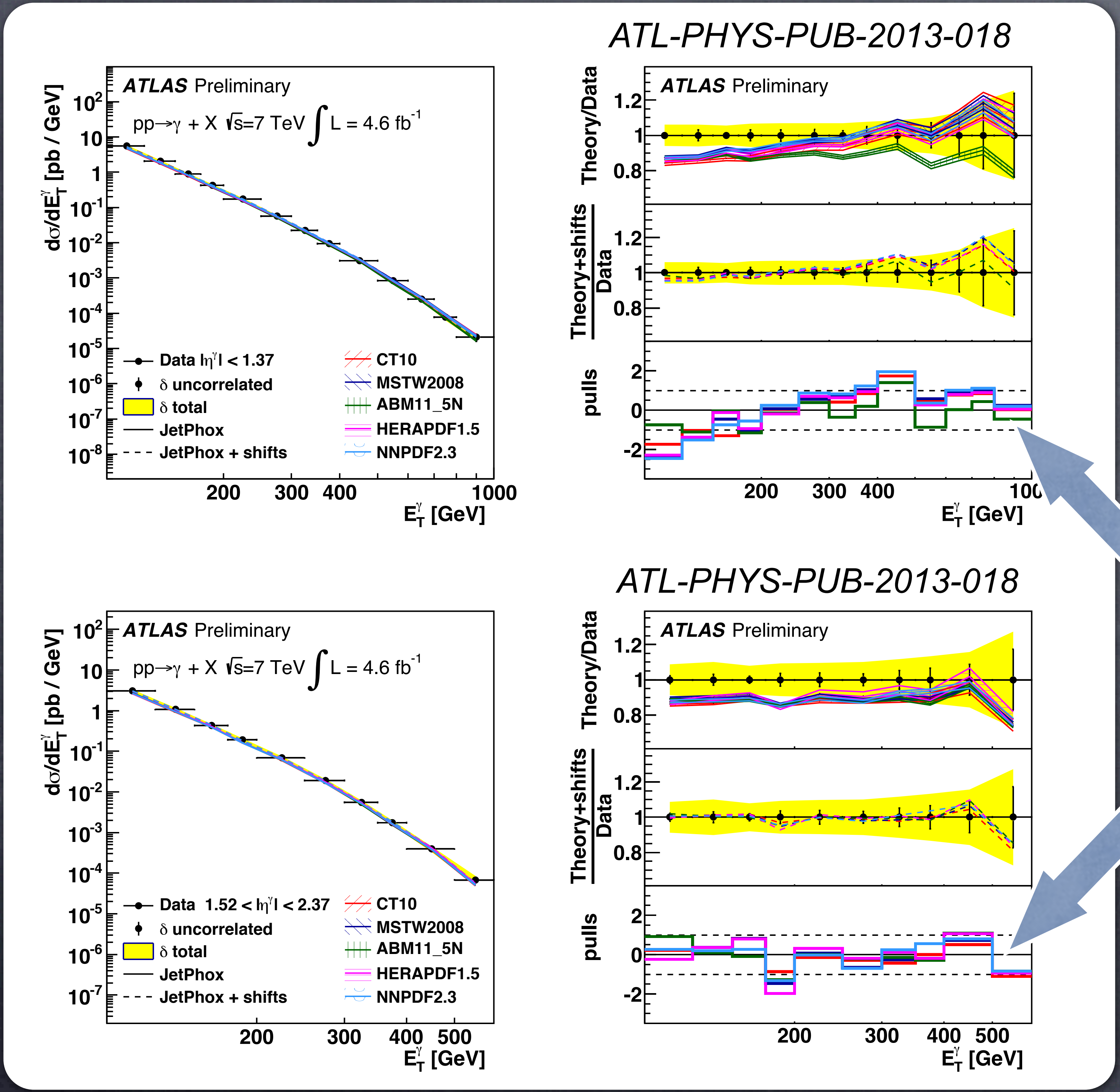

agreement of data and theory quantified via χ^2 (or pulls) using HERAFitter

significant pulls between data and NLO prediction using different PDFs:

- strong sensitivity to g(x)
- large scale uncertainties

NNLO needed !

Strong coupling

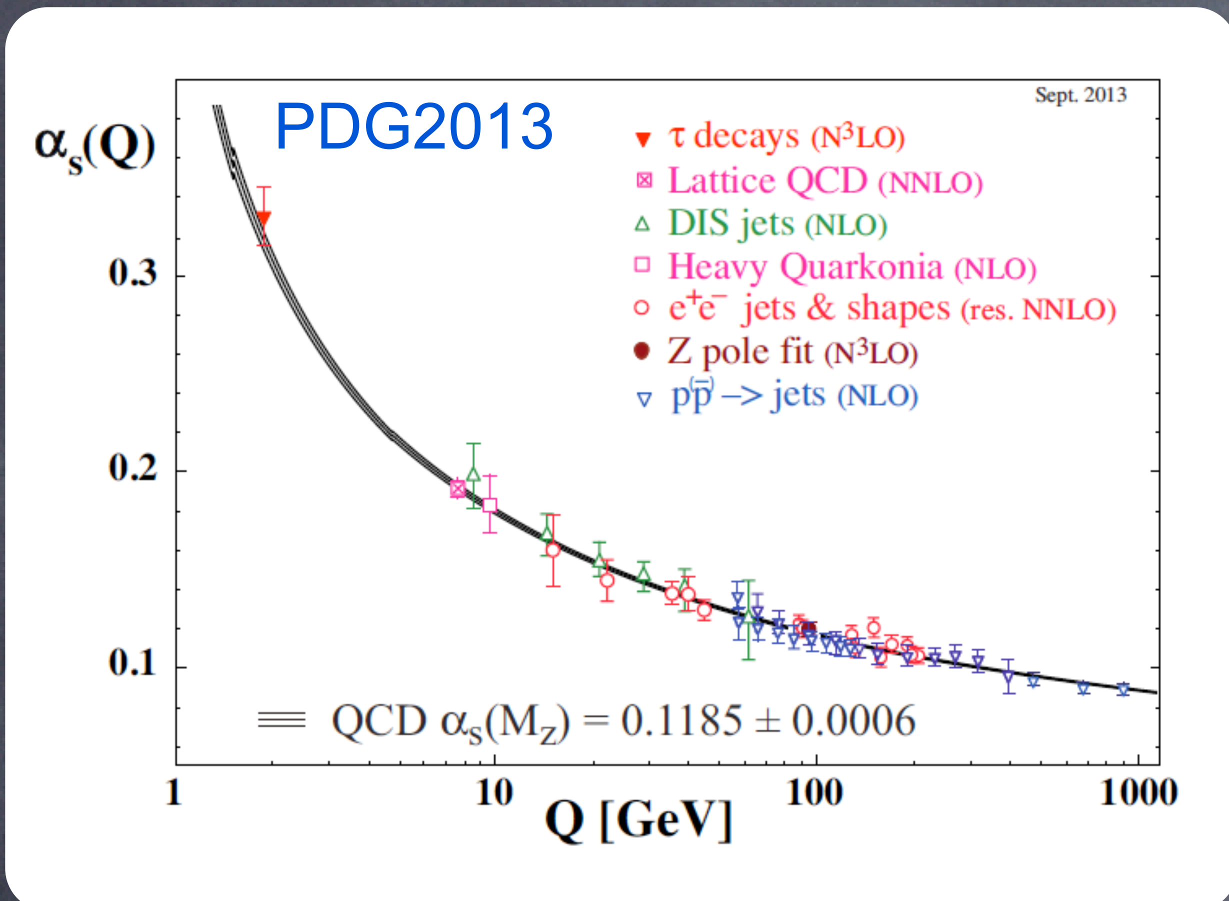

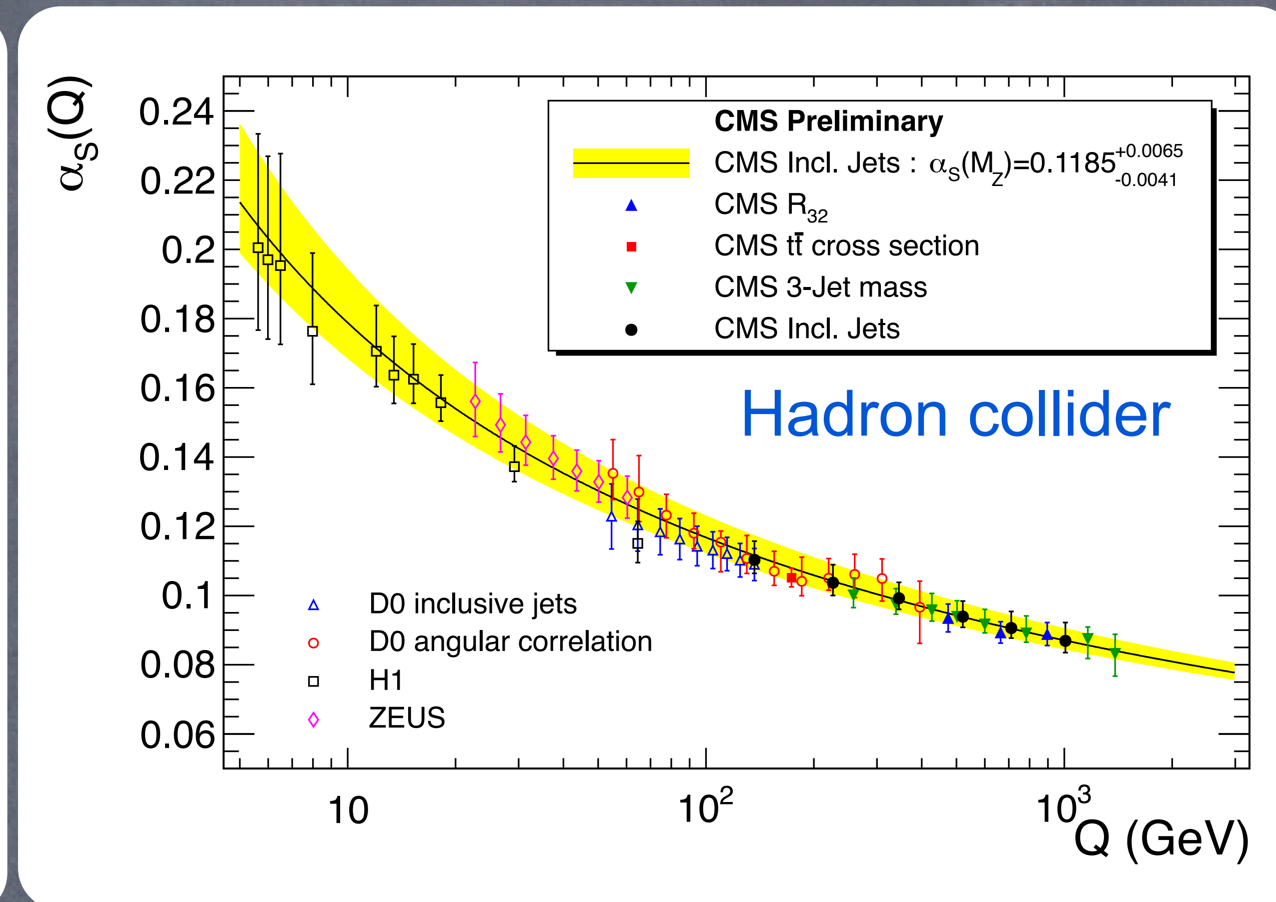

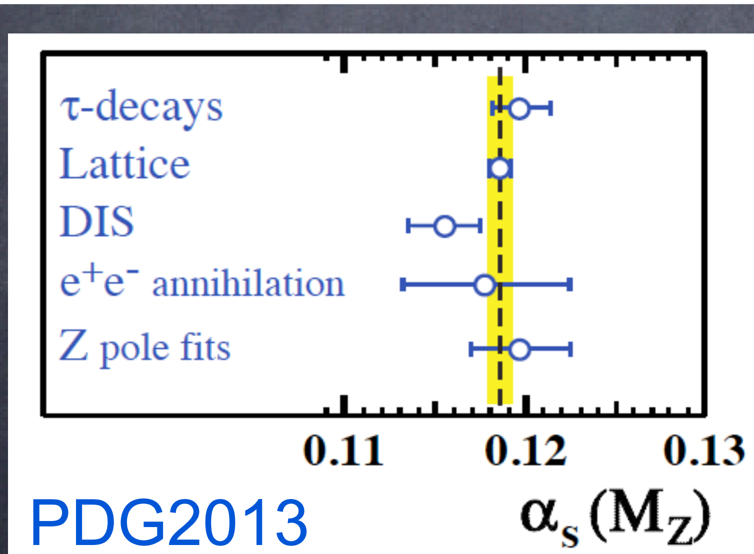

$$\alpha_s(M_Z^2) = 0.1185 \pm 0.0006$$

LHC 7 TeV (without theory uncertainty)

Incl. jets: $\alpha_S(m_Z)= 0.1185 \pm 0.0019_{exp} \pm 0.0028_{PDF}$

R32: $\alpha_S(m_Z)= 0.1148 \pm 0.0014_{exp} \pm 0.0018_{PDF}$

3jet mass: $\alpha_S(m_Z)= 0.1160 ^{+0.0068}_{-0.0021}$ (exp+PDF)

PDF fit: $\alpha_S(m_Z) = 0.1192^{+0.0017}_{-0.0015}$ (exp)

top-pairs: $\alpha_S(m_Z) = 0.1151^{+0.0033}_{-0.0032}$ (total, theory 1%)

Theory uncertainties: progress at NNLO

Scale dependence of the inclusive jet cross section for
pp @ √s = 8 TeV, anti-kT, R = 0.7
|y| < 4.4 and 80 GeV < pT < 97 GeV

Phys.Rev.Lett. 110 (2013) 16, 162003

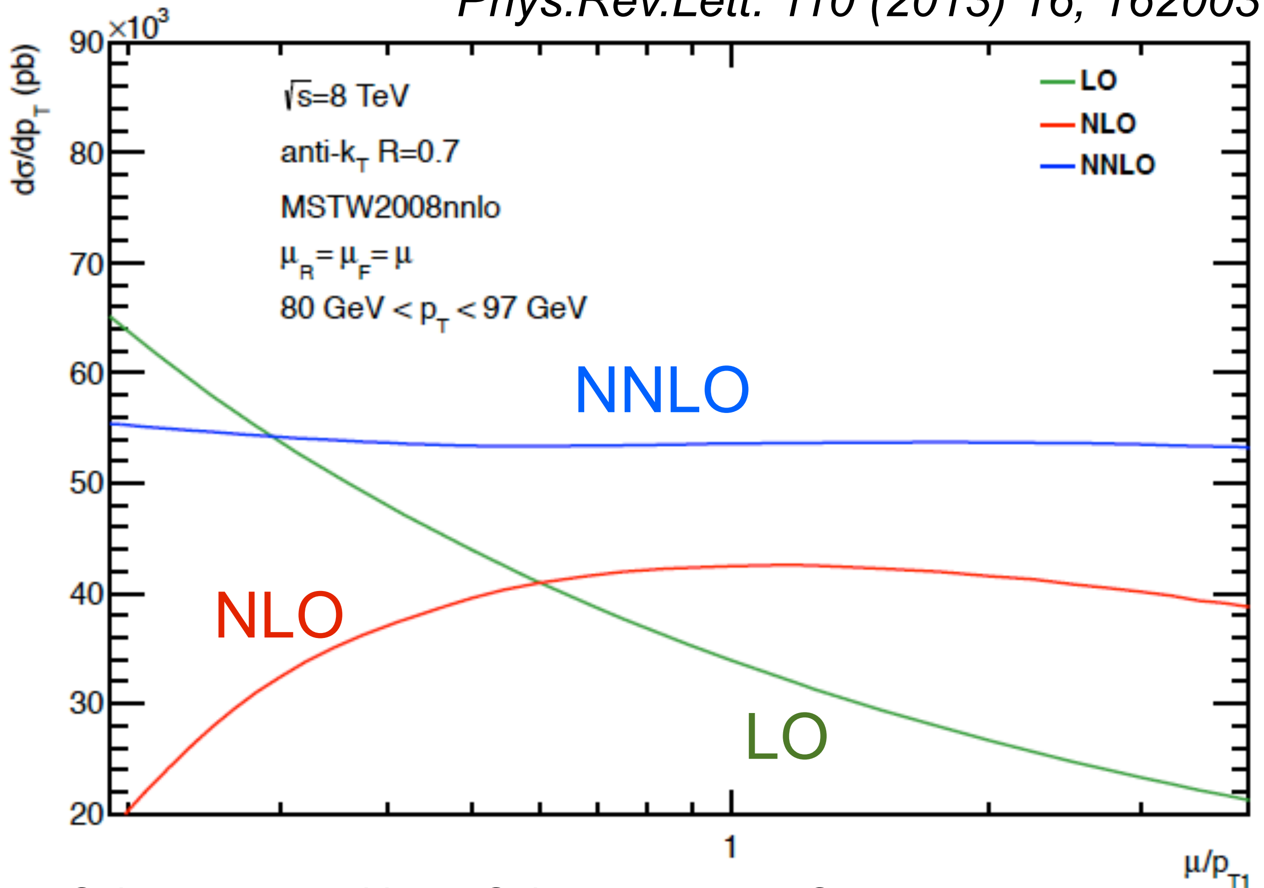

A. Gehrmann-De Ridder, T. Gehrmann, E.W.N. Glover, J. Pires

significant progress in theory calculation of pp collisions

Comparison data/theory using ATLAS jet PDF

Ratio of jet cross sections at 2.76 and 7 TeV vs NLO QCD ⊗ ATLAS jet PDF

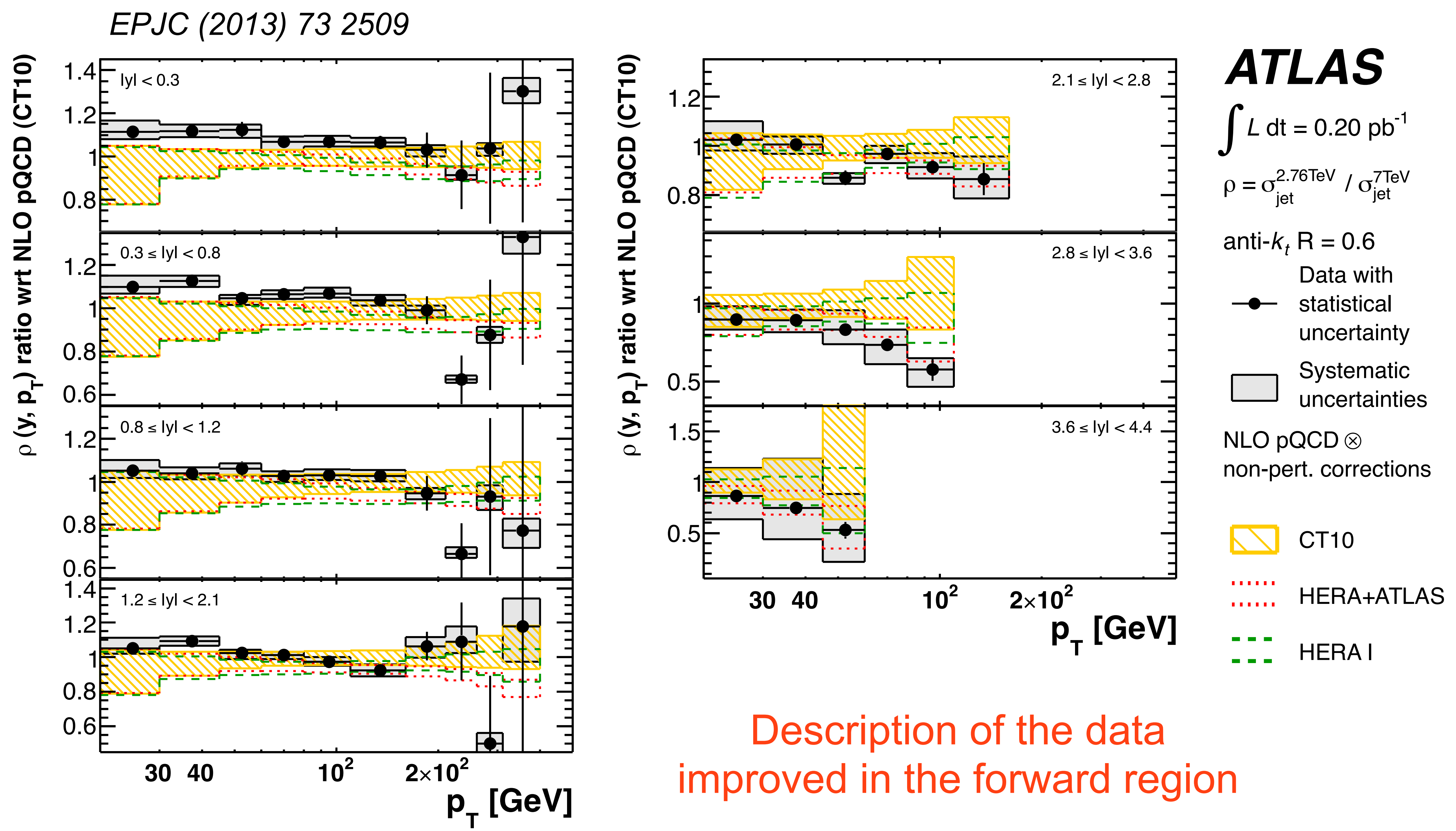

Description of the data improved in the forward region

Jet reconstruction (e.g. at CMS)

CMS detector

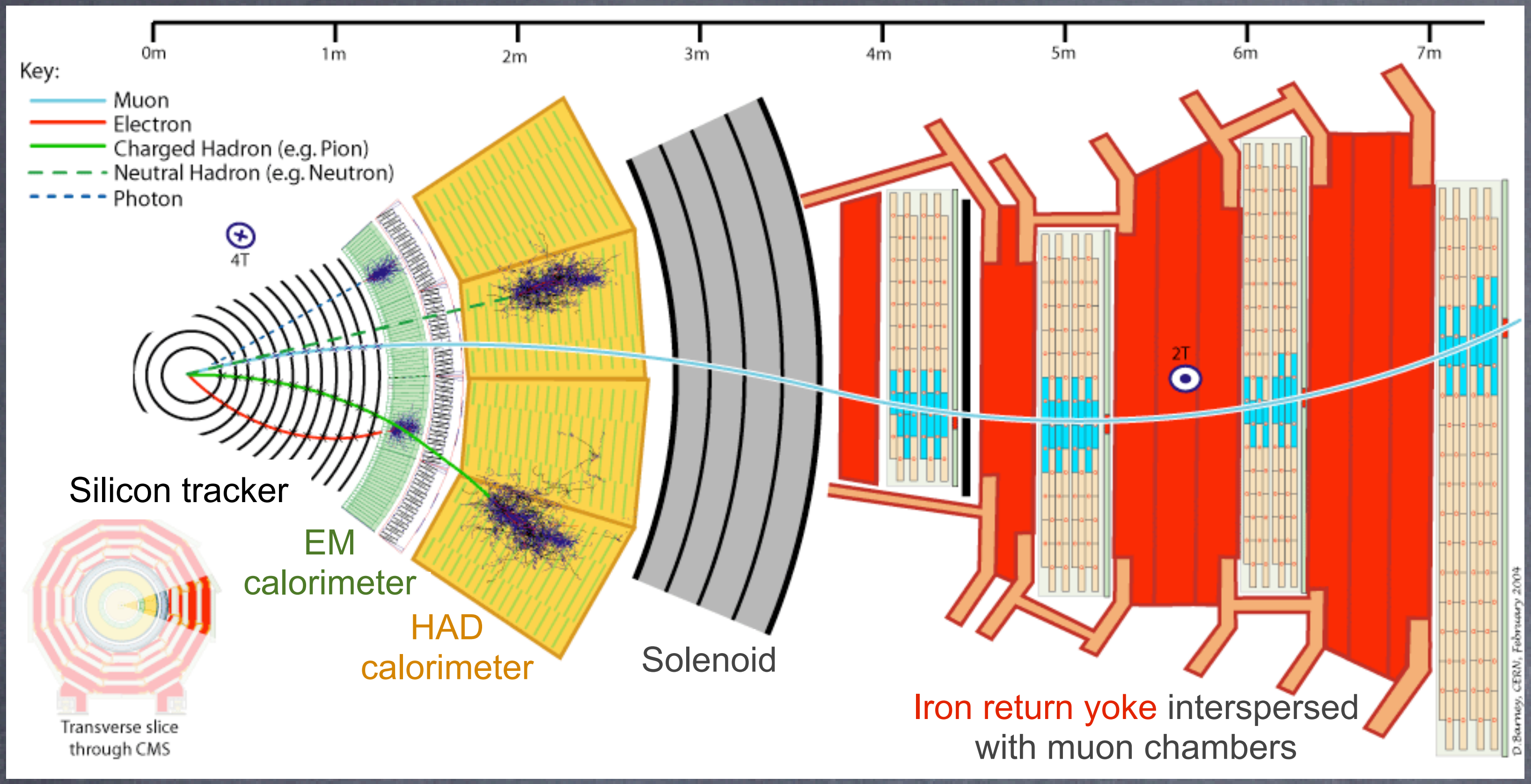

Acceptance:
Tracking: $|\eta|<2.5$
Central calorimetry $|\eta|<3$
Forward calorimetry $3<|\eta|<5$

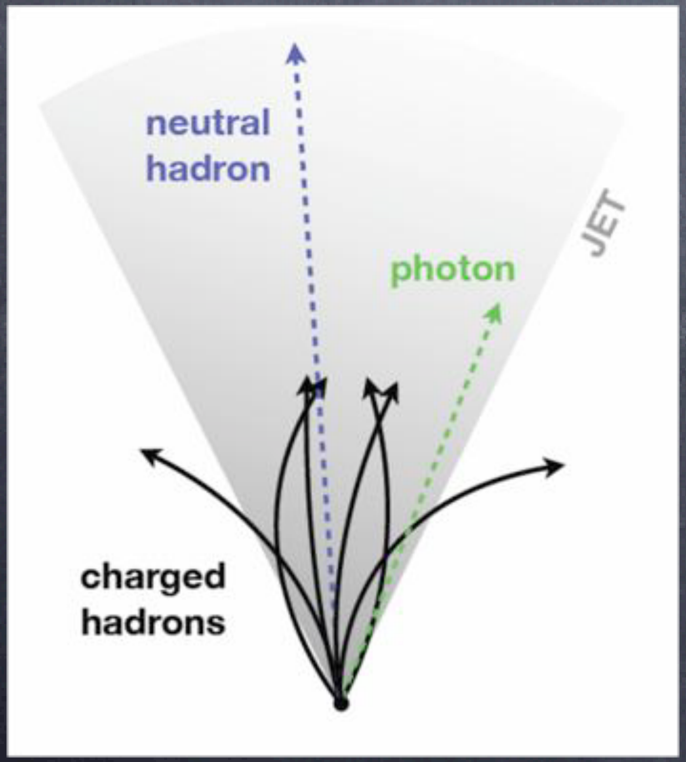

CMS global event reconstruction: reconstructs and identifies all stable particles in the event, through the optimal combination of all sub-detectors.

Particle Flow jets are the output of anti-k_T algorithm, running on the reconstructed particles. Infrared and collinear safe, different R used.

Jet p_T resolution ≈ 9% at 100 GeV

Searches for new phenomena with dijets

New phenomena could appear as resonances in dijet mass distribution

Invariant mass of the di-jet system

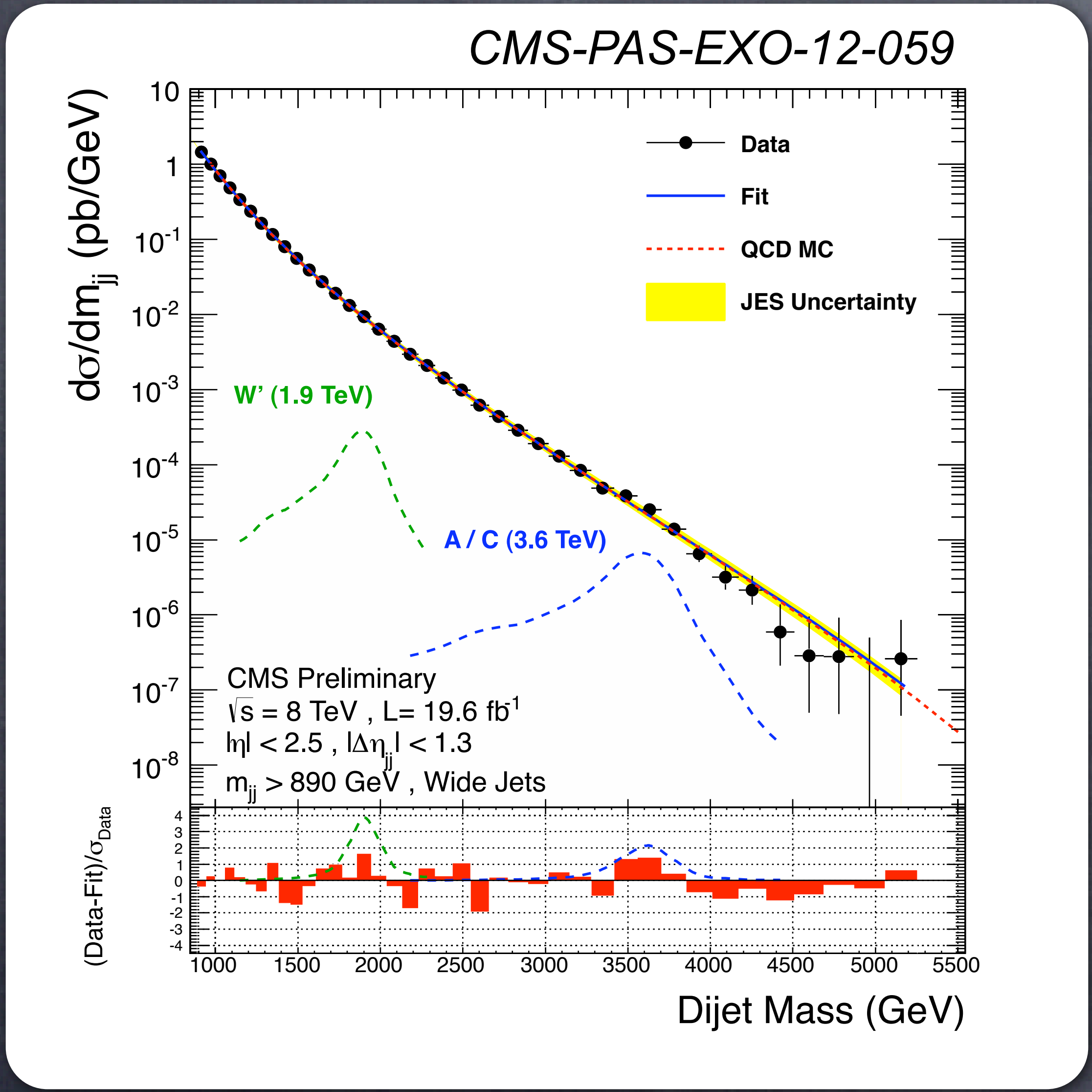

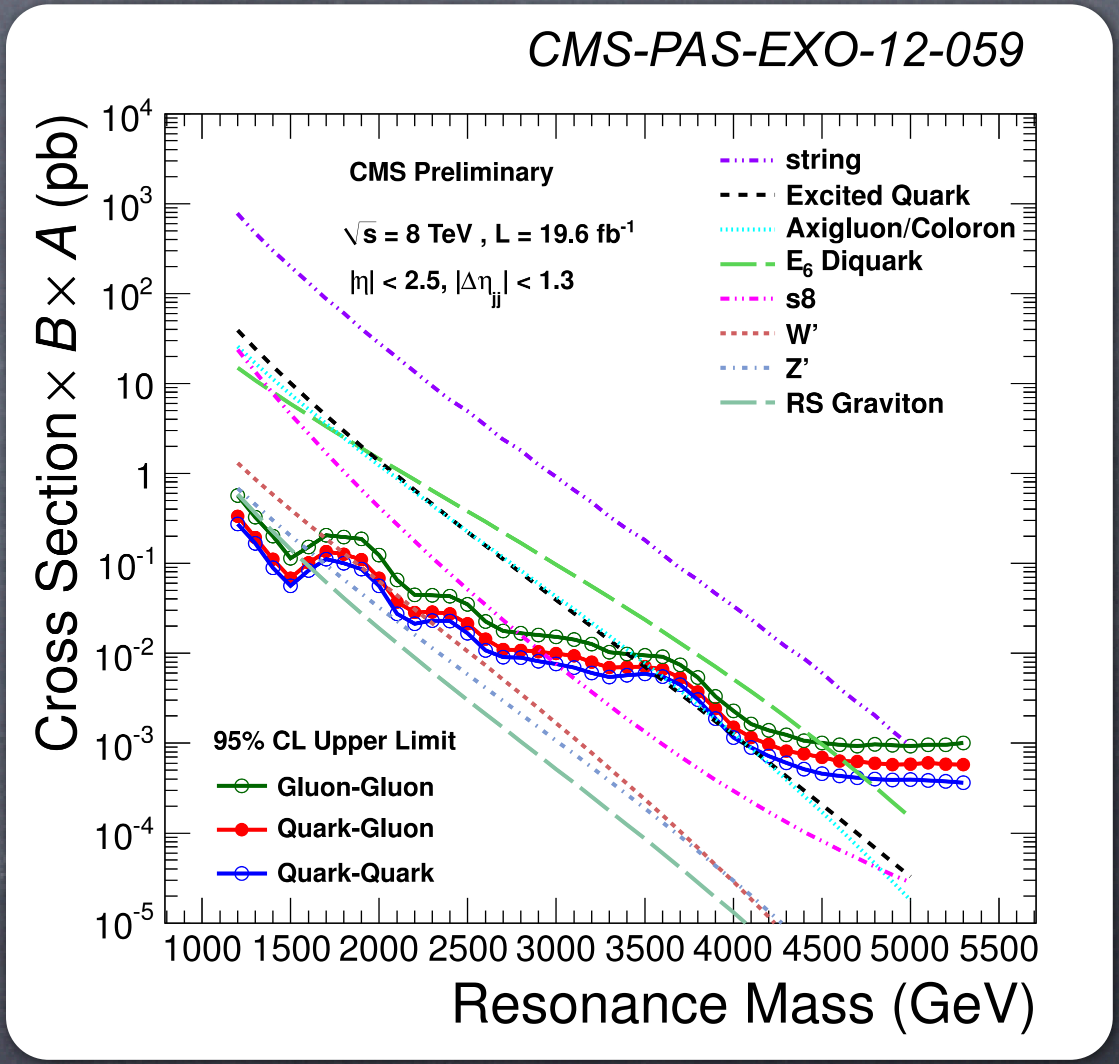

Fit with a *data-driven* smooth function
(only for resonant effects, CI absorbed)

large angular and mass range is explored
limits set on a variety of hypotheses

Ultimate QCD tests: di-jet production

Di-jet production at ATLAS $\sqrt{s}$=7 TeV (L=4.5 fb^{-1}) compared to NLO QCD (NLOJet++)corrected for non-perturbative and EWK effects

NLO QCD describes measurements very well for both jet sizes *(probe effects beyond fixed order)*